How spin conductive are oligo(p-phenylenes) in trityl-based biradicals

Kevin L. Kopp[a], Andrea Pellegrini[b], Stefan Grimme[c], Olav Schiemann[a]*

[a] *Clausius Institute of Physical and Theoretical Chemistry, University of Bonn, Wegelerstraße 12, 53115 Bonn, Germany*

[b] *Department of Industrial Chemistry "Toso Montanari", University of Bologna, Via P. Gobetti 85, 40129 Bologna, Italy*

[c] *Mulliken-Centre, Clausius-Institute for Physical and Theoretical Chemistry, University of Bonn, Wegelerstraße 12, 53115 Bonn, Germany*

*E-mail: schiemann@uni-bonn.de

Table of contents

1. General Procedures and Instrumentation

NMR spectroscopy: NMR spectra were recorded at room temperature on Avance I 400, Avance III 500, or Avance III HD 700 spectrometers (Bruker BioSpin, Ettlingen, Germany). All chemical shifts are referenced to the residual hydrogen peaks of the deuterated NMR solvents.

Mass spectrometry: MALDI(+)-spectra were recorded on a Bruker Daltonics UltraFlex TOF/TOF spectrometer with *trans*-2-[-3(4-*tert*-Butylphenyl)-2-methyl-2-propenylidene]malononitrile (DCTB) as the matrix (Bruker Daltonics, Bremen, Germany). ESI-spectra were recorded on an Orbitrap XL mass spectrometer (Thermo Fisher Scientific, Bremen, Germany) with a Dionex Ultimate 3000 autosampler. EI-spectra were recorded on a MAT 95 XL sector field device (Thermo Finnigan, Bremen, Germany).

EPR spectroscopy: Cw EPR measurements at X-band frequencies (~9.4 GHz) were performed on a Bruker EMXmicro spectrometer (Bruker Biospin, Ettlingen, Germany). Measurements at room temperature were done using a Bruker 4119HS resonator, while for measurements down to 100 K a Bruker 4119HS resonator in combination with an ER 4141VT temperature control system was used, which operates with a continuous flow of nitrogen gas. Measurements below 100 K were recorded using an ER4122SHQE resonator, an ER4122HV liquid helium cryostat, and a Mercury iTC503 temperature controller (sensor type ESR900, Oxford Instruments).

Pulsed EPR measurements at Q-band frequencies (~33.7 GHz) were performed on a Bruker Elexsys E580 EPR spectrometer equipped with an ER5106QT-II resonator and a 150 W TWT-amplifier (Applied Systems Engineering, Fort Worth, TX, USA). All spectra were recorded using quadrature detection. The temperature was adjusted to 80 K using a CF935 helium gas-flow cryostat (Oxford Instruments, Abingdon, UK) in combination with an Oxford Instruments iTC503 temperature controller.

For the EPR measurements, a 50 µM (molar concentration; or 500 µM when indicated) solution of each of the radicals was prepared in toluene-d8, transferred into a Q-band tube, degassed repeatedly, and finally flame-sealed under vacuum while still frozen.

Medium pressure liquid chromatography (MPLC): The analytical MPLC was performed using a Sepacore X10 system from Büchi (Essen, Germany) and using Büchi Flashpure Select 12 g cartridges (Silica 25 µm spherical). For each run, a constant flowrate of 20 mL/min was used with tetrahydrofuran/n-hexane as the eluent. The sample was injected into the system by dissolving it in a minimal amount of dichloromethane.

Synthesis: Chemicals were purchased from commercial suppliers and used without further purification. Where indicated, solvents were degassed by applying three freeze-pump-thaw cycles. Thin layer chromatography was conducted using 250 µm F254 silica plates provided by Merck, and spots were visualized with UV-light at 254 nm. Spots of trityl alcohols can be stained selectively by irradiating the TLC-plate for 5 min with UV-light at 254 nm (5 W). For column chromatography, silica gel (60 Å pore size, 40-63 µm particle size) purchased from Merck was used. Solvents were generally removed under reduced pressure by a rotary evaporator, products were further dried in an oil-pump vacuum at 10^{-3} mbar. Unless indicated otherwise; standard Schlenk techniques were used in the setup of the chemical reactions. Trityl alcohol **7** and the reference compound **Mono•** were synthesized according to the literature procedure.[1,2]

Trityl alcohol **7** showed an impurity with a mass that is 46.02 au heavier than the expected compound. In addition, the ^{1}H-NMR (Figure S1) spectrum of **7** shows next to the signal of the central alcohol group of **7** at 6.68 ppm an additional one at 6.65 ppm, which corresponds to the alcohol group of **A**. If the integral of the latter one is set to 1, the integral of the aromatic signals of **A** between 8 and 7.4 ppm amount to 5, and are comprised of a doublet at 7.95 ppm with an integral of 2, a triplet at 7.61 ppm

with an integral of 1, and a triplet at 7.43 ppm with an integral of 2. This pattern is indicative of a benzene group and explains the additional signal in the mass. We determined that **A** is a side product formed during the carboxylation step in the synthesis of **7**. **A** is present in all synthesized trityl compounds but constitutes less than 5% of the overall product (determined via the integral of the additional alcohol signal in the ^{1}H-NMR spectrum).

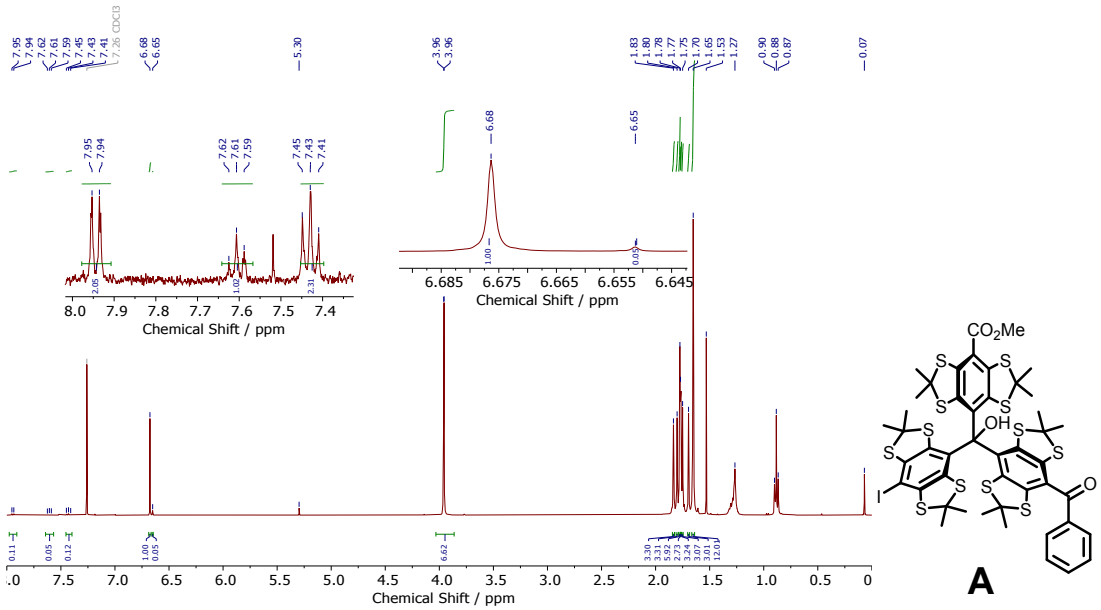

Figure S1: ^{1}H-NMR spectrum of trityl alcohol **7** and **A**. The signals belonging to **A** are of low intensity, and are shown as zoom-ins. The Lewis-structure of **A** is shown on the right.

2. Synthesis

2.1. 2,2''',5,5'''-Tetramethyl-4,4'''-bis(trimethylsilyl)-p-quaterphenyl (22)

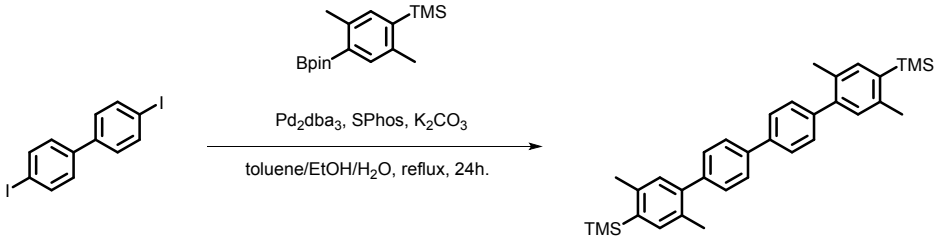

4,4'-Diiodobiphenyl (300.0 mg, 0.7389 mmol), 2-[2,5-dimethyl-4-(trimethylsilyl)phenyl]-4,4,5,5-tetramethyl-1,3,2-dioxaborolan (539.7 mg, 1.774 mmol), Pd_2dba_3 (18.7 mg, 20.4 µmol), SPhos (33.4 mg, 81.4 µmol), and K_2CO_3 (337.8 mg, 2.444 mmol) were placed in a flame-dried and argon-flushed Schlenk flask. The flask was evacuated and flushed again with argon. The solids were dissolved in degassed toluene (4.1 mL), EtOH (1.6 mL), and H_2O (2.4 mL). The reaction mixture was then stirred and refluxed for 24 hours. Afterwards, the reaction was allowed to cool to room temperature, and the phases were separated. The aqueous phase was extracted with DCM (3x20 mL). The combined organic phases were washed with water (2x20 mL) and brine (20 mL), dried over magnesium sulfate, and the solvents were removed under reduced pressure. The crude product was subjected to column chromatography on silica eluting with cyclohexane/DCM; 1:1 (v/v) (R_f = 0.18) to obtain 285.3 mg (1.563 mmol, yield: 76%) of an off-white solid.

^{1}H-NMR (500 MHz, $CDCl_3$) δ: 7.70 (d, $^3J_{H,H}$ = 8.1 Hz, 4H), 7.44 (d, $^3J_{H,H}$ = 8.1 Hz, 4H), 7.38 (s, 2H), 7.12 (s, 2H), 2.48 (s, 6H), 2.33 (s, 6H), 0.38 (s, 18H).

^{13}C-NMR (125 MHz, $CDCl_3$) δ: 142.1, 140.9, 140.9, 139.3, 137.3, 136.7, 131.5, 131.3, 129.6, 126.7, 22.4, 20.0.

HRMS (EI+, m/z, [M]+): calc. for $C_{34}H_{42}Si_2$, 506.2825; found 506.2815.

2.2. 4,4'''-Diiodo-2,2''',5,5'''-Tetramethyl-p-quaterphenyl (23)

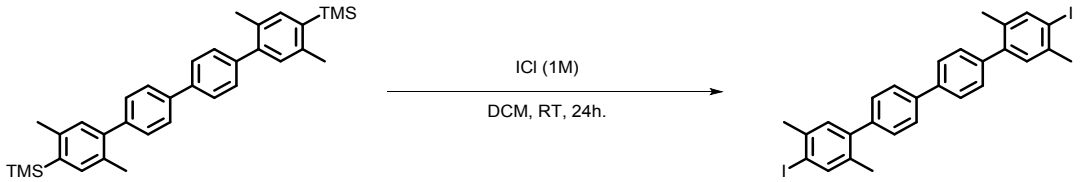

2,2''',5,5'''-Tetramethyl-4,4'''-bis(trimethylsilyl)-p-quaterphenyl (203.0 mg, 0.400 mmol) was placed in a flame-dried and argon-flushed Schlenk flask. The flask was evacuated and flushed again with argon. The solid was dissolved in DCM and a 1M solution of iodine monochloride in DCM (1.18 mL, 1.18 mmol) was added dropwise at room temperature. The reaction mixture was stirred for 24 hours at room temperature. Afterwards, the solvent was removed under reduced pressure, and the residue was redissolved in 20 mL of DCM. The organic phase was washed with water (2x20 mL) and brine (20 mL), dried over magnesium sulfate, and the solvents was removed under reduced pressure. The crude product was subjected to column chromatography on silica eluting with cyclohexane/DCM; 2:1 (v/v) (R_f = 0.58) to obtain 248.0 mg (0.4000 mmol, yield: 99%) of an off-white solid.

^{1}H-NMR (500 MHz, $CDCl_3$) δ: 7.76 (s, 2H), 7.68 (d, $^3J_{H,H}$ = 8.4 Hz, 4H), 7.39 (d, $^3J_{H,H}$ = 8.4 Hz, 4H), 7.15 (s, 2H), 2.44 (s, 6H), 2.26 (s, 6H).

^{13}C-NMR (125 MHz, $CDCl_3$) δ: 141.7, 140.6, 140.1, 139.5, 138.9, 134.9, 131.1, 129.6, 127.0, 99.9, 27.6, 19.7.

HRMS (APCI+, m/z, [M]+): calc. for $C_{28}H_{24}I_2$, 613.9962; found 613.9969.

2.3. 4,4’’’- Bis(4,4,5,5-tetramethyl-1,3,2-dioxaborolan-2-yl)-2,2''',5,5'''-tetramethyl-p-quaterphenyl (11)

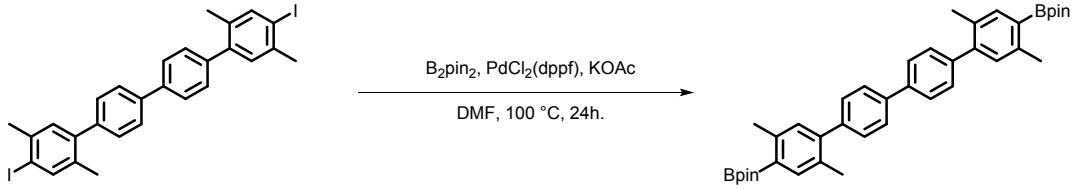

4,4’’’-Diiodo-2,2''',5,5'''-Tetramethyl-p-quaterphenyl (143.2 mg, 0.2331 mmol), B_2pin_2 (236.8 mg, 0.9325 mmol), $PdCl_2$(dppf) (34.0 mg, 46.5 µmol), and KOAc (137.3 mg, 1.399 mmol) were placed in a flame-dried and argon-flushed Schlenk flask. The flask was evacuated and flushed again with argon. The solids were then dissolved in DMF and the reaction mixture was stirred for 24 hours at 100 °C. Afterwards, the reaction was cooled to room temperature, and the mixture was diluted with 20 mL of DCM. The solution was washed with water (3x50 mL) and the solvents were then removed under reduced pressure. The crude product was subjected to column chromatography on silica eluting with cyclohexane/DCM; 1:1 (v/v) (R_f = 0.35) to obtain 57.3 mg (0.0933 mmol, yield: 40%) of an off-white solid.

^{1}H-NMR (500 MHz, $CDCl_3$) δ: 7.71 (s, 2H), 7.69 (d, $^3J_{H,H}$ = 8.4 Hz, 4H), 7.42 (d, $^3J_{H,H}$ = 8.4 Hz, 4H), 7.12 (s, 2H), 2.56 (s, 6H), 2.31 (s, 6H), 1.37 (s, 24H).

^{13}C-NMR (125 MHz, $CDCl_3$) δ: 144.0, 142.5, 141.1, 139.5, 138.2, 131.7, 131.5, 129.7, 126.8, 83.6, 25.1, 21.8, 19.9.

HRMS (EI+, m/z, [M]+): calc. for $C_{28}H_{24}I_2$, 614.3739; found 614.3734.

2.4. 2’’,3’’,5’’,6’’-Tetramethoxy-2,2’’’’,5,5’’’’-tetramethyl-1,4’’’’-bis(trimethylsilyl)-p-quinquephenyl (25)

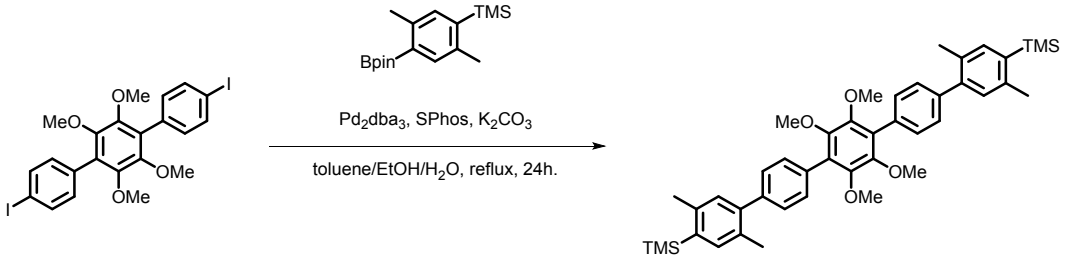

1,4-Bis(4’-iodophenyl)-2,3,5,6-tetramethoxybenzene (1000.0 mg, 1.661 mmol), 2-[2,5-dimethyl-4-(trimethylsilyl)phenyl]-4,4,5,5-tetramethyl-1,3,2-dioxaborolan (1510.0 mg, 4.962 mmol), Pd_2dba_3 (60.0 mg, 65.5 µmol), SPhos (120.0 mg, 292.3 µmol), and K_2CO_3 (920.0 mg, 6.657 mmol) were placed in a flame-dried and argon-flushed Schlenk flask. The flask was evacuated and flushed again with argon. The solids were dissolved in degassed toluene (35 mL), EtOH (15 mL), and H_2O (20 mL). The reaction mixture was then stirred and refluxed for 24 hours. Afterwards, the reaction was allowed to cool to room temperature, and the phases were separated. The aqueous phase was extracted with DCM (3x50 mL). The combined organic phases were washed with water (2x50 mL) and brine (50 mL), dried over magnesium sulfate, and the solvents were removed under reduced pressure. The crude product was subjected to column chromatography on silica eluting with cyclohexane/DCM; 1:1 (v/v) (R_f = 0.36) to obtain 843.0 mg (1.199 mmol, yield: 72%) of an off-white solid.

^{1}H-NMR (500 MHz, $CDCl_3$) δ: 7.49 (d, $^3J_{H,H}$ = 8.3 Hz, 4H), 7.43 (d, $^3J_{H,H}$ = 8.3 Hz, 4H), 7.39 (s, 2H), 7.17 (s, 2H), 3.67 (s, 12H), 2.49 (s, 6H), 2.34 (s, 6H), 0.38 (s, 18H).

^{13}C-NMR (125 MHz, $CDCl_3$) δ: 147.4, 142.6, 141.0, 140.8, 137.3, 136.8, 132.4, 131.7, 131.5, 130.2, 130.0, 128.8, 61.1, 22.6, 20.2.

HRMS (MALDI+, DCTB-Matrix, m/z, [M]+): calc. for $C_{44}H_{54}O_4Si_2$, 702.3555; found 702.3550.

2.5. 1,4’’’’-Diiodo-2’’,3’’,5’’,6’’-tetramethoxy-2,2’’’’,5,5’’’’-tetramethyl-p-quinquephenyl (26)

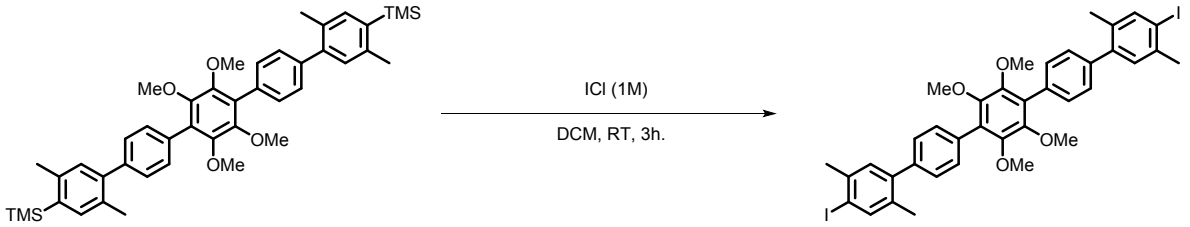

2’’,3’’,5’’,6’’-Tetramethoxy-2,2’’’’,5,5’’’’-tetramethyl-1,4’’’’-bis(trimethylsilyl)-p-quinquephenyl (750.0 mg, 1.067 mmol) was placed in a flame-dried and argon-flushed Schlenk flask. The flask was evacuated and flushed again with argon. The solid was dissolved in DCM and a 1m solution of iodine monochloride in DCM (2.668 mL, 2.668 mmol) was added dropwise at room temperature. The reaction mixture was stirred for 3 hours at room temperature. Afterwards, the solvent was removed under reduced pressure, and the residue was redissolved in 20 mL of DCM. The organic phase was washed with water (2x20 mL) and brine (20 mL), dried over magnesium sulfate, and the solvents was removed under reduced pressure. The crude product was subjected to column chromatography on silica eluting with cyclohexane/DCM; 1:1 (v/v) (R_f = 0.56) to obtain 610.0 mg (0.7526 mmol, yield: 71%) of an off-white solid.

^{1}H-NMR (500 MHz, $CDCl_3$) δ: 7.76 (s, 2H), 7.49 (d, $^3J_{H,H}$ = 8.3 Hz, 4H), 7.38 (d, $^3J_{H,H}$ = 8.3 Hz, 4H), 7.20 (s, 2H), 3.66 (s, 12H), 2.45 (s, 6H), 2.27 (s, 6H).

^{13}C-NMR (125 MHz, $CDCl_3$) δ: 147.3, 142.1, 140.5, 139.9, 138.8, 135.0, 132.7, 131.2, 130.1, 130.1, 128.7, 99.8, 61.1, 27.6, 19.7.

HRMS (MALDI+, DCTB-Matrix, m/z, [M]+): calc. for $C_{38}H_{36}I_2O_4$, 810.0698; found 810.0726.

2.6. 1,4’’’’-Bis(4,4,5,5-tetramethyl-1,3,2-dioxaborolan-2-yl)-2’’,3’’,5’’,6’’-tetramethoxy-2,2’’’’,5,5’’’’-tetramethyl-p-quinquephenyl (12)

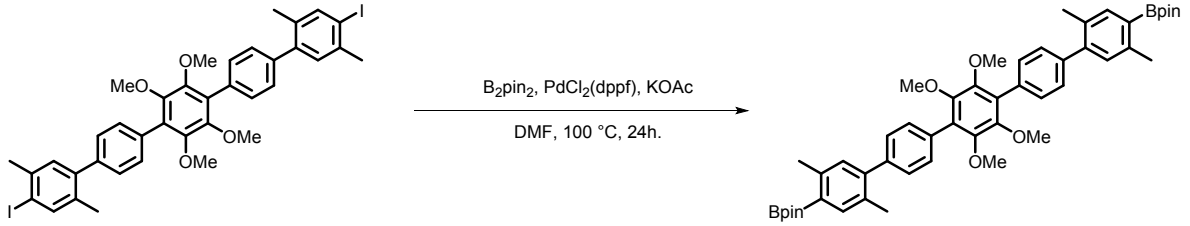

1,4’’’’-Diiodo-2’’,3’’,5’’,6’’-tetramethoxy-2,2’’’’,5,5’’’’-tetramethyl-p-quinquephenyl (351.9 mg, 0.4342 mmol), B_2pin_2 (441.5 mg, 1.739 mmol), $PdCl_2$(dppf) (65.0 mg, 0.0888 mmol), and KOAc (258.7 mg, 2.636 mmol) were placed in a flame-dried and argon-flushed Schlenk flask. The flask was evacuated and flushed again with argon. The solids were then dissolved in DMF and the reaction mixture was stirred for 24 hours at 100 °C. Afterwards, the reaction was cooled to room temperature, and the mixture was diluted with 20 mL of DCM. The solution was washed with water (3x50 mL) and the solvents were then removed under reduced pressure. The crude product was subjected to column chromatography on silica eluting with cyclohexane/DCM; 1:2 (v/v) (R_f = 0.29) to obtain 239.0 mg (0.2948 mmol, yield: 68%) of an off-white solid.

^{1}H-NMR (500 MHz, $CDCl_3$) δ: 7.71 (s, 2H), 7.50 (d, $^3J_{H,H}$ = 8.3 Hz, 4H), 7.41 (d, $^3J_{H,H}$ = 8.3 Hz, 4H), 7.17 (s, 2H), 3.67 (s, 12H), 2.57 (s, 6H), 2.33 (s, 6H), 1.38 (s, 24H).

^{13}C-NMR (125 MHz, $CDCl_3$) δ: 147.3, 144.3, 142.4, 138.1, 132.5, 131.7, 131.6, 130.1, 130.0, 128.7, 83.6, 61.1, 25.1, 21.8, 20.0.

HRMS (MALDI+, DCTB-Matrix, m/z, [M]+): calc. for $C_{50}H_{60}B_2O_8$, 810.4485; found 810.4468.

2.7. General procedure for the synthesis of bistrityl alcohols

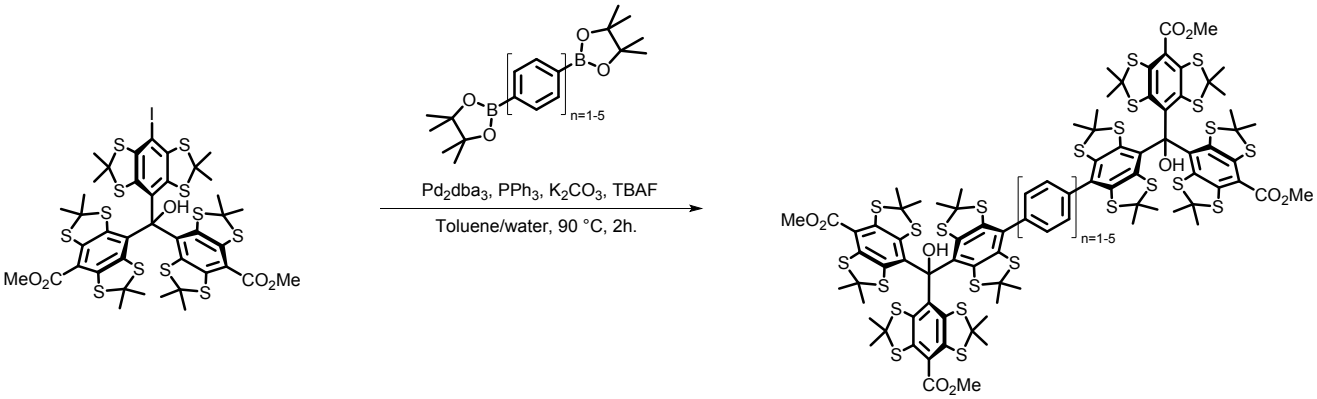

Trityl alcohol **7** (100.0 mg, 0.0887 mmol), 0.5 equivalents of the respective polyphenyl linker, Pd_2dba_3 (8.1 mg, 8.8 µmol), PPh_3 (9.3 mg, 35 µmol), and TBAF (5.0 mg, 35 µmol) were placed in a flame-dried and argon-flushed Schlenk flask. The flask was evacuated and flushed again with argon. The solids were dissolved in degassed toluene (6 mL) and a degassed 2M solution of potassium carbonate (4 mL) was added. The reaction mixture was then stirred and heated to 90 °C for 2h. Afterwards, the reaction was allowed to cool to room temperature, and the phases were separated. The aqueous phase was extracted with DCM (3x20 mL). The combined organic phases were washed with water (2x20 mL) and brine (40 mL), dried over magnesium sulfate, and the solvents were removed under reduced pressure. The crude product was subjected to column chromatography on silica eluting with n-hexane/ethyl acetate; 3:1 (v/v) to obtain the indicated amount of a yellow solid.

2.7.1. 1,4-Bis[{Bis(8-methoxycarbonyl-2,2,6,6-tetramethylbenzo-[1,2-d;4,5-d']-bis-[1,3]dithiol-4-yl)-(8-yl-2,2,6,6-tetramethylbenzo-[1,2-d;4,5-d']-bis-[1,3]dithiol-4-yl)}-methanol]-benzene (14)
Linker: 1,4-Bis(4,4,5,5-tetramethyl-1,3,2-dioxaborolan-2-yl)-benzene (14.6 mg, 0.0442 mmol).

Yield: 76.5 mg (0.0368 mmol, 83%) (R_f=0.36).

^{1}H-NMR (500 MHz, $CDCl_3$) δ: 7.53-7.50 (m, 2H), 7.32 (br. s, 2H), 7.76 (s, 2H), 3.97 (s, 12H), 1.83 (s, 6H), 1.81 (s, 6H), 1.80 (s, 12H), 1.78 (s, 6H), 1.72 (s, 18H), 1.68 (s, 6H), 1.67 (s, 6H), 1.67 (s, 6H), 1.62 (s, 6H).

^{13}C-NMR (125 MHz, $CDCl_3$) δ: 166.8, 166.8, 142.1, 142.1, 141.8, 141.6, 140.9, 140.9, 140.5, 139.5, 139.3, 139.3, 139.3, 138.9, 138.7, 135.1, 135.0, 134.9, 133.0, 129.6, 121.1, 84.3, 62.5, 62.1, 61.7, 61.7, 61.5, 61.4, 60.9, 60.8, 52.5, 52.5, 34.9, 34.7, 33.9, 33.4, 31.6, 30.9, 30.9, 30.4, 30.4, 30.3, 29.8, 29.8, 29.4, 28.3, 28.2, 27.7.

HRMS (MALDI+, DCTB-matrix, m/z, $[M]^+$): calc. for $C_{88}H_{90}O_{10}S_{24}$, 2073.9826; found 2073.9854.

2.7.2. 4,4'-Bis[{Bis(8-methoxycarbonyl-2,2,6,6-tetramethylbenzo-[1,2-d;4,5-d']-bis-[1,3]dithiol-4-yl)-(8-yl-2,2,6,6-tetramethylbenzo-[1,2-d;4,5-d']-bis-[1,3]dithiol-4-yl)}-methanol]-biphenyl (15)
Linker: 1,4'-Bis(4,4,5,5-tetramethyl-1,3,2-dioxaborolan-2-yl)-biphenyl (18.0 mg, 0.0443 mmol).

Yield: 59.2 mg (0.0275 mmol, 63%) (R_f=0.36).

^{1}H-NMR (700 MHz, $CDCl_3$) δ: 7.77-7.69 (m, 4H), 7.52 (s, 2H), 7.34 (s, 2H), 6.77 (s, 2H), 3.97 (s, 12H), 1.84 (s, 6H), 1.83 (s, 6H), 1.81 (s, 6H), 1.80 (s, 6H), 1.78 (s, 6H), 1.75 (s, 6H), 1.73 (s, 6H), 1.71 (s, 6H), 1.69 (s, 6H), 1.68 (s, 6H), 1.67 (s, 6H), 1.62 (s, 6H).

^{13}C-NMR (176 MHz, $CDCl_3$) δ: 166.8, 166.8, 142.1, 142.1, 141.9, 141.5, 140.9, 140.7, 140.5, 140.3, 139.6, 139.2, 138.9, 138.7, 138.0, 135.1, 134.9, 133.1, 129.5, 129.2, 129.0, 128.5, 127.4, 121.1, 121.1, 115.8, 84.3, 62.6, 62.1, 61.7, 61.6, 60.9, 60.7, 52.5, 52.5, 35.0, 34.7, 34.1, 33.4, 31.5, 30.9, 30.4, 29.9, 29.8, 29.5, 28.2, 28.0, 27.7.

HRMS (MALDI+, DCTB-matrix, m/z, $[M]^+$): calc. for $C_{94}H_{94}O_{10}S_{24}$, 2150.0139; found 2150.0149.

2.7.3. 4,4''-Bis[{Bis(8-methoxycarbonyl-2,2,6,6-tetramethylbenzo-[1,2-d;4,5-d']-bis-[1,3]dithiol-4-yl)-(8-yl-2,2,6,6-tetramethylbenzo-[1,2-d;4,5-d']-bis-[1,3]dithiol-4-yl)}-methanol]-p-terphenyl (16)
Linker: 1,4''-Bis(4,4,5,5-tetramethyl-1,3,2-dioxaborolan-2-yl)-p-terphenyl (21.4 mg, 0.0444 mmol).

Yield: 26.6 mg (0.0119 mmol, 27%) (R_f=0.38).

^{1}H-NMR (500 MHz, $CDCl_3$) δ: 7.79-7.65 (m, 8H), 7.52 (s, 2H), 7.35 (s, 2H), 6.76 (s, 2H), 3.97 (s, 12H), 1.85 (s, 6H), 1.84 (s, 6H), 1.82 (s, 6H), 1.80 (s, 6H), 1.79 (s, 6H), 1.75 (s, 6H), 1.74 (s, 6H), 1.72 (s, 6H), 1.69 (s, 6H), 1.68 (s, 6H), 1.67 (s, 6H), 1.62 (s, 6H).

^{13}C-NMR (125 MHz, $CDCl_3$) δ: 166.8, 166.8, 142.1, 142.1, 141.9, 141.5, 140.9, 140.7, 140.5, 140.3, 139.8, 139.6, 139.3, 139.3, 138.9, 138.7, 138.0, 135.1, 134.9, 133.1, 129.5, 129.1, 127.6, 127.3, 121.1, 121.1, 84.4, 62.6, 62.1, 61.7, 61.6, 61.0, 60.7, 52.5, 52.5, 35.0, 34.7, 34.1, 33.4, 31.5, 30.9, 30.4, 30.4, 29.9, 29.8, 29.5, 28.3, 28.0, 27.7.

HRMS (ESI+, m/z, $[M+Na]^+$): calc. for $C_{100}H_{98}O_{10}S_{24}$, 2249.0349; found 2249.0335.

2.7.4. 4,4'''-Bis[{Bis(8-methoxycarbonyl-2,2,6,6-tetramethylbenzo-[1,2-d;4,5-d']-bis-[1,3]dithiol-4-yl)-(8-yl-2,2,6,6-tetramethylbenzo-[1,2-d;4,5-d']-bis-[1,3]dithiol-4-yl)}-methanol]-2,2''',5,5'''-tetramethyl-p-quaterphenyl (17)
Linker: 4,4'''- Bis(4,4,5,5-tetramethyl-1,3,2-dioxaborolan-2-yl)-2,2''',5,5'''-tetramethyl-p-quaterphenyl (27.2 mg, 0.0443 mmol).

Yield: 73.4 mg (0.0311 mmol, 70%) (R_f=0.37).

^{1}H-NMR (700 MHz, $CDCl_3$) δ: 7.72 (d, $^3J_{H,H}$ = 8.2 Hz, 4H), 7.49 (d, $^3J_{H,H}$ = 8.2 Hz, 4H), 7.25 (s, 2H), 7.00 (s, 2H), 6.79 (s, 2H), 3.98 (s, 6H), 3.97 (s, 6H), 2.31 (s, 6H), 2.30 (s, 6H), 1.86 (s, 6H), 1.84 (s, 12H), 1.82-1.81 (m, 6H), 1.80-1.80 (m, 6H), 1.78-1.78 (m, 6H), 1.72-1.71 (m, 6H), 1.69 (s, 6H), 1.68 (s, 6H), 1.67 (s, 12H), 1.62 (s, 6H).

^{13}C-NMR (125 MHz, $CDCl_3$) δ:166.7, 166.6, 142.1, 142.1, 141.9, 141.7, 141.3, 140.7, 140.6, 140.4, 140.0, 139.3, 139.1, 138.9, 138.8, 138.2, 137.9, 135.3, 134.9, 133.2, 132.0, 131.8, 130.9, 130.3, 129.9, 129.8, 128.9, 126.6, 126.6, 121.0, 84.1, 84.1, 62.6, 62.5, 61.8, 61.7, 61.6, 60.8, 60.8, 60.8, 52.4, 52.4, 35.3, 35.3, 34.8, 33.0, 31.0, 30.3, 30.2, 30.0, 29.7, 29.6, 29.6, 28.5, 27.7, 27.3, 27.0, 26.9, 20.5, 20.1, 19.2, 18.5.

HRMS (ESI+, m/z, $[M]^+$): calc. for $C_{110}H_{110}O_{10}S_{24}$, 2360.1396; found 2360.1326.

2.7.5. 4,4''''-Bis[{Bis(8-methoxycarbonyl-2,2,6,6-tetramethylbenzo-[1,2-d;4,5-d']-bis-[1,3]dithiol-4-yl)-(8-yl-2,2,6,6-tetramethylbenzo-[1,2-d;4,5-d']-bis-[1,3]dithiol-4-yl)}-methanol]-2,2''',5,5'''-tetramethyl-2'',3'',5'',6''-tetramethoxy-2,2'''',5,5''''-tetramethyl-p-quinquephenyl (18)
Linker: 1,4''''-Bis(4,4,5,5-tetramethyl-1,3,2-dioxaborolan-2-yl)-2'',3'',5'',6''-tetramethoxy-2,2'''',5,5''''-tetramethyl-p-quinquephenyl (36.0 mg, 0.0444 mmol).

Yield: 102.0 mg (0.0399 mmol, 90%) (R_f=0.47).

^{1}H-NMR (500 MHz, $CDCl_3$) δ: 7.51 (d, $^3J_{H,H}$ = 8.5 Hz, 4H), 7.49 (d, $^3J_{H,H}$ = 8.5 Hz, 4H), 7.30 (s, 2H), 7.01 (s, 2H), 6.77 (s, 2H), 3.98 (s, 6H), 3.97 (s, 6H), 3.66 (s, 12H), 2.33 (s, 6H), 2.31 (s, 6H), 1.86 (s, 6H), 1.85 (s, 6H), 1.84 (s, 6H), 1.81 (s, 6H), 1.80 (s, 6H), 1.78 (s, 6H), 1.71 (s, 6H), 1.70 (s, 6H), 1.69 (s, 6H), 1.68 (s, 12H), 1.63 (s, 6H).

^{13}C-NMR (125 MHz, $CDCl_3$) δ: 166.8, 166.8, 166.8, 147.4, 142.2, 142.2, 142.1, 142.0, 141.4, 140.8, 140.6, 140.5, 140.1, 139.4, 139.1, 139.0, 138.4, 138.1, 135.5, 135.1, 133.4, 132.4, 132.2, 132.0, 131.0, 130.4, 130.2, 130.0, 129.0, 121.2, 84.3, 62.7, 61.9, 61.8, 61.1, 61.0, 60.9, 52.5, 52.5, 35.4, 35.0, 33.2, 31.3, 30.9, 30.4, 30.1, 29.7, 28.7, 27.9, 27.4, 27.2, 20.3, 19.3.

HRMS (MALDI+, DCTB-Matrix, m/z, $[M]^+$): calc. for $C_{120}H_{122}O_{14}S_{24}$, 2554.2126; found 2554.2141.

2.7.6. 1,4-Bis[{Bis(8-methoxycarbonyl-2,2,6,6-tetramethylbenzo-[1,2-d;4,5-d']-bis-[1,3]dithiol-4-yl)-(8-yl-2,2,6,6-tetramethylbenzo-[1,2-d;4,5-d']-bis-[1,3]dithiol-4-yl)}-methanol]-*p*-xylene (19)

Linker: 1,4-Bis(4,4,5,5-tetramethyl-1,3,2-dioxaborolan-2-yl)-2,5-dimethylbenzene (15.9 mg, 0.0443 mmol).

Yield: 71.5 mg (0.0340 mmol, 77%) (R_f=0.42).

^{1}H-NMR (500 MHz, $CDCl_3$) δ: 7.08-6.81 (m, 2H), 6.78-6.68 (m, 2H), 3.99-3.95 (m, 12H), 2.33-2.06 (m, 6H), 1.88-1.57 (m, 72H).

^{13}C-NMR (125 MHz, $CDCl_3$) δ: 166.8, 166.8, 166.8, 142.1, 142.1, 142.1, 142.1, 141.9, 141.9, 141.5, 141.5, 140.9, 140.9, 140.5, 140.5, 140.4, 140.0, 139.9, 139.2, 139.2, 139.0, 139.0, 138.9, 138.8, 138.2, 138.1, 138.0, 135.4, 135.4, 135.2, 135.2, 132.2, 131.8, 130.3, 128.9, 128.8, 121.1, 121.1, 84.3, 84.3, 62.6, 62.5, 62.1, 62.0, 61.8, 61.6, 61.5, 61.5, 61.0, 60.9, 60.9, 52.6, 52.6, 35.6, 35.5, 35.4, 35.1, 34.9, 33.0, 33.0, 31.5, 31.5, 31.1, 30.3, 30.1, 30.0, 29.9, 29.9, 29.8, 29.8, 27.9, 27.7, 27.5, 27.4, 27.1, 27.1, 27.1, 27.1, 19.5, 19.3, 15.4.

HRMS (MALDI+, DCTB-Matrix, m/z, $[M]^+$): calc. for $C_{90}H_{94}O_{10}S_{24}$, 2104.0135; found 2104.0065.

2.8. General procedure for radical generation

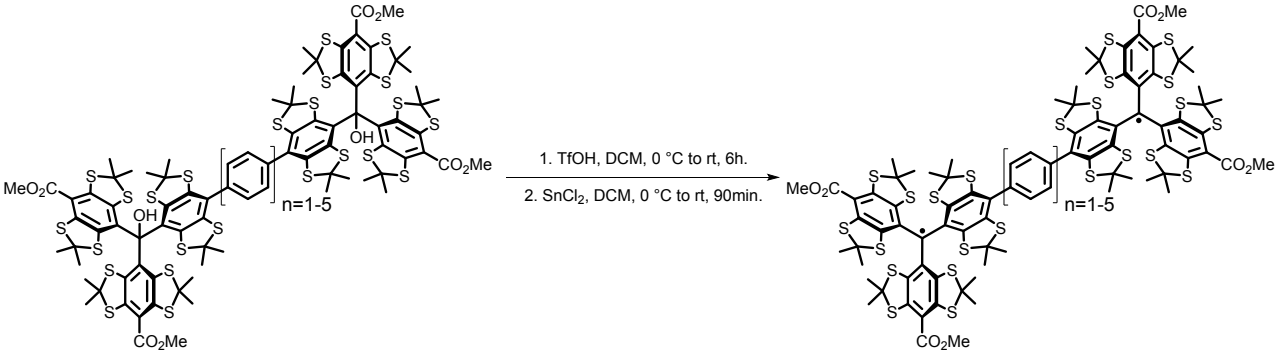

1 equivalent of the respective trityl bisalcohol was placed in a flame-dried and argon-flushed Schlenk flask. The flask was evacuated and flushed again with argon. The solid was then dissolved in DCM and cooled to 0 °C using an ice-bath and triflic acid (4 eq.) was added. The reaction mixture was allowed to reach room temperature and was stirred for 6 hours. It was then cooled to 0 °C again and tin(II)chloride (2 eq.) dissolved in a minimal amount of THF was added. The reaction was again allowed to reach room temperature and was stirred for an additional 90min. Afterwards, the reaction mixture was washed with water (3x10 mL) and brine (10 mL). The organic solution was dried over magnesium sulfate and the solvent was removed under reduced pressure. The crude product was subjected to column chromatography on silica eluting with cyclohexane/ethyl acetate; 3:1 (v/v) to obtain the indicated amount of a green solid.

2.8.1. 1,4-Bis[{Bis(8-methoxycarbonyl-2,2,6,6-tetramethylbenzo-[1,2-d;4,5-d']-bis-[1,3]dithiol-4-yl)-(8-yl-2,2,6,6-tetramethylbenzo-[1,2-d;4,5-d']-bis-[1,3]dithiol-4-yl)}-methyl radical]-benzene (1$^{\bullet\bullet}$)

Substrate: 1,4-Bis[{Bis(8-methoxycarbonyl-2,2,6,6-tetramethylbenzo-[1,2-d;4,5-d']-bis-[1,3]dithiol-4-yl)-(8-yl-2,2,6,6-tetramethylbenzo-[1,2-d;4,5-d']-bis-[1,3]dithiol-4-yl)}-methanol]-benzene (48.2 mg, 0.0232 mmol).

Yield: 25.8 mg (0.0126 mmol, 54%) (R_f=0.32).

HRMS (MALDI+, DCTB-Matrix, m/z, $[M]^+$): calc. for $C_{88}H_{88}O_8S_{24}$, 2041.9766; found 2041.9669.

2.8.2. 4,4'-Bis[{Bis(8-methoxycarbonyl-2,2,6,6-tetramethylbenzo-[1,2-d;4,5-d']-bis-[1,3]dithiol-4-yl)-(8-yl-2,2,6,6-tetramethylbenzo-[1,2-d;4,5-d']-bis-[1,3]dithiol-4-yl)}-methyl radical]-biphenyl (2••)

Substrate: 4,4'-Bis[{Bis(8-methoxycarbonyl-2,2,6,6-tetramethylbenzo-[1,2-d;4,5-d']-bis-[1,3]dithiol-4-yl)-(8-yl-2,2,6,6-tetramethylbenzo-[1,2-d;4,5-d']-bis-[1,3]dithiol-4-yl)}-methanol]-biphenyl (57.0 mg, 0.0265 mmol)

Yield: 40.0 mg (0.0190 mmol, 71%) (R_f=0.32).

HRMS (ESI+, m/z, $[M]^+$): calc. for $C_{94}H_{92}O_8S_{24}$, 2119.0160; found 2119.0029.

2.8.3. 4,4''-Bis[{Bis(8-methoxycarbonyl-2,2,6,6-tetramethylbenzo-[1,2-d;4,5-d']-bis-[1,3]dithiol-4-yl)-(8-yl-2,2,6,6-tetramethylbenzo-[1,2-d;4,5-d']-bis-[1,3]dithiol-4-yl)}-methyl radical]-*p*-terphenyl (3••)

Substrate: 4,4''-Bis[{Bis(8-methoxycarbonyl-2,2,6,6-tetramethylbenzo-[1,2-d;4,5-d']-bis-[1,3]dithiol-4-yl)-(8-yl-2,2,6,6-tetramethylbenzo-[1,2-d;4,5-d']-bis-[1,3]dithiol-4-yl)}-methanol]-p-terphenyl (26.6 mg, 0.0119 mmol)

Yield: 18.5 mg (0.0084 mmol, 71%) (R_f=0.32).

HRMS (MALDI+, DCTB-Matrix, m/z, $[M]^+$): calc. for $C_{100}H_{96}O_8S_{24}$, 2194.0397; found 2194.0334.

2.8.4. 4,4'''-Bis[{Bis(8-methoxycarbonyl-2,2,6,6-tetramethylbenzo-[1,2-d;4,5-d']-bis-[1,3]dithiol-4-yl)-(8-yl-2,2,6,6-tetramethylbenzo-[1,2-d;4,5-d']-bis-[1,3]dithiol-4-yl)}-methyl radical]-2,2''',5,5'''-tetramethyl-*p*-quaterphenyl (4••)

Substrate: 4,4'''-Bis[{Bis(8-methoxycarbonyl-2,2,6,6-tetramethylbenzo-[1,2-d;4,5-d']-bis-[1,3]dithiol-4-yl)-(8-yl-2,2,6,6-tetramethylbenzo-[1,2-d;4,5-d']-bis-[1,3]dithiol-4-yl)}-methanol]-2,2''',5,5'''-tetramethyl- p-quaterphenyl (40.0 mg, 0.0169 mmol)

Yield: 28.1 mg (0.0121 mmol, 72%) (R_f=0.38).

HRMS (MALDI+, DCTB-Matrix, m/z, $[M]^+$): calc. for $C_{110}H_{108}O_8S_{24}$, 2326.1341; found 2326.1351.

2.8.5. 4,4''''-Bis[{Bis(8-methoxycarbonyl-2,2,6,6-tetramethylbenzo-[1,2-d;4,5-d']-bis-[1,3]dithiol-4-yl)-(8-yl-2,2,6,6-tetramethylbenzo-[1,2-d;4,5-d']-bis-[1,3]dithiol-4-yl)}-methanol]-2,2''',5,5'''-tetramethyl-2'',3'',5'',6''-tetramethoxy-2,2'''',5,5''''-tetramethyl-*p*-quinquephenyl (5••)

Substrate: 4,4''''-Bis[{Bis(8-methoxycarbonyl-2,2,6,6-tetramethylbenzo-[1,2-d;4,5-d']-bis-[1,3]dithiol-4-yl)-(8-yl-2,2,6,6-tetramethylbenzo-[1,2-d;4,5-d']-bis-[1,3]dithiol-4-yl)}-methanol]-2,2''',5,5'''-tetramethyl-2'',3'',5'',6''-tetramethoxy-2,2'''',5,5''''-tetramethyl-p-quinquephenyl (50.0 mg, 0.0195 mmol)

Yield: 46.7 mg (0.0185 mmol, 95%) (R_f=0.38).

HRMS (MALDI+, DCTB-Matrix, m/z, $[M]^+$): calc. for $C_{120}H_{120}O_{12}S_{24}$, 2522.2081; found 2522.2068.

2.8.6. 1,4-Bis[{Bis(8-methoxycarbonyl-2,2,6,6-tetramethylbenzo-[1,2-d;4,5-d']-bis-[1,3]dithiol-4-yl)-(8-yl-2,2,6,6-tetramethylbenzo-[1,2-d;4,5-d']-bis-[1,3]dithiol-4-yl)}-methyl radical]-*p*-benzene (6••)

Substrate: 1,4-Bis[{Bis(8-methoxycarbonyl-2,2,6,6-tetramethylbenzo-[1,2-d;4,5-d']-bis-[1,3]dithiol-4-yl)-(8-yl-2,2,6,6-tetramethylbenzo-[1,2-d;4,5-d']-bis-[1,3]dithiol-4-yl)}-methanol]-*p*-xylene (40.0 mg, 0.0190 mmol).

Yield: 28.5 mg (0.0138 mmol, 73%) (R_f=0.37).

HRMS (MALDI+, DCTB-Matrix, m/z, $[M]^+$): calc. for $C_{90}H_{92}O_8S_{24}$, 2070.0080; found 2070.0034.

3. Analytical Data

3.1. NMR-Spectra

3.1.1. 2,2''',5,5'''-Tetramethyl-4,4'''-bis(trimethylsilyl)-p-quaterphenyl

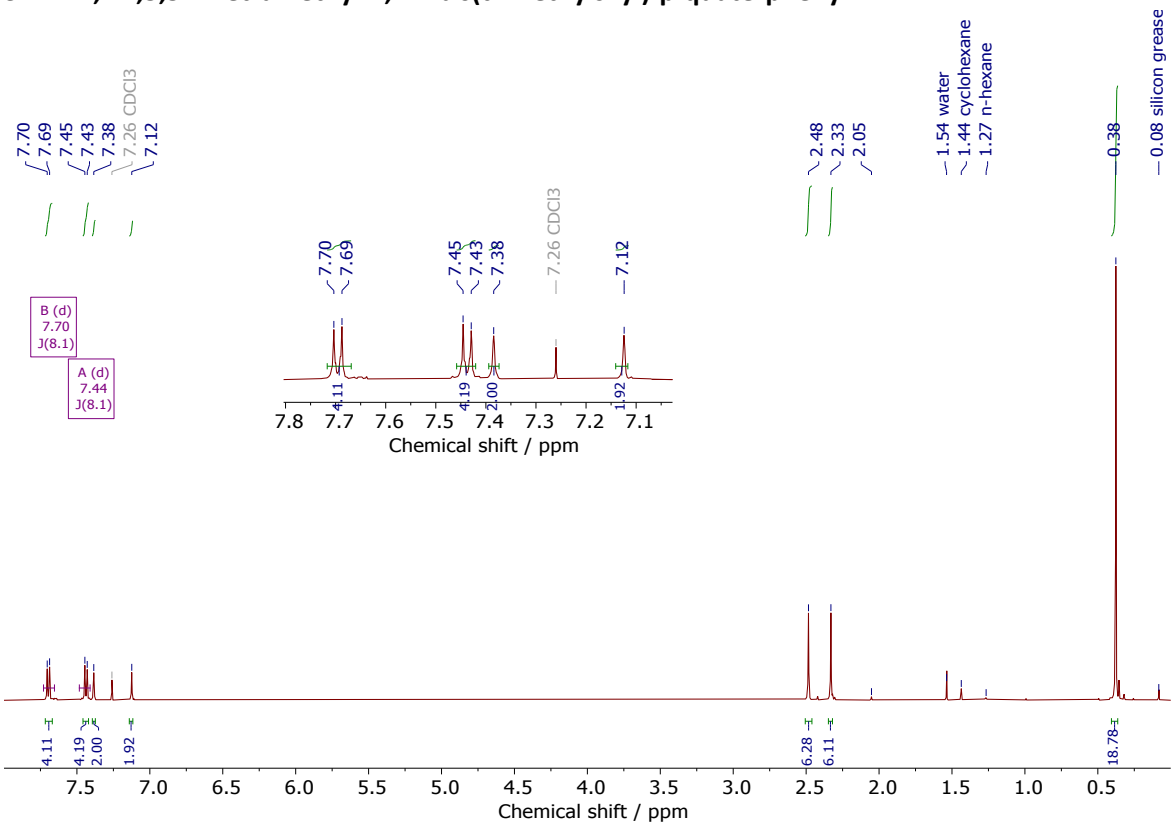

Figure S2: ^{1}H-NMR, 500 MHz, $CDCl_3$.

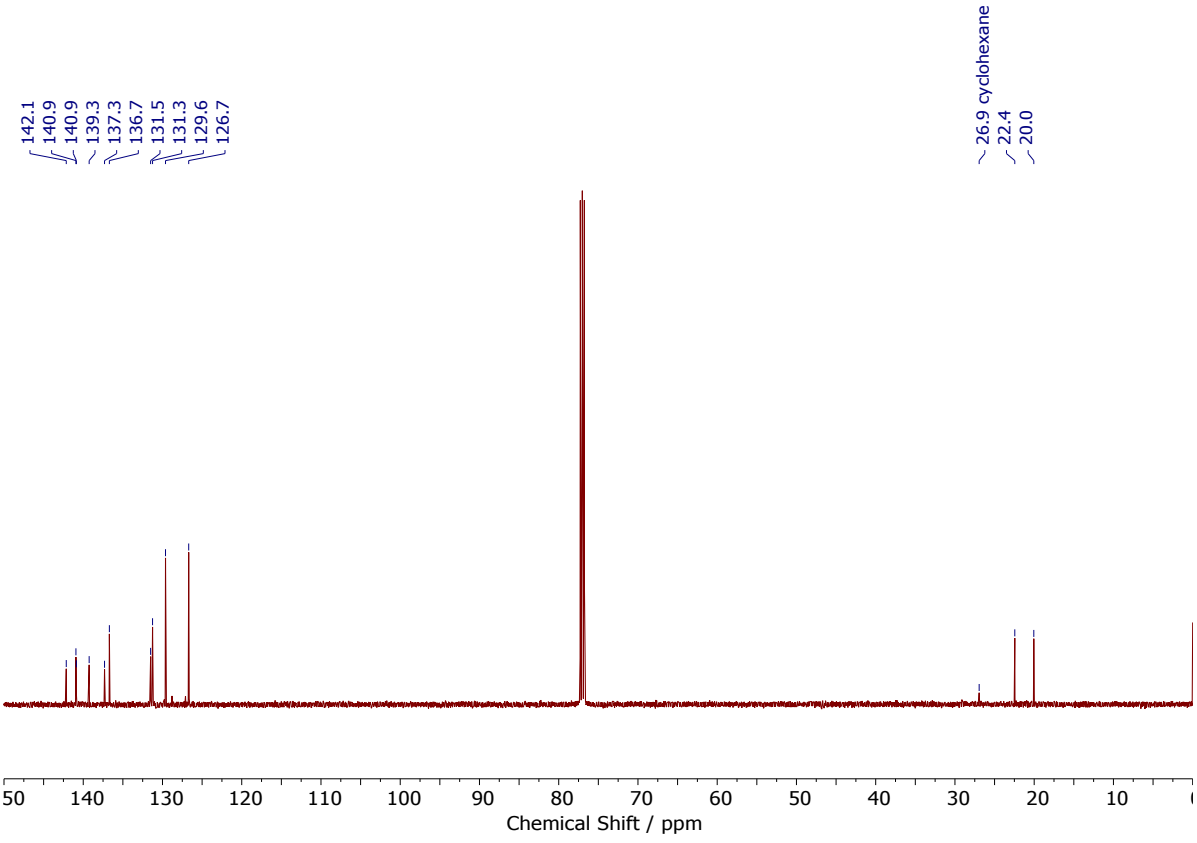

Figure S3: $^{13}C\{^{1}H\}$-NMR, 125 MHz, $CDCl_3$.

3.1.2. 4,4’’’-Diiodo-2,2’’’,5,5’’’-Tetramethyl-p-quaterphenyl

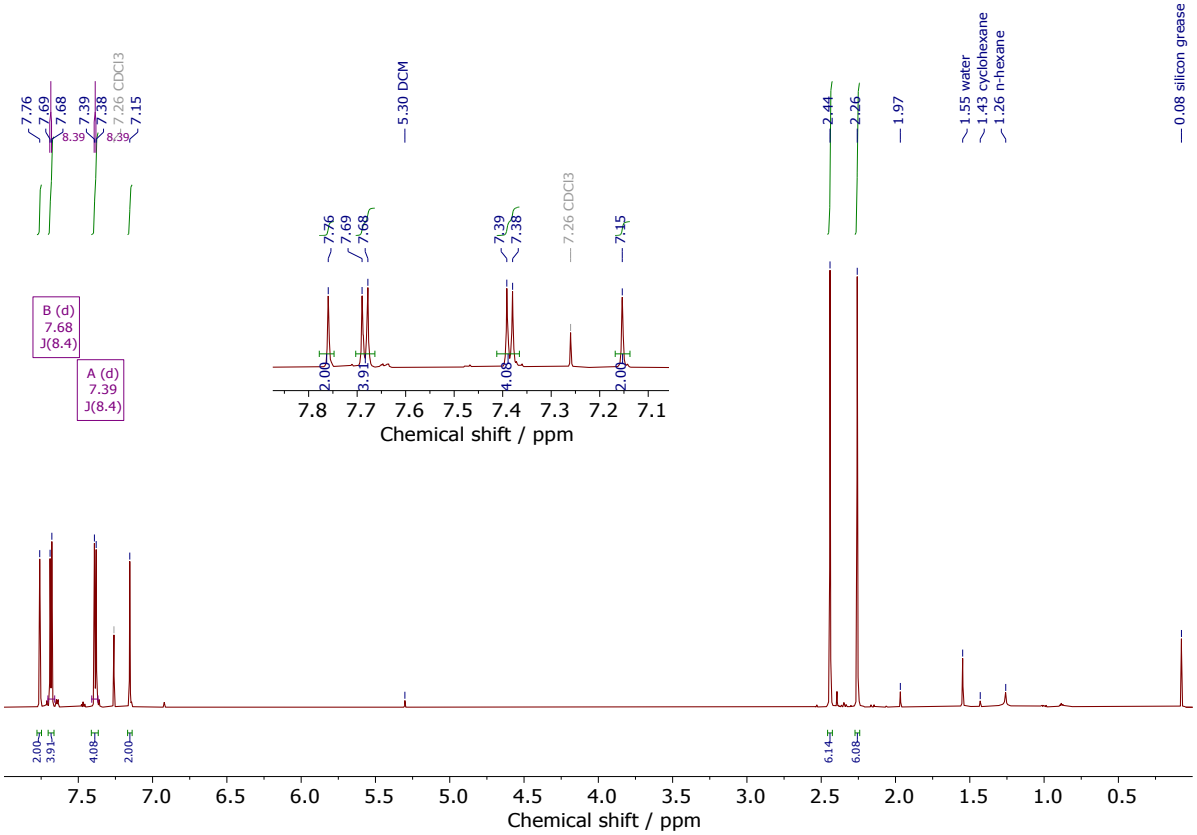

Figure S4: ^{1}H-NMR, 700 MHz, $CDCl_3$.

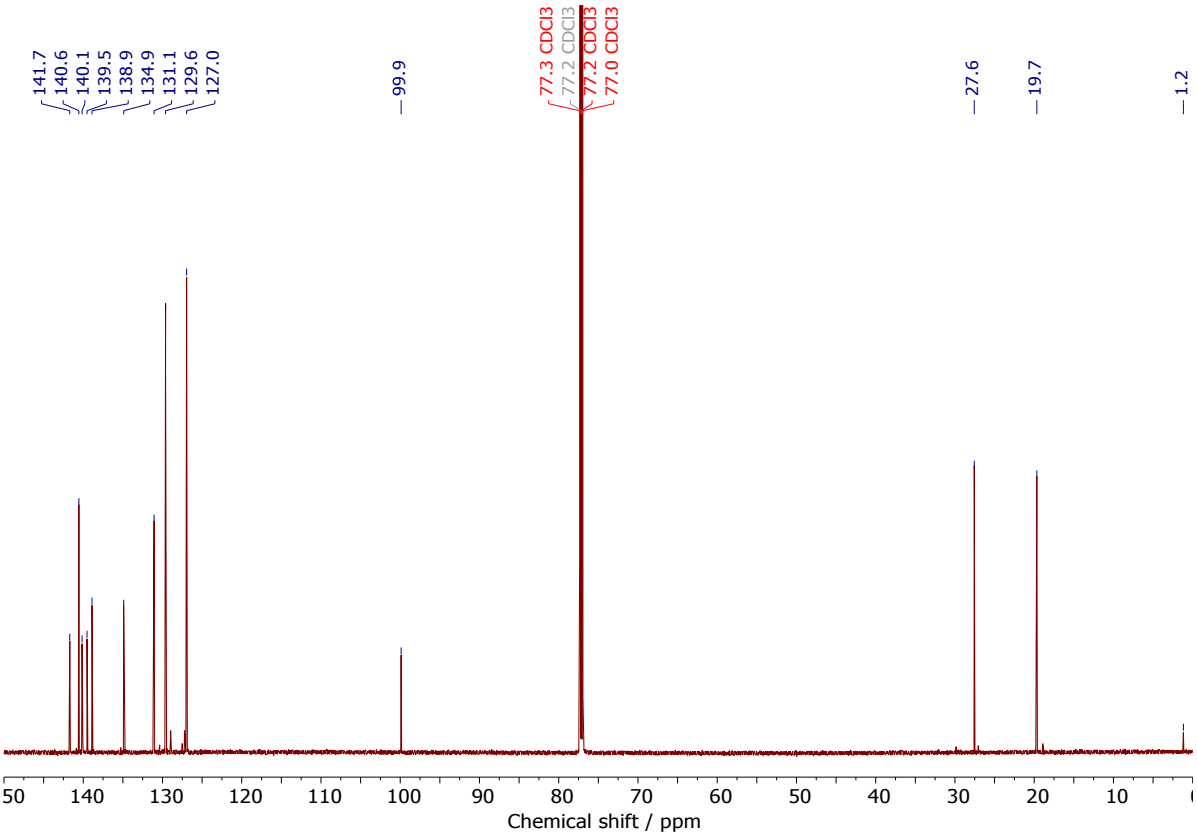

Figure S5: $^{13}C\{^{1}H\}$-NMR, 175 MHz, $CDCl_3$.

3.1.3. 4,4’’’-Bis(4,4,5,5-tetramethyl-1,3,2-dioxaborolan-2-yl)-2,2''',5,5'''-tetramethyl-p-quaterphenyl

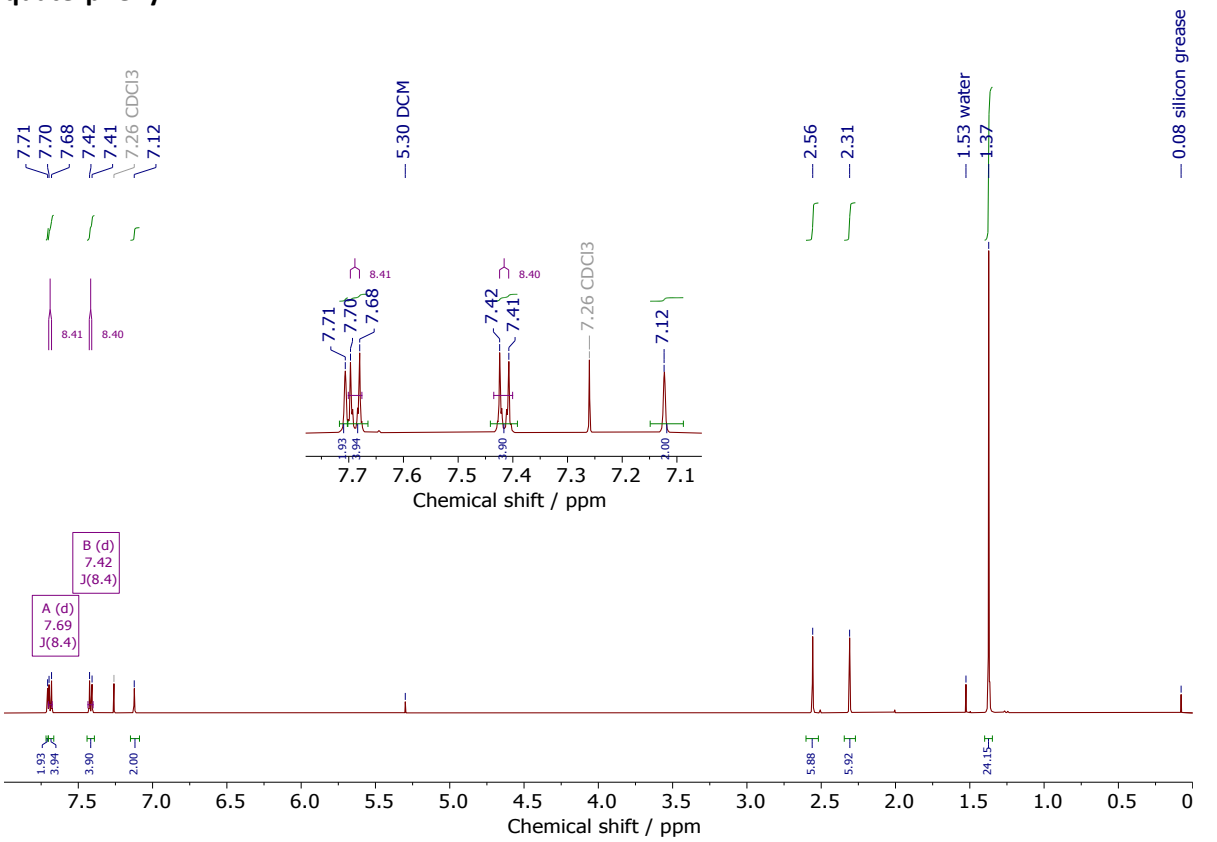

Figure S6: ^{1}H-NMR, 500 MHz, $CDCl_3$.

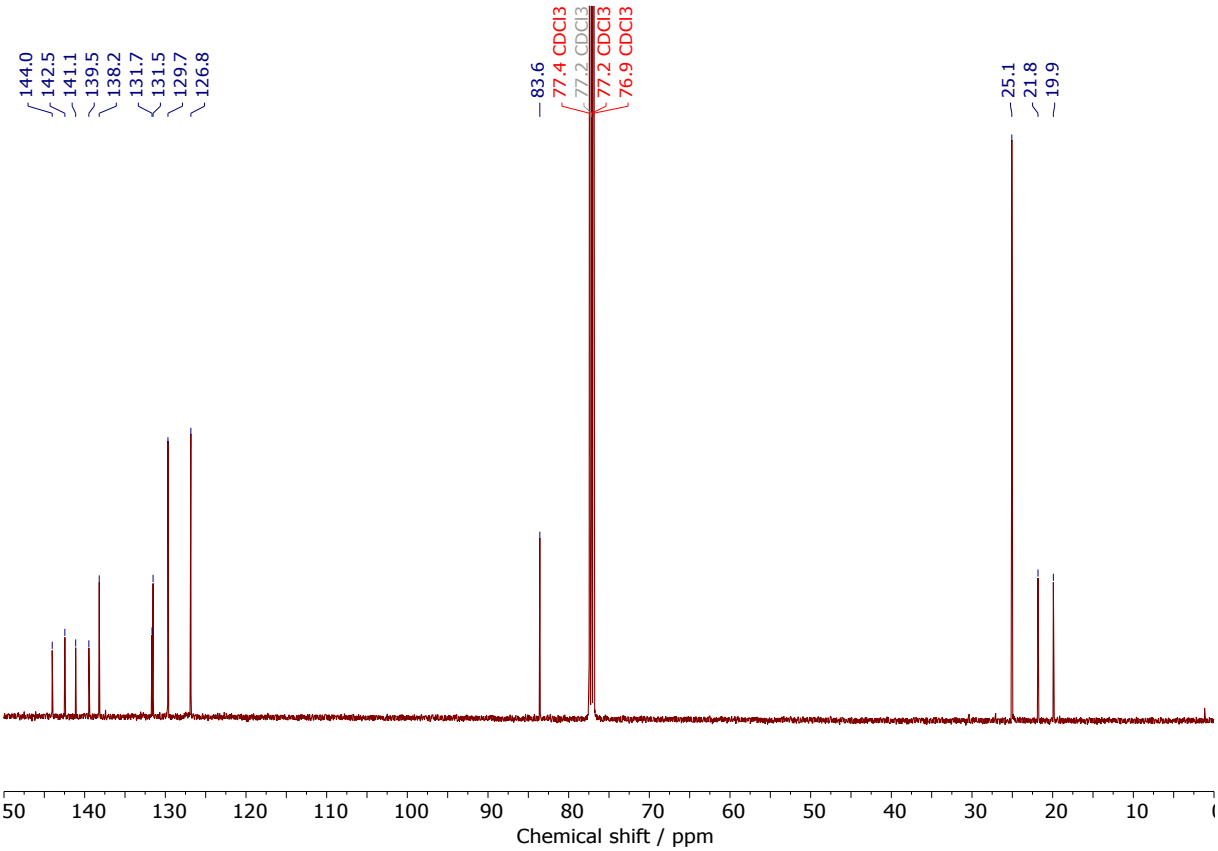

Figure S7: $^{13}C\{^{1}H\}$-NMR, 125 MHz, $CDCl_3$.

3.1.4. 2'',3'',5'',6''-Tetramethoxy-2,2'''',5,5''''-tetramethyl-1,4''''-bis(trimethylsilyl)-p-quinquephenyl

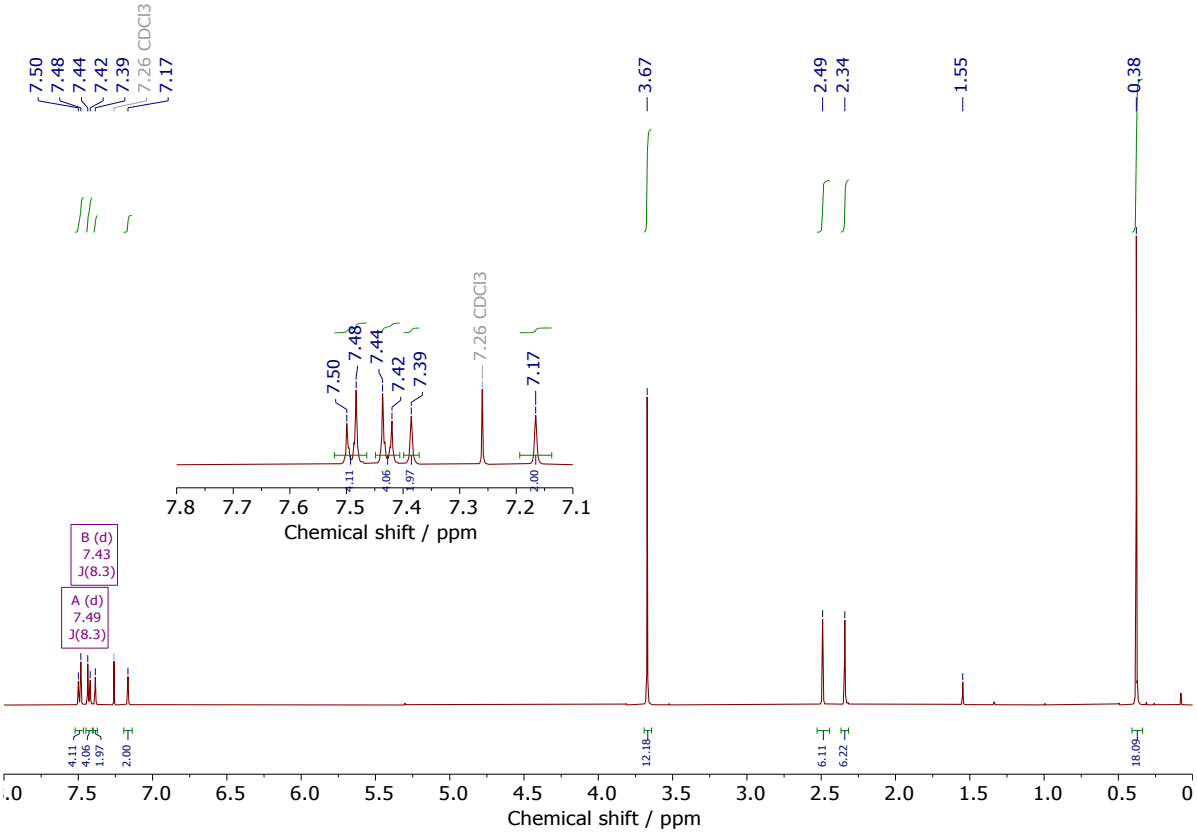

Figure S8: ^{1}H-NMR, 500 MHz, $CDCl_3$.

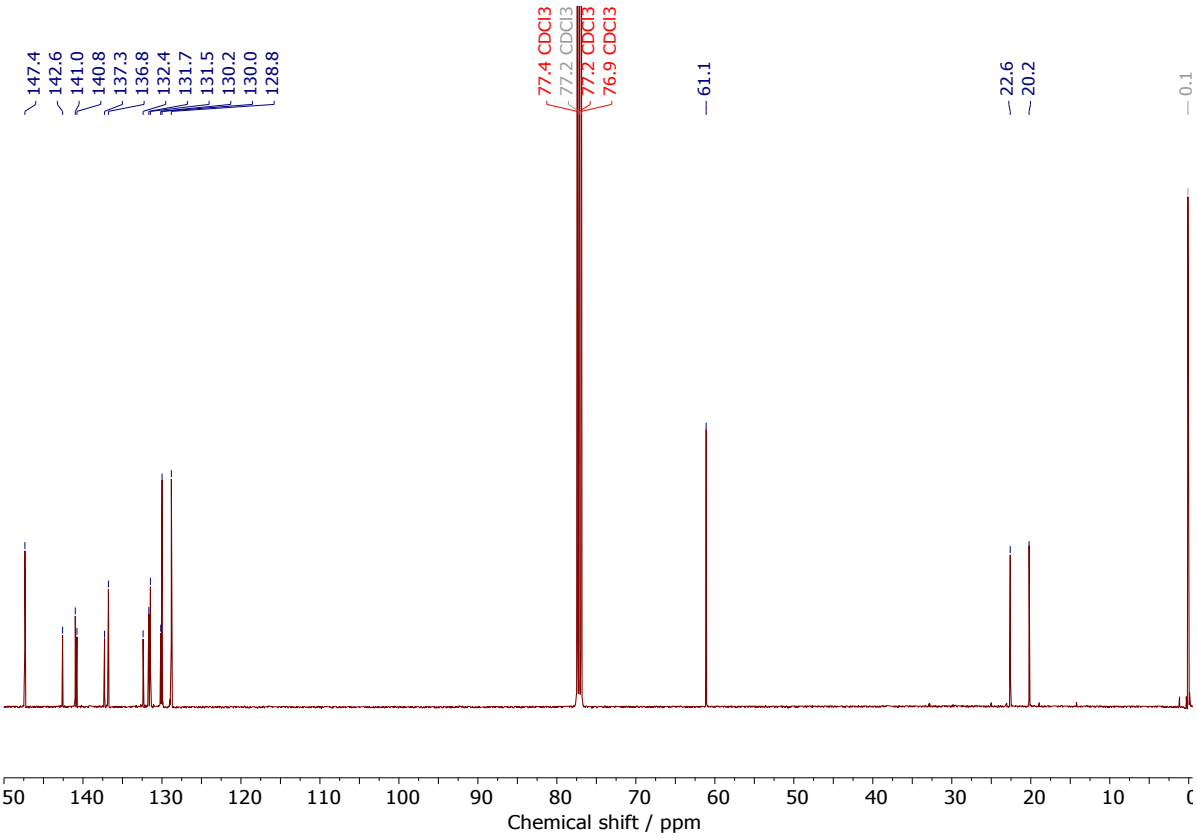

Figure S9: $^{13}C\{^{1}H\}$-NMR, 125 MHz, $CDCl_3$.

3.1.5. 1,4’’’’-Diiodo-2’’,3’’,5’’,6’’-tetramethoxy-2,2’’’’,5,5’’’’-tetramethyl-p-quinquephenyl

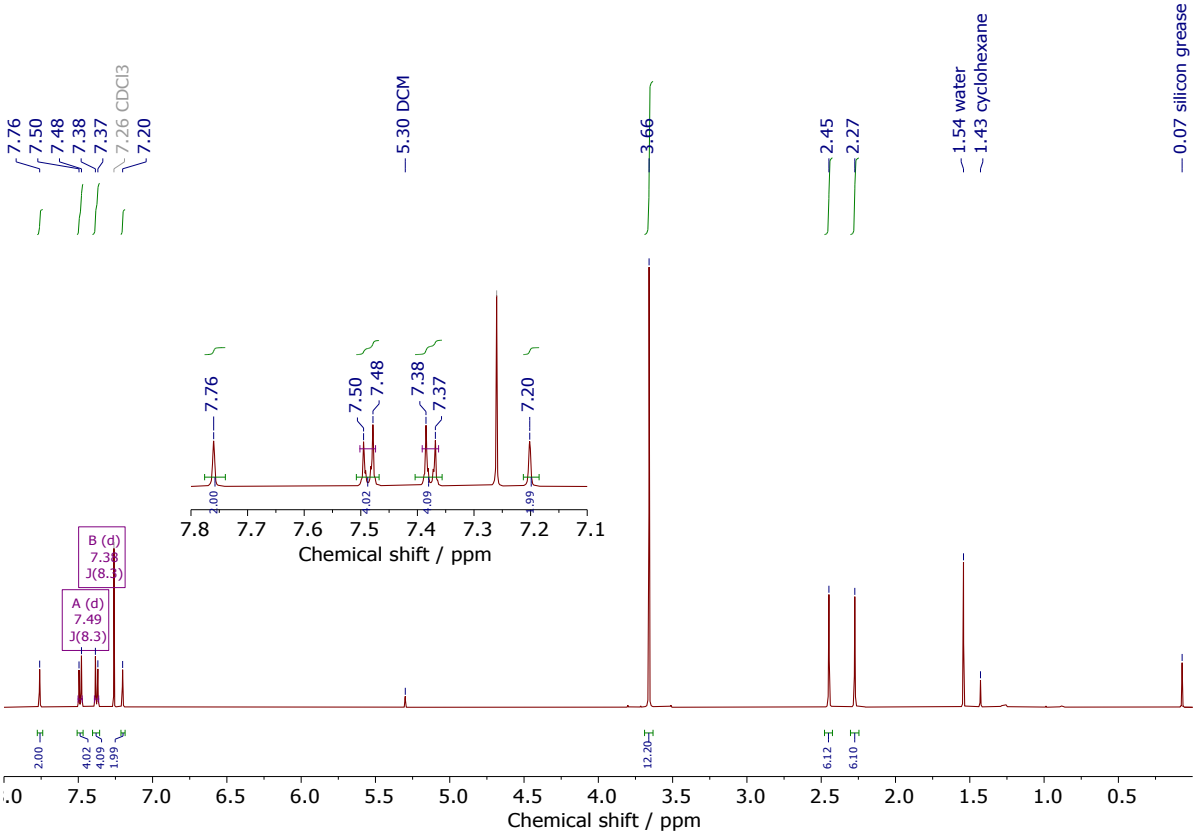

Figure S10: ^{1}H-NMR, 500 MHz, $CDCl_3$.

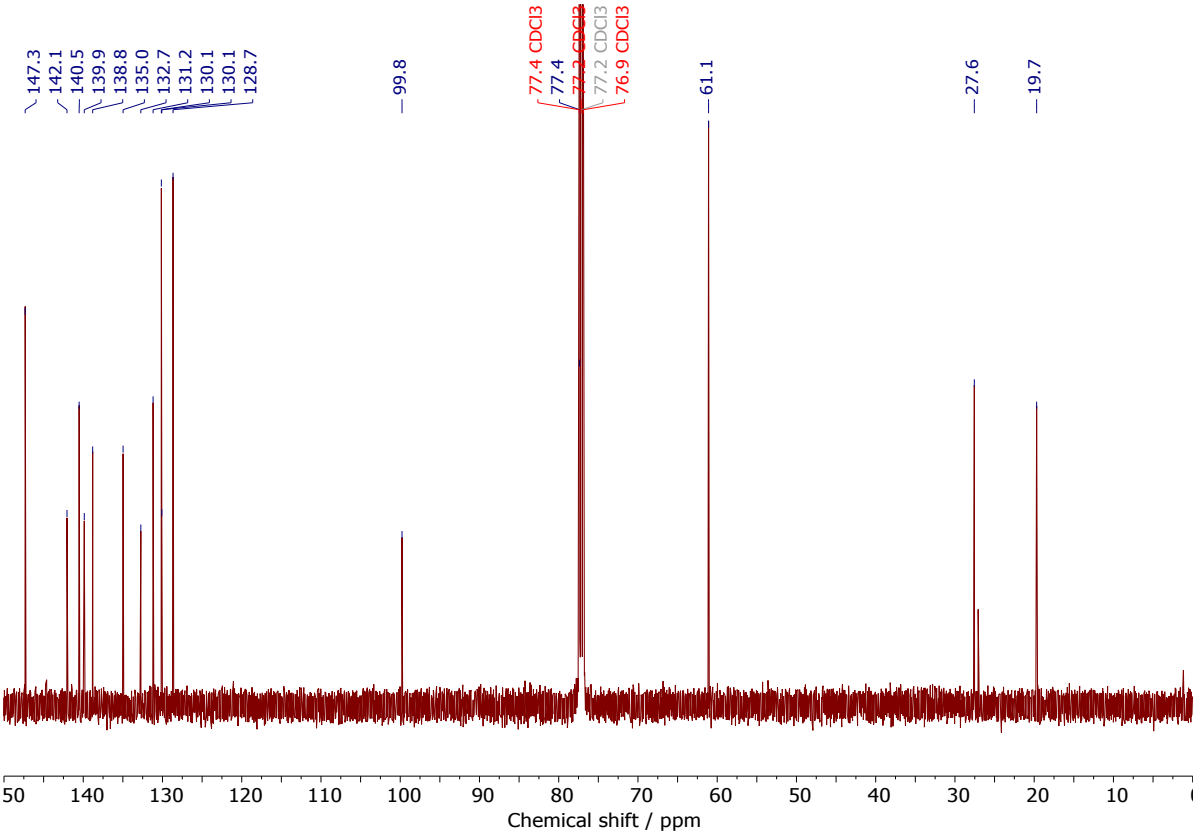

Figure S11: $^{13}C\{^{1}H\}$-NMR, 125 MHz, $CDCl_3$.

3.1.6. 1,4’’’’-Bis(4,4,5,5-tetramethyl-1,3,2-dioxaborolan-2-yl)-2’’,3’’,5’’,6’’-tetramethoxy-2,2’’’’,5,5’’’’-tetramethyl-p-quinquephenyl

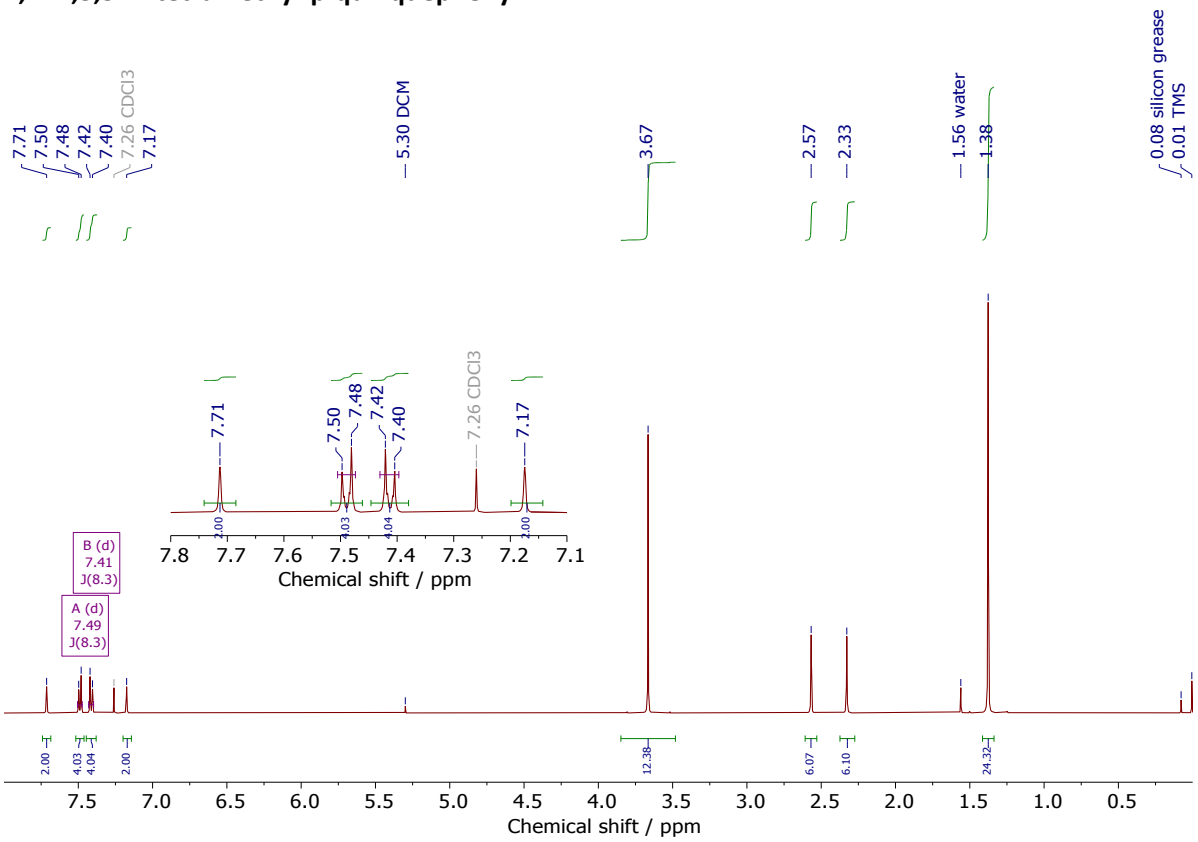

Figure S12: ^{1}H-NMR, 500 MHz, $CDCl_3$.

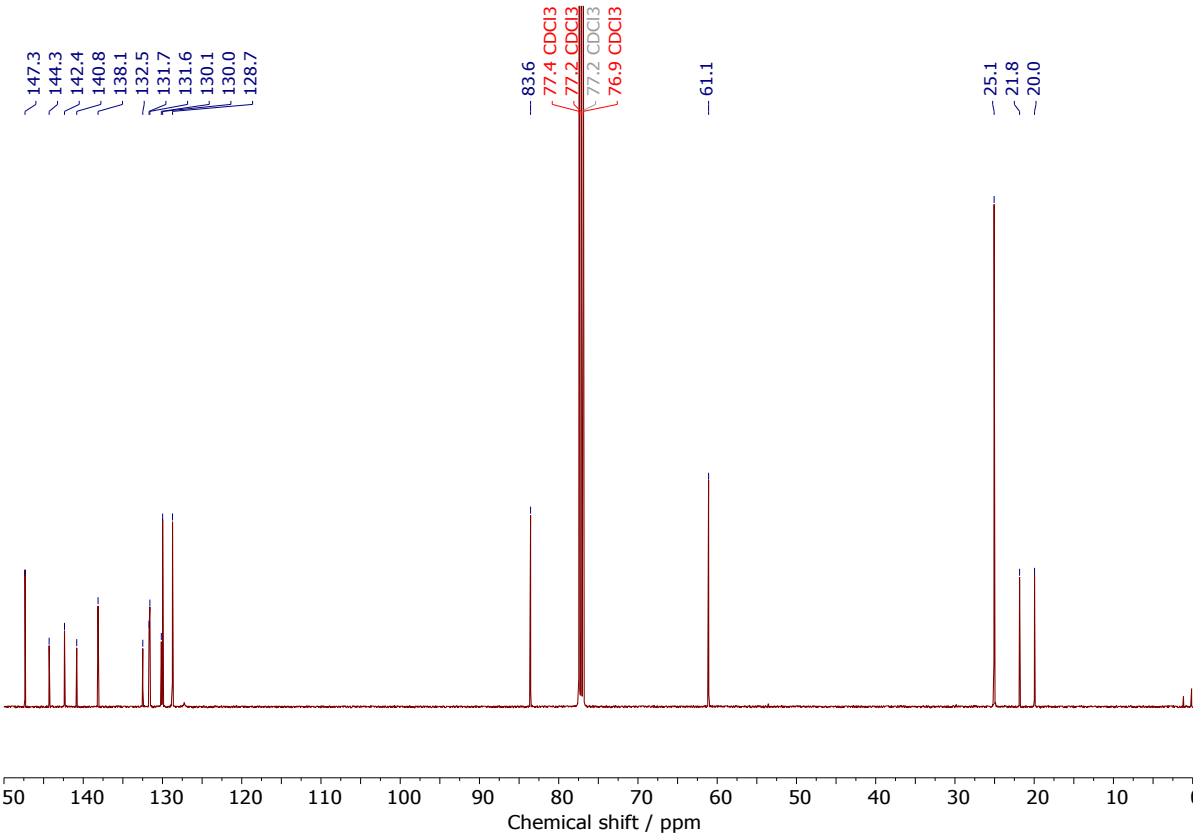

Figure S13: $^{13}C\{^{1}H\}$-NMR, 125 MHz, $CDCl_3$.

3.1.7. 1,4-Bis[{Bis(8-methoxycarbonyl-2,2,6,6-tetramethylbenzo-[1,2-d;4,5-d']-bis-[1,3]dithiol-4-yl)-(8-yl-2,2,6,6-tetramethylbenzo-[1,2-d;4,5-d']-bis-[1,3]dithiol-4-yl)}-methanol]-benzene

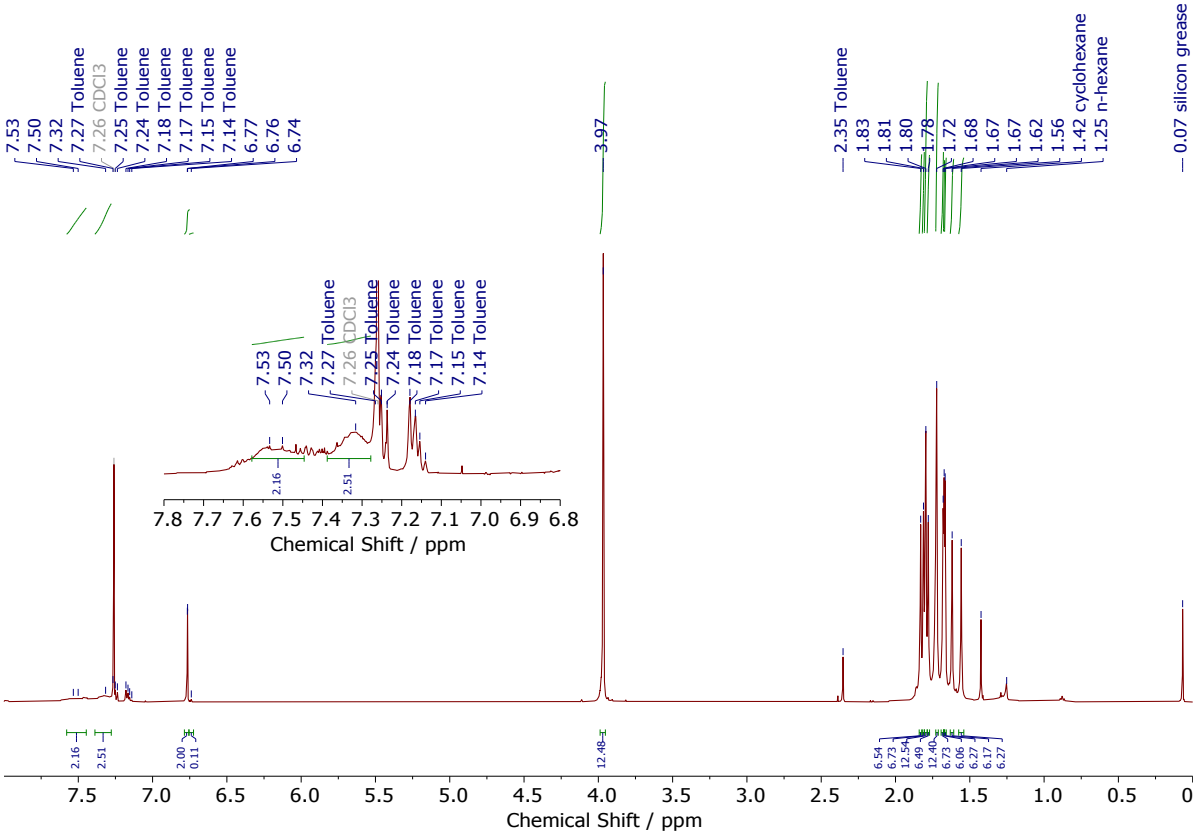

Figure S14: ^{1}H-NMR, 500 MHz, $CDCl_3$ (Impurity 5%).

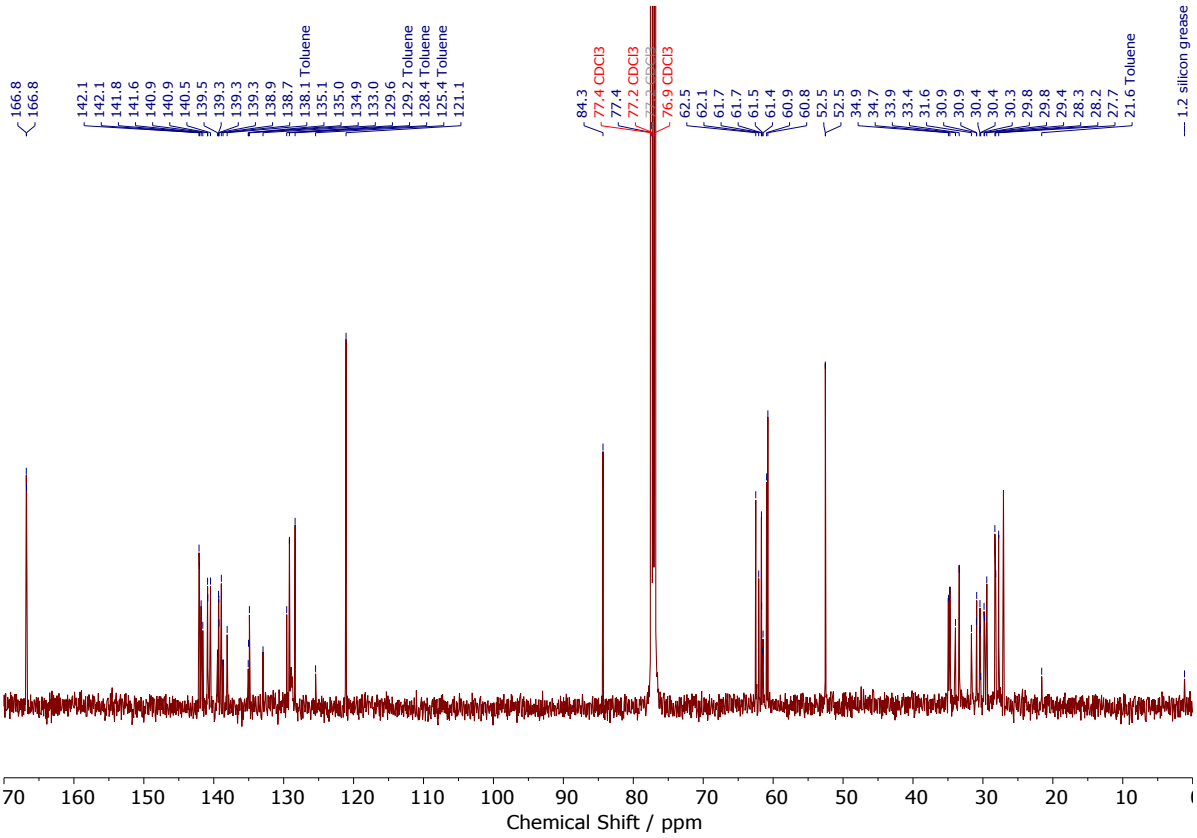

Figure S15: $^{13}C\{^{1}H\}$-NMR, 125 MHz, $CDCl_3$.

3.1.8. 4,4'-Bis[{Bis(8-methoxycarbonyl-2,2,6,6-tetramethylbenzo-[1,2-d;4,5-d']-bis-[1,3]dithiol-4-yl)-(8-yl-2,2,6,6-tetramethylbenzo-[1,2-d;4,5-d']-bis-[1,3]dithiol-4-yl)}-methanol]-biphenyl

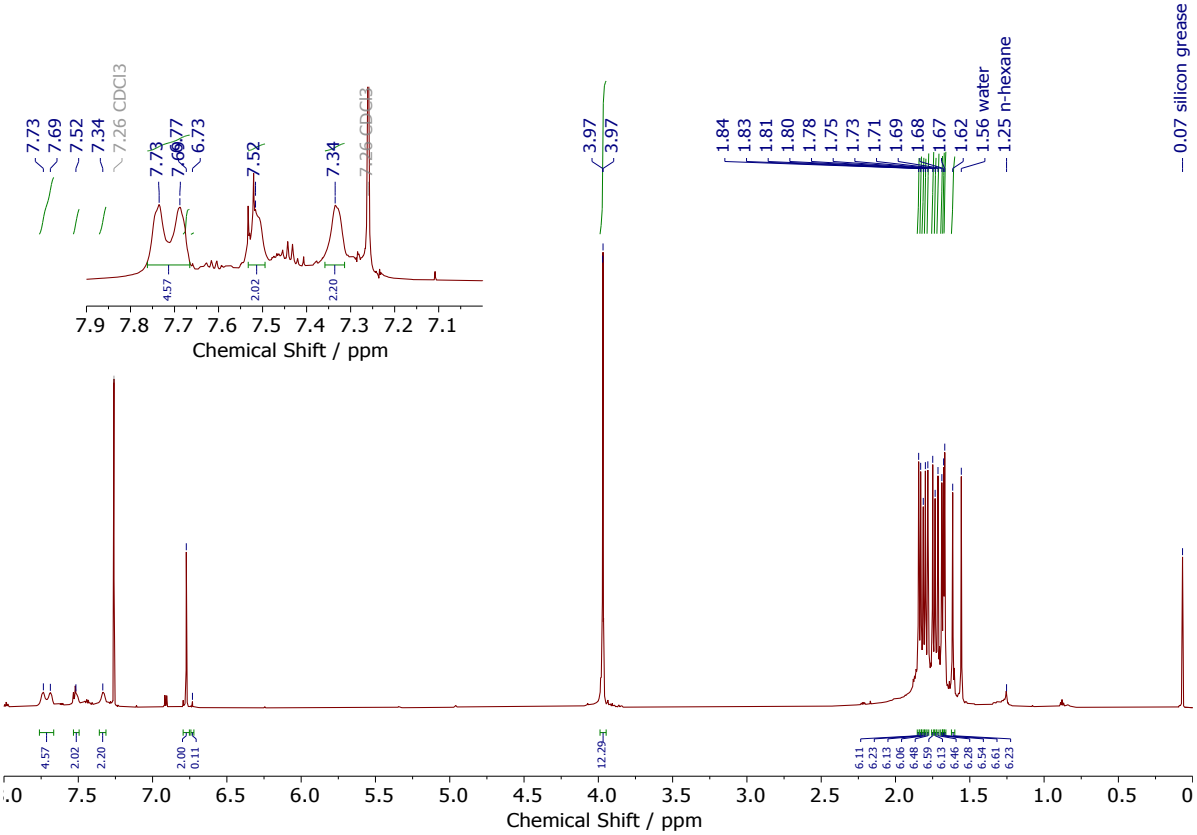

Figure S16: ^{1}H-NMR, 700 MHz, $CDCl_3$ (Impurity 5%).

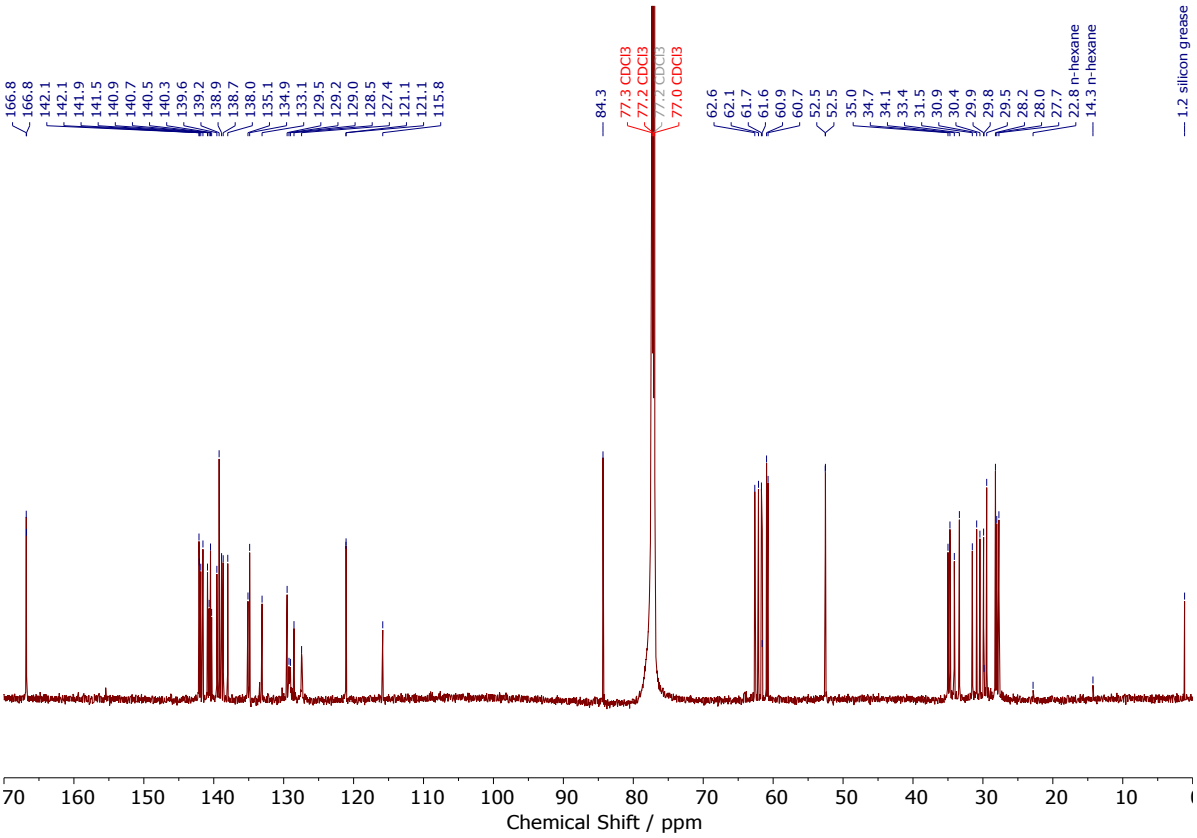

Figure S17: $^{13}C\{^{1}H\}$-NMR, 175 MHz, $CDCl_3$.

3.1.9. 4,4''-Bis[{Bis(8-methoxycarbonyl-2,2,6,6-tetramethylbenzo-[1,2-d;4,5-d']-bis-[1,3]dithiol-4-yl)-(8-yl-2,2,6,6-tetramethylbenzo-[1,2-d;4,5-d']-bis-[1,3]dithiol-4-yl)}-methanol]-p-terphenyl

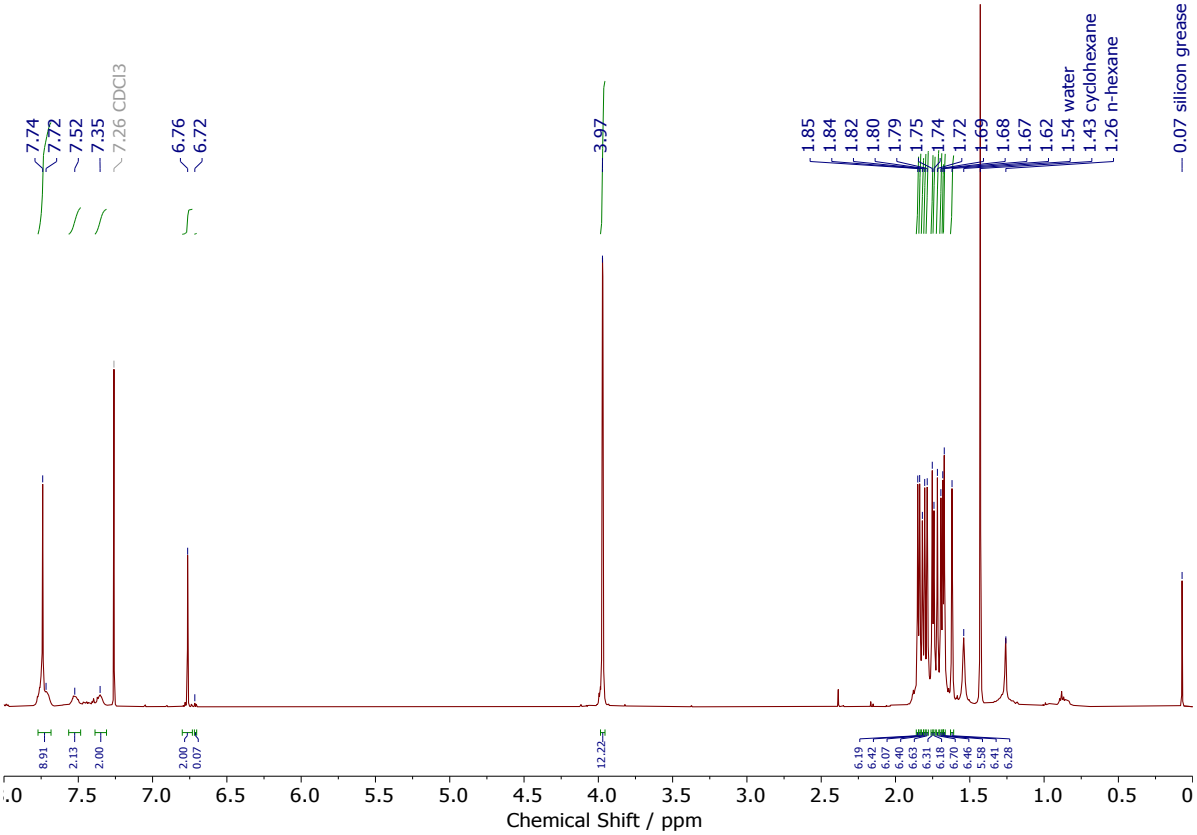

Figure S18: ^{1}H-NMR, 500 MHz, $CDCl_3$ (Impurity 3%).

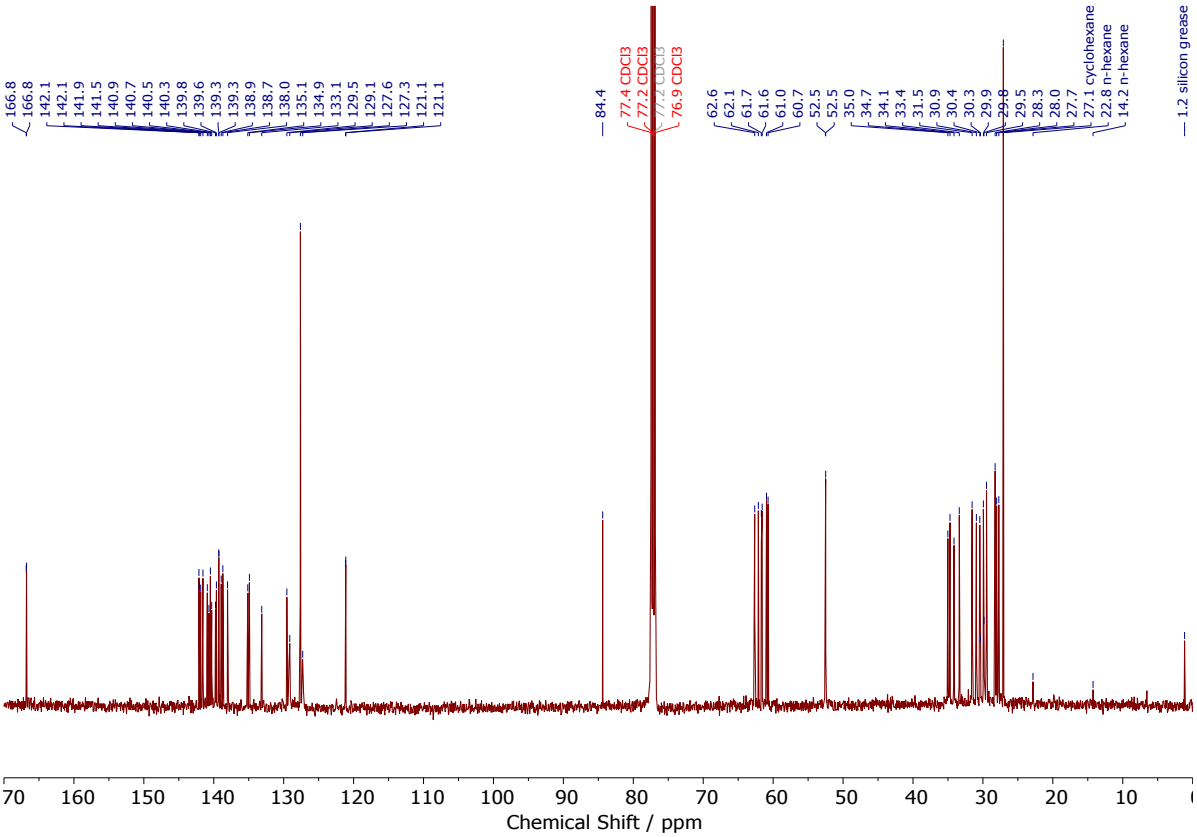

Figure S19: $^{13}C\{^{1}H\}$-NMR, 125 MHz, $CDCl_3$.

3.1.10. 4,4'''-Bis[{Bis(8-methoxycarbonyl-2,2,6,6-tetramethylbenzo-[1,2-d;4,5-d']-bis-[1,3]dithiol-4-yl)-(8-yl-2,2,6,6-tetramethylbenzo-[1,2-d;4,5-d']-bis-[1,3]dithiol-4-yl)}-methanol]-2,2''',5,5'''-tetramethyl-p-quaterphenyl

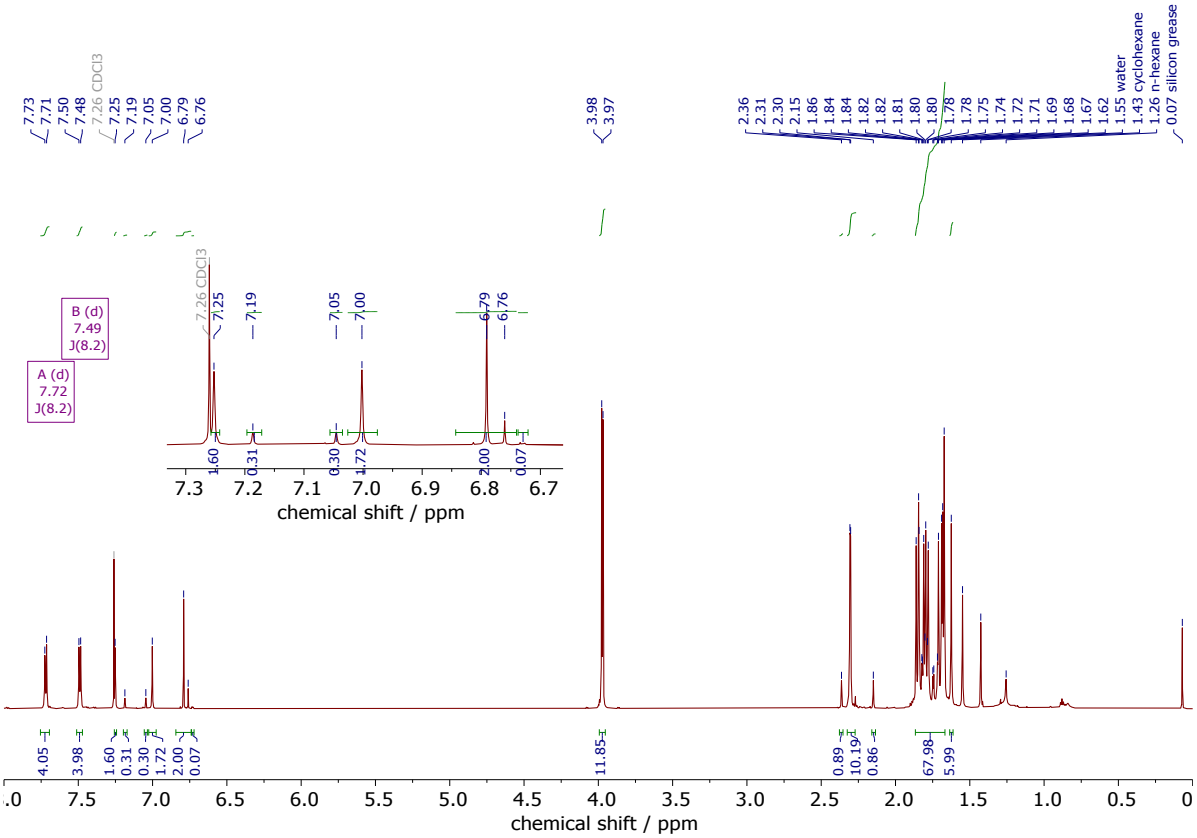

Figure S20: ^{1}H-NMR, 700 MHz, $CDCl_3$ (Impurity 3%).

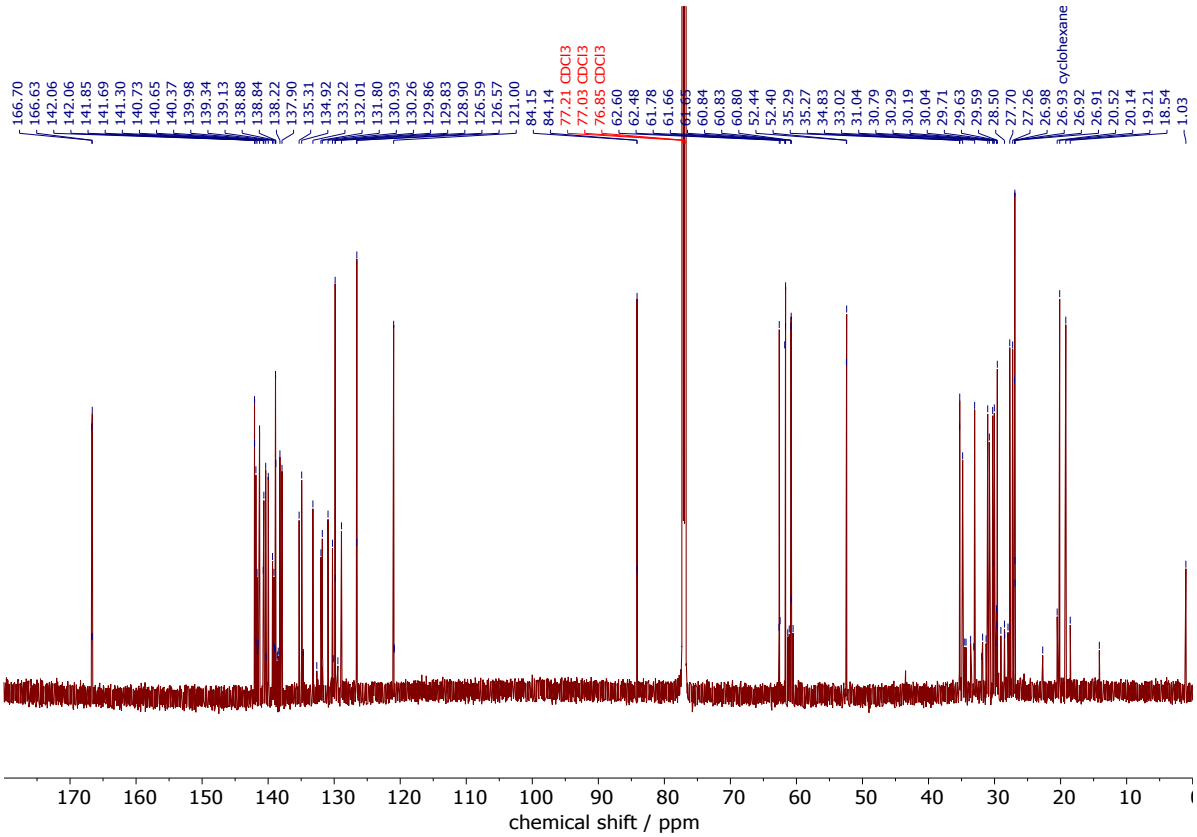

Figure S21: $^{13}C\{^{1}H\}$-NMR, 175 MHz, $CDCl_3$.

3.1.11. 4,4’’’’-Bis[{Bis(8-methoxycarbonyl-2,2,6,6-tetramethylbenzo-[1,2-d;4,5-d’]-bis-[1,3]dithiol-4-yl)-(8-yl-2,2,6,6-tetramethylbenzo-[1,2-d;4,5-d’]-bis-[1,3]dithiol-4-yl)}-methanol]-2,2’’’,5,5’’’-tetramethyl-2’’,3’’,5’’,6’’-tetramethoxy-2,2’’’’,5,5’’’’-tetramethyl-p-quinquephenyl

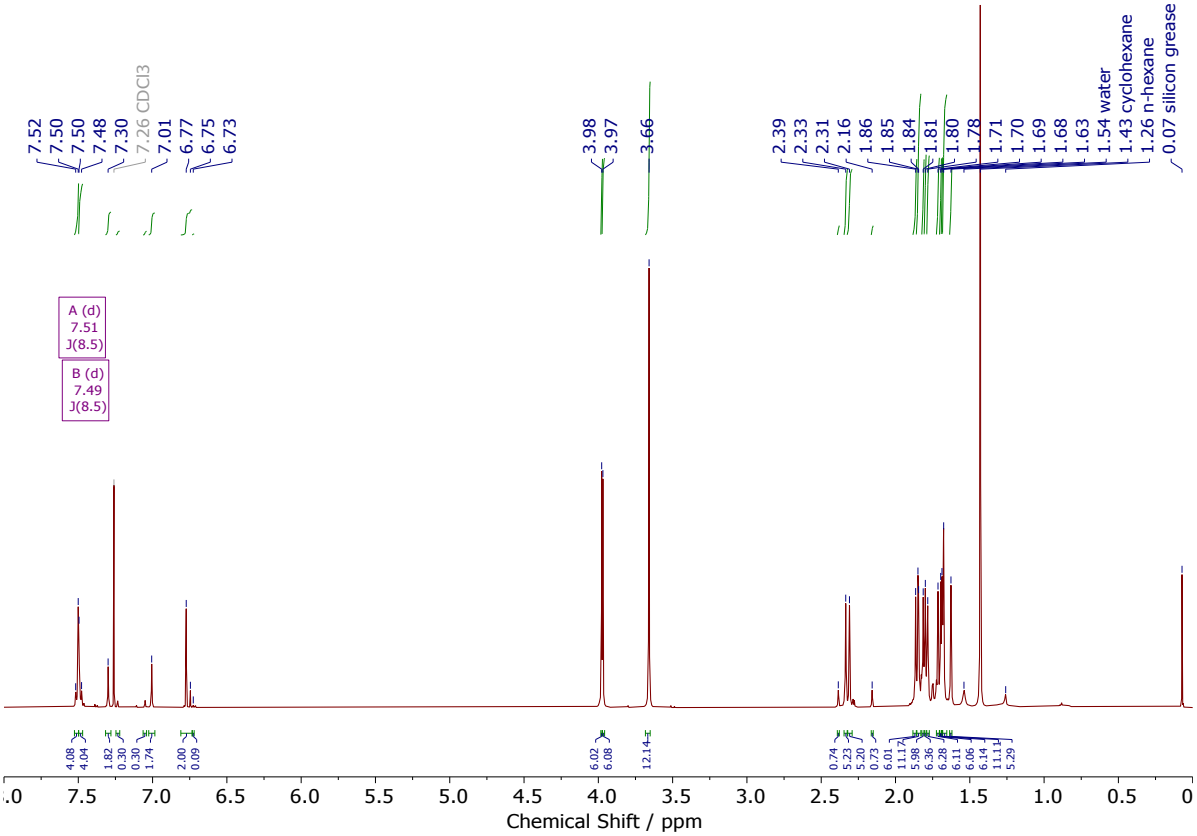

Figure S22: ^{1}H-NMR, 500 MHz, $CDCl_3$ (Impurity 4%).

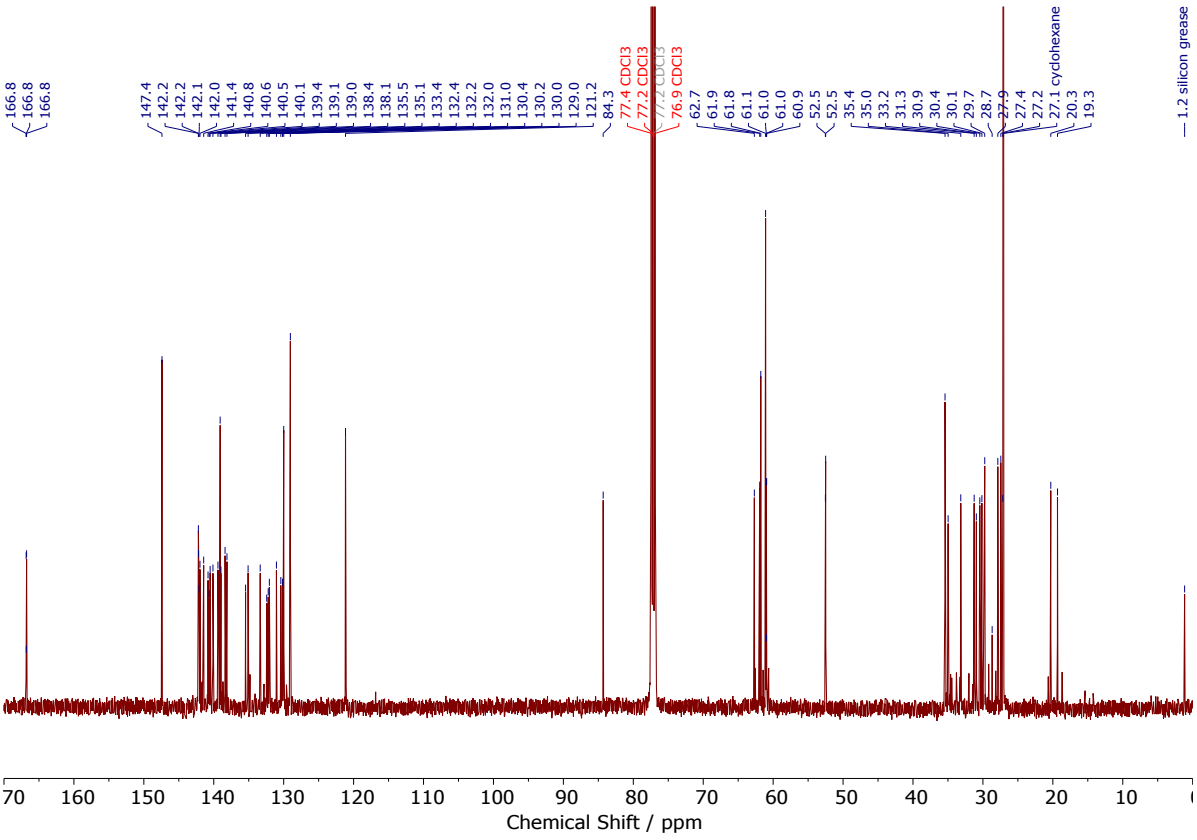

Figure S23: $^{13}C\{^{1}H\}$-NMR, 125 MHz, $CDCl_3$.

3.1.12. 1,4-Bis[{Bis(8-methoxycarbonyl-2,2,6,6-tetramethylbenzo-[1,2-d;4,5-d']-bis-[1,3]dithiol-4-yl)-(8-yl-2,2,6,6-tetramethylbenzo-[1,2-d;4,5-d']-bis-[1,3]dithiol-4-yl)}-methanol]-*p*-xylene

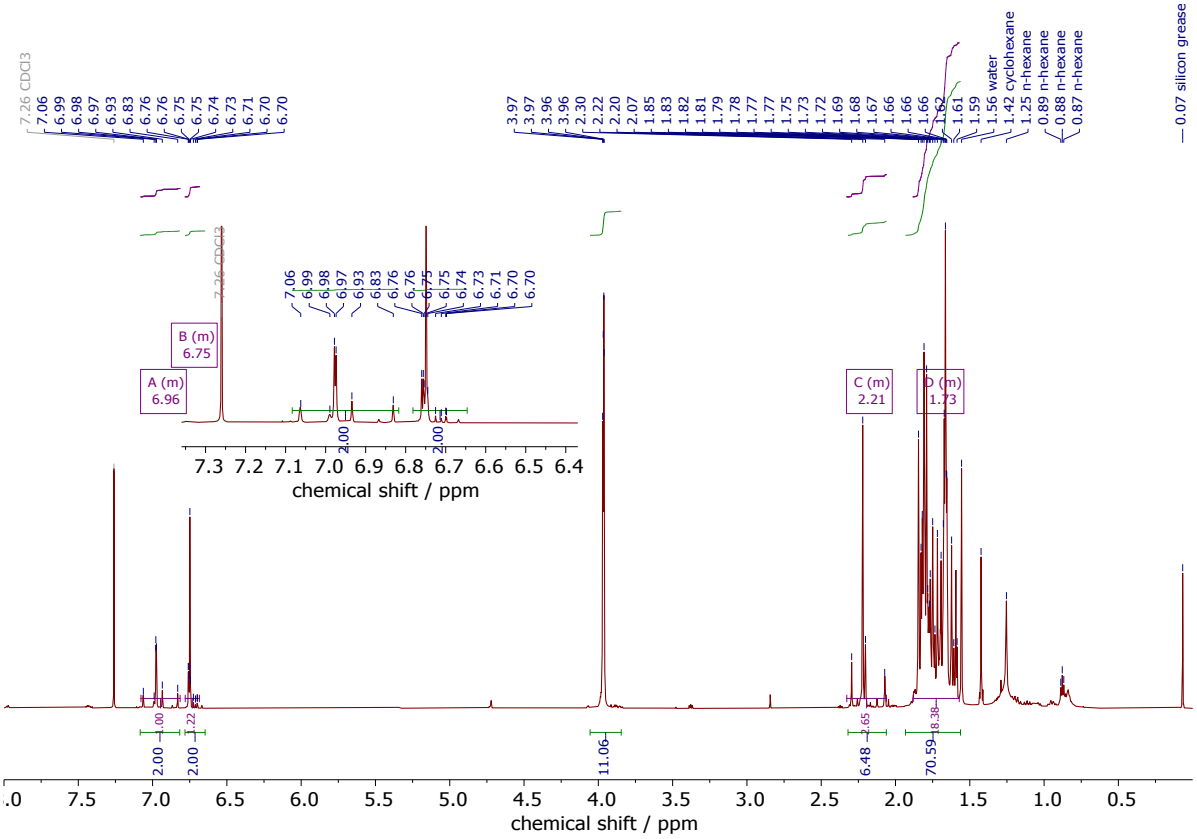

Figure S24: ^{1}H-NMR, 700 MHz, $CDCl_3$ (Impurity 4%).

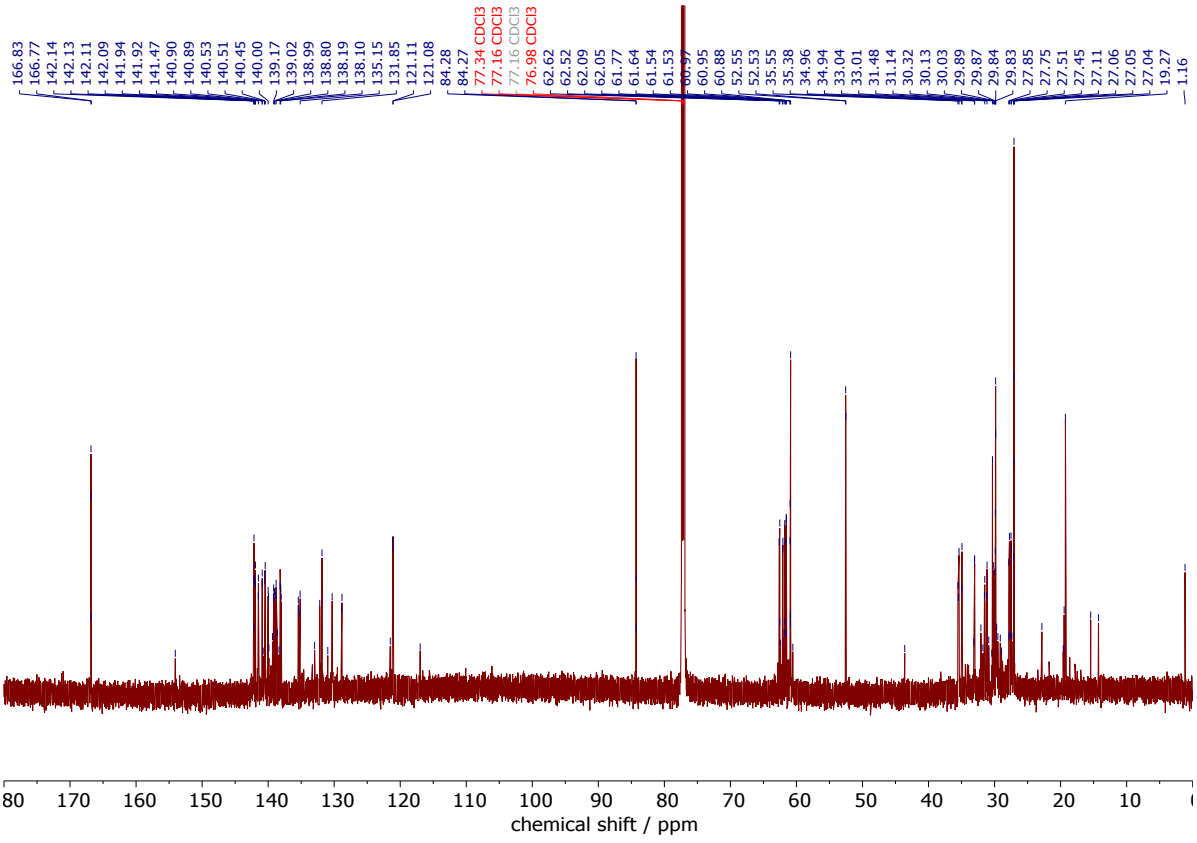

Figure S25: $^{13}C\{^{1}H\}$-NMR, 175 MHz, $CDCl_3$.

3.2. High-Resolution Mass Spectra

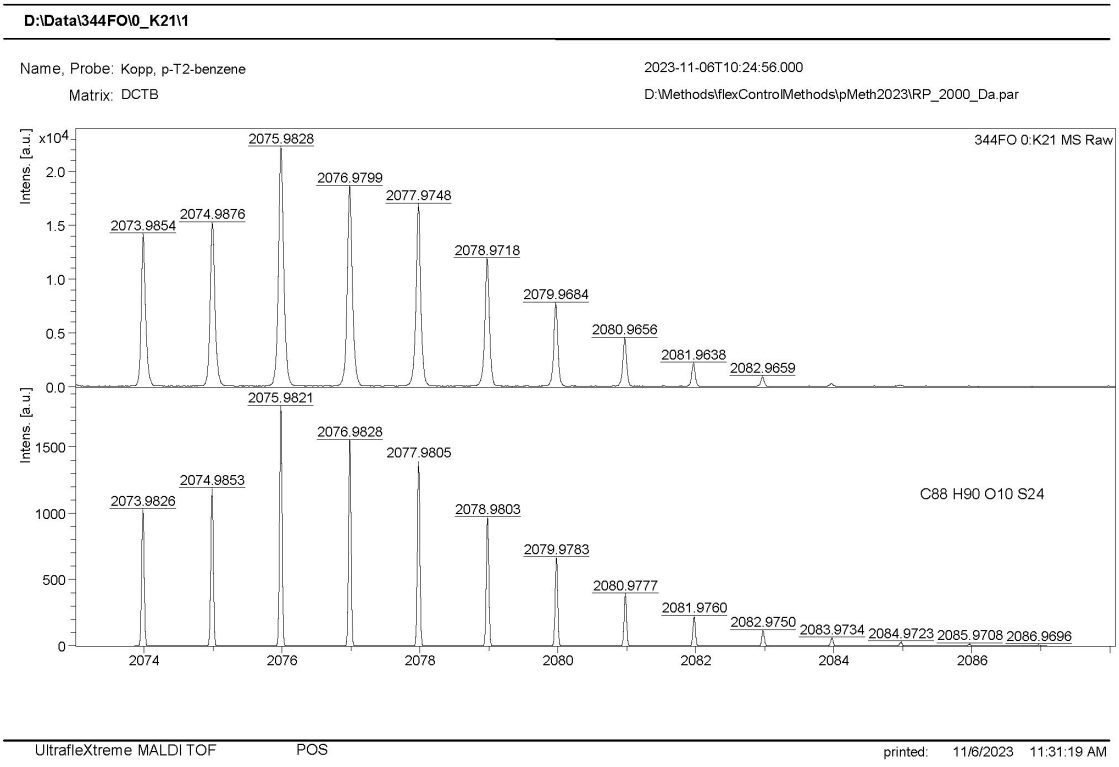

Figure S26: MALDI(+)-HRMS of 1,4-Bis[{Bis(8-methoxycarbonyl-2,2,6,6-tetramethylbenzo-[1,2-d;4,5-d']-bis-[1,3]dithiol-4-yl)-(8-yl-2,2,6,6-tetramethylbenzo-[1,2-d;4,5-d']-bis-[1,3]dithiol-4-yl)}-methanol]-benzene.

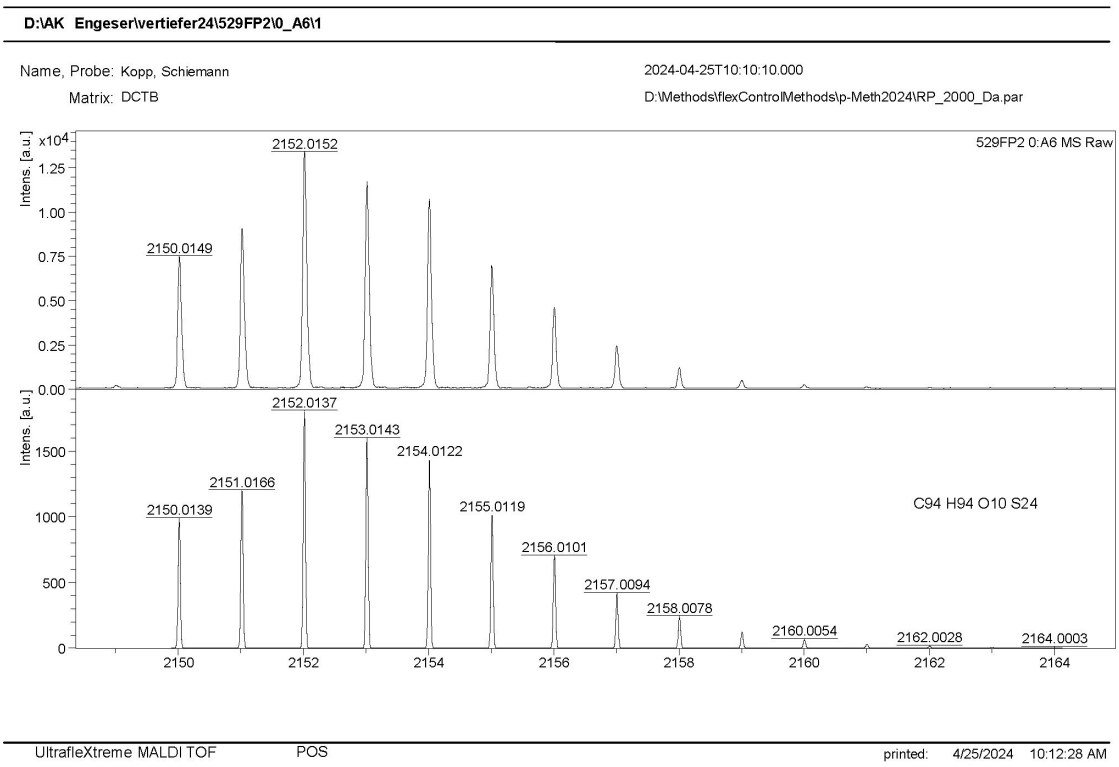

Figure S27: MALDI(+)-HRMS of 4,4'-Bis[{Bis(8-methoxycarbonyl-2,2,6,6-tetramethylbenzo-[1,2-d;4,5-d']-bis-[1,3]dithiol-4-yl)-(8-yl-2,2,6,6-tetramethylbenzo-[1,2-d;4,5-d']-bis-[1,3]dithiol-4-yl)}-methanol]-biphenyl.

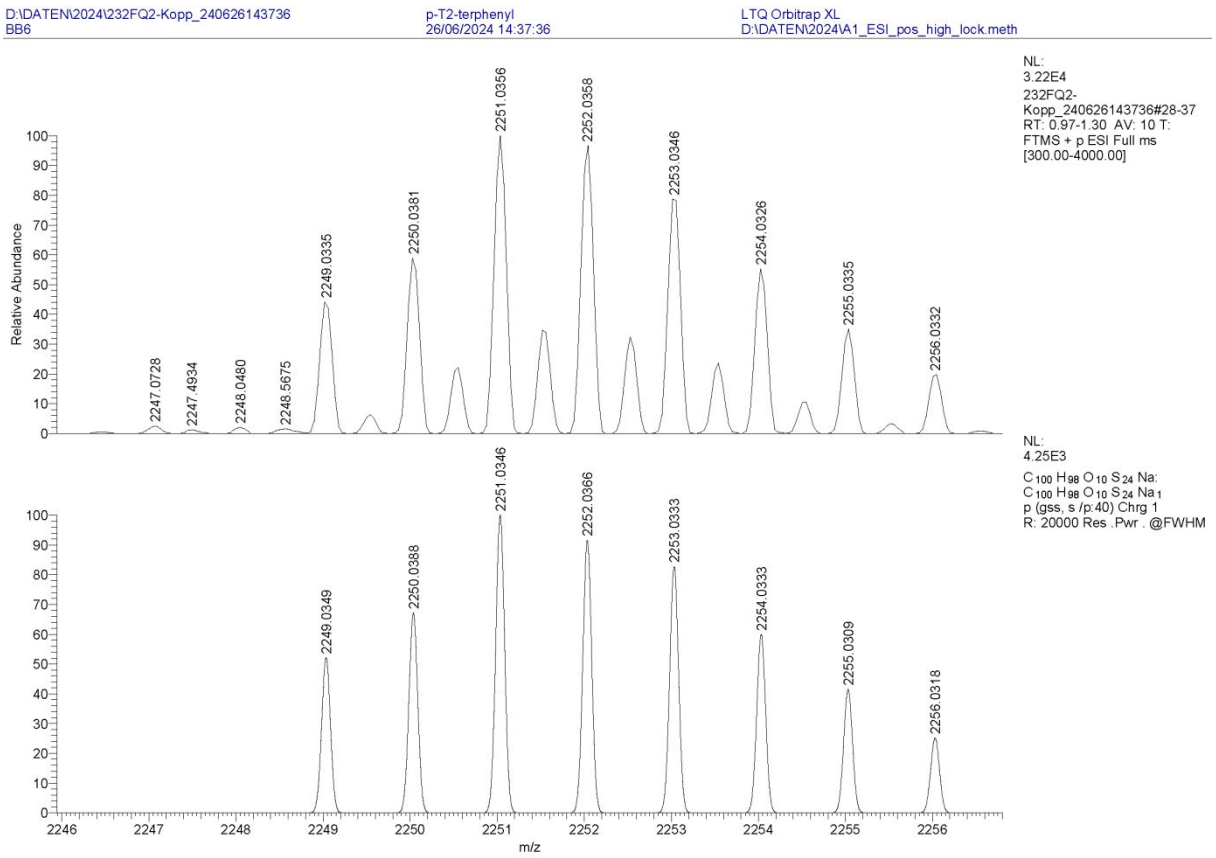

Figure S28: ESI(+)-HRMS of 4,4''-Bis[{Bis(8-methoxycarbonyl-2,2,6,6-tetramethylbenzo-[1,2-d;4,5-d']-bis-[1,3]dithiol-4-yl)-(8-yl-2,2,6,6-tetramethylbenzo-[1,2-d;4,5-d']-bis-[1,3]dithiol-4-yl)}-methanol]-p-terphenyl.

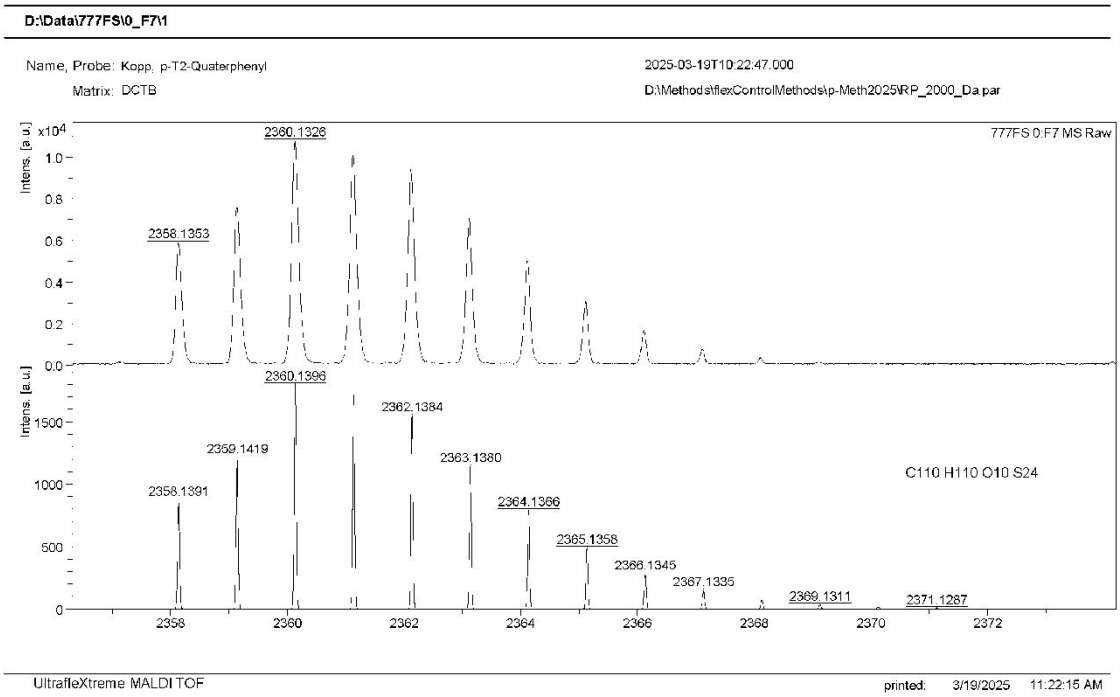

Figure S29: MALDI(+)-HRMS of 4,4'''-Bis[{Bis(8-methoxycarbonyl-2,2,6,6-tetramethylbenzo-[1,2-d;4,5-d']-bis-[1,3]dithiol-4-yl)-(8-yl-2,2,6,6-tetramethylbenzo-[1,2-d;4,5-d']-bis-[1,3]dithiol-4-yl)}-methanol]-2,2''',5,5'''-tetramethyl-p-quaterphenyl.

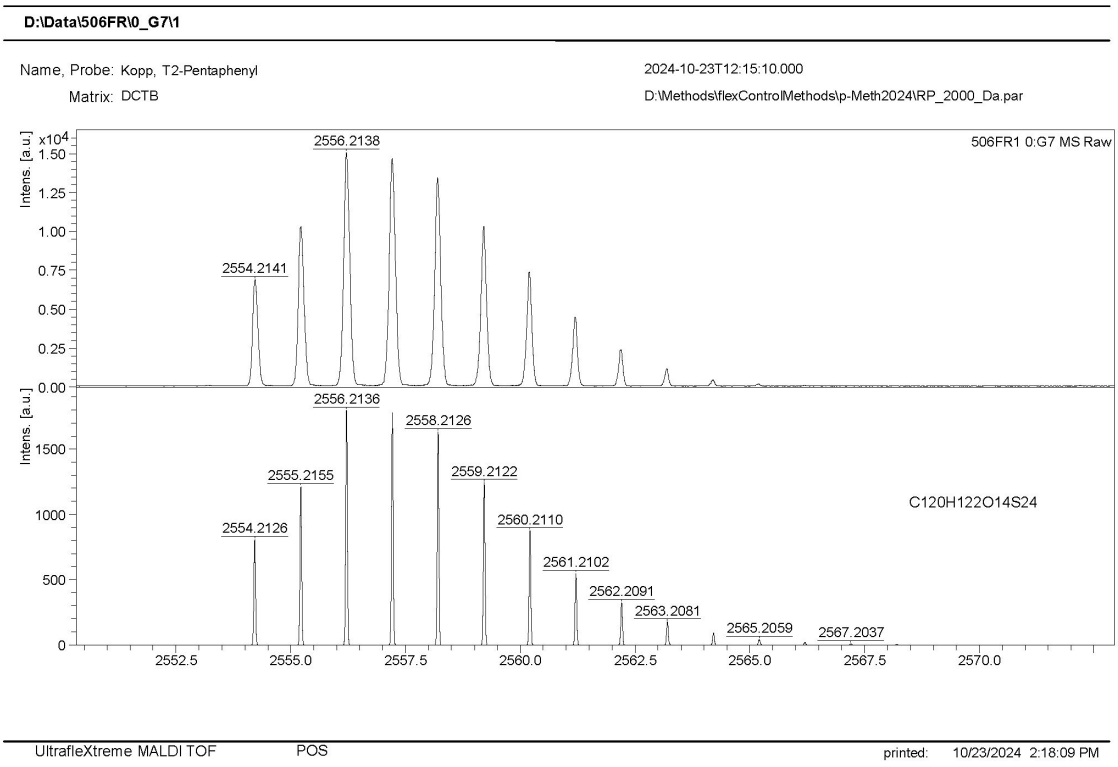

Figure S30: MALDI(+)-HRMS of 4,4’’’’-Bis[{Bis(8-methoxycarbonyl-2,2,6,6-tetramethylbenzo-[1,2-d;4,5-d’]-bis-[1,3]dithiol-4-yl)-(8-yl-2,2,6,6-tetramethylbenzo-[1,2-d;4,5-d’]-bis-[1,3]dithiol-4-yl)}-methanol]-2,2''',5,5'''-tetramethyl-2’’,3’’,5’’,6’’-tetramethoxy-2,2’’’’,5,5’’’’-tetramethyl-p-quinquephenyl.

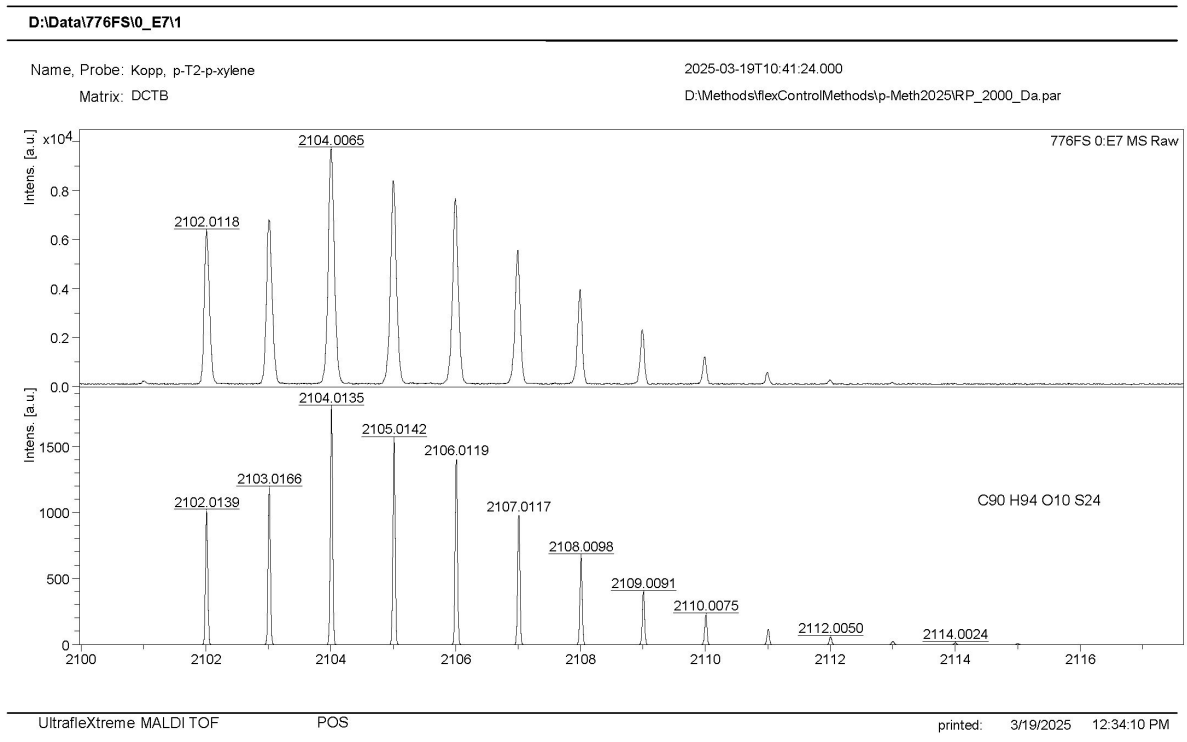

Figure S31: MALDI(+)-HRMS of 1,4-Bis[{Bis(8-methoxycarbonyl-2,2,6,6-tetramethylbenzo-[1,2-d;4,5-d’]-bis-[1,3]dithiol-4-yl)-(8-yl-2,2,6,6-tetramethylbenzo-[1,2-d;4,5-d’]-bis-[1,3]dithiol-4-yl)}-methanol]-*p-xylene*.

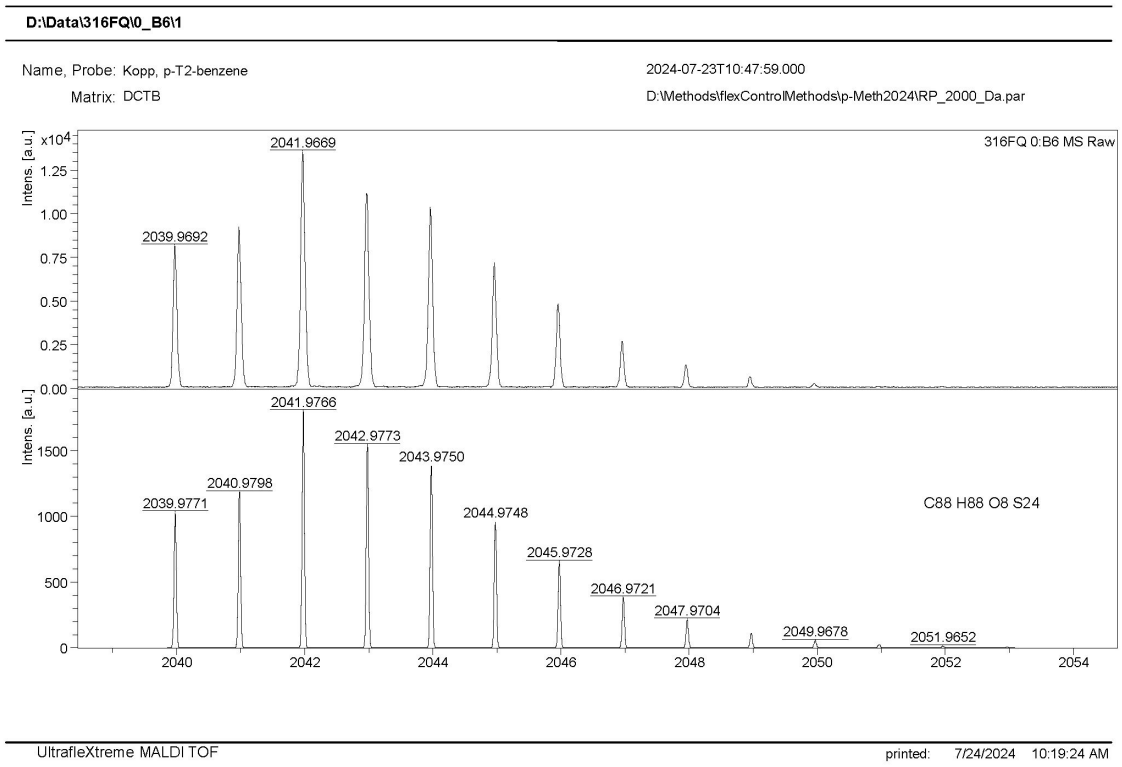

Figure S32: MALDI(+)-HRMs of 1,4-Bis[{Bis(8-methoxycarbonyl-2,2,6,6-tetramethylbenzo-[1,2-d;4,5-d']-bis-[1,3]dithiol-4-yl)-(8-yl-2,2,6,6-tetramethylbenzo-[1,2-d;4,5-d']-bis-[1,3]dithiol-4-yl)}-methyl radical]-benzene **1••**.

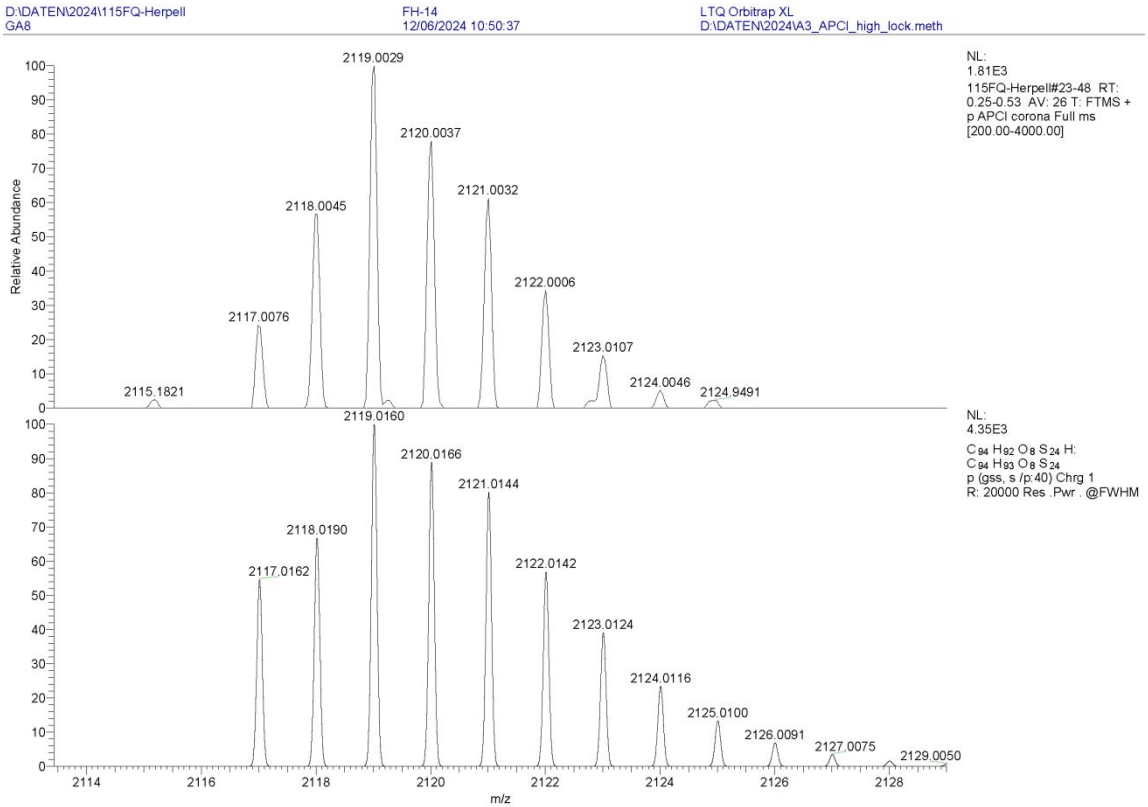

Figure S33: APCI(+)-HRMS of 4,4'-Bis[{Bis(8-methoxycarbonyl-2,2,6,6-tetramethylbenzo-[1,2-d;4,5-d']-bis-[1,3]dithiol-4-yl)-(8-yl-2,2,6,6-tetramethylbenzo-[1,2-d;4,5-d']-bis-[1,3]dithiol-4-yl)}-methyl radical]-biphenyl **2••**.

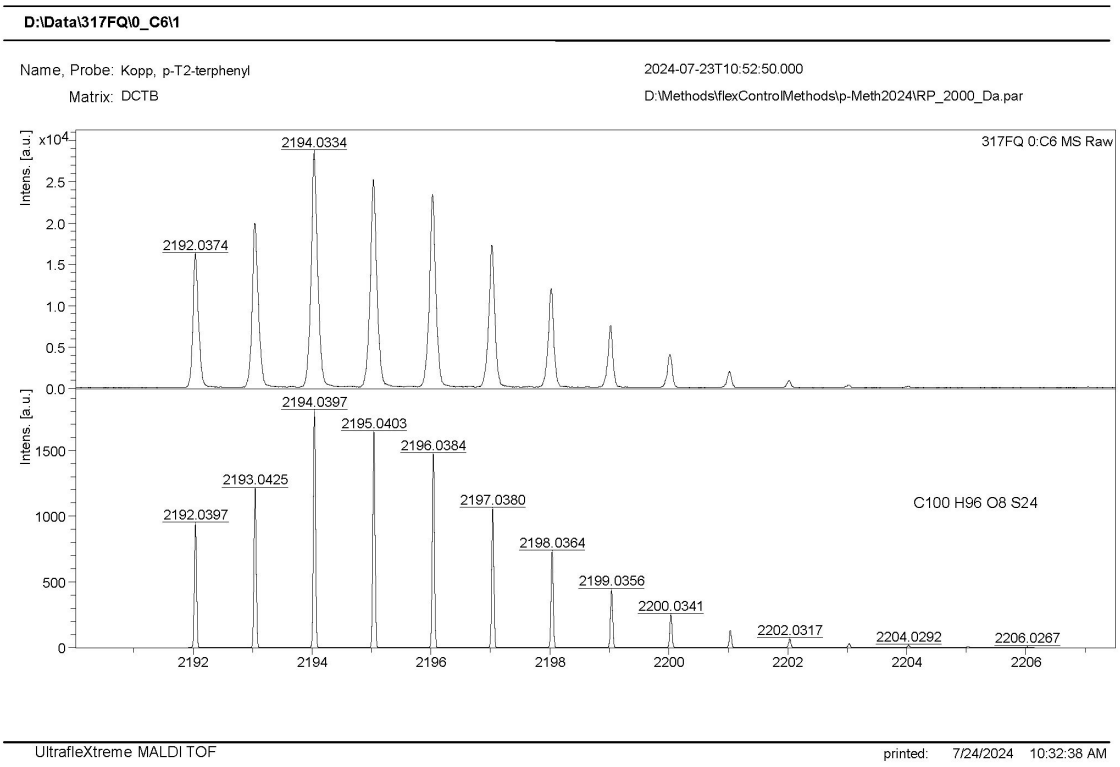

Figure S34: MALDI(+)-HRMS of 4,4''-Bis[{Bis(8-methoxycarbonyl-2,2,6,6-tetramethylbenzo-[1,2-d;4,5-d']-bis-[1,3]dithiol-4-yl)-(8-yl-2,2,6,6-tetramethylbenzo-[1,2-d;4,5-d']-bis-[1,3]dithiol-4-yl)}-methyl radical]-p-terphenyl **3••**.

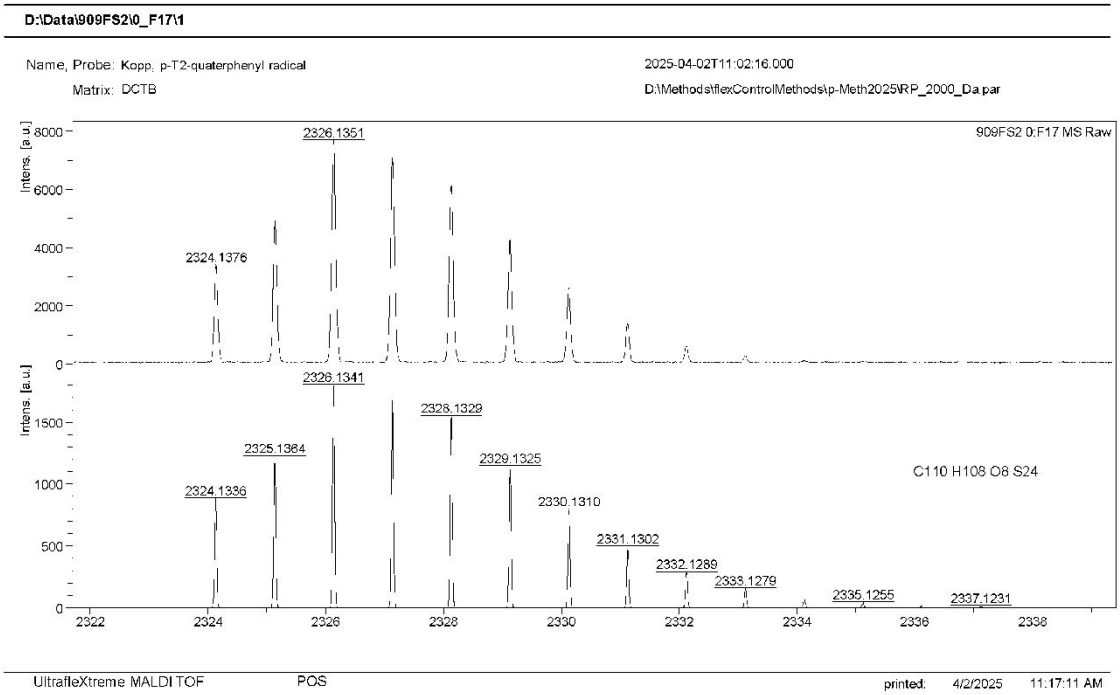

Figure S35: MALDI(+)-HRMS of 4,4'''-Bis[{Bis(8-methoxycarbonyl-2,2,6,6-tetramethylbenzo-[1,2-d;4,5-d']-bis-[1,3]dithiol-4-yl)-(8-yl-2,2,6,6-tetramethylbenzo-[1,2-d;4,5-d']-bis-[1,3]dithiol-4-yl)}-methyl radical]-2,2''',5,5'''-tetramethyl- p-quaterphenyl **4••**.

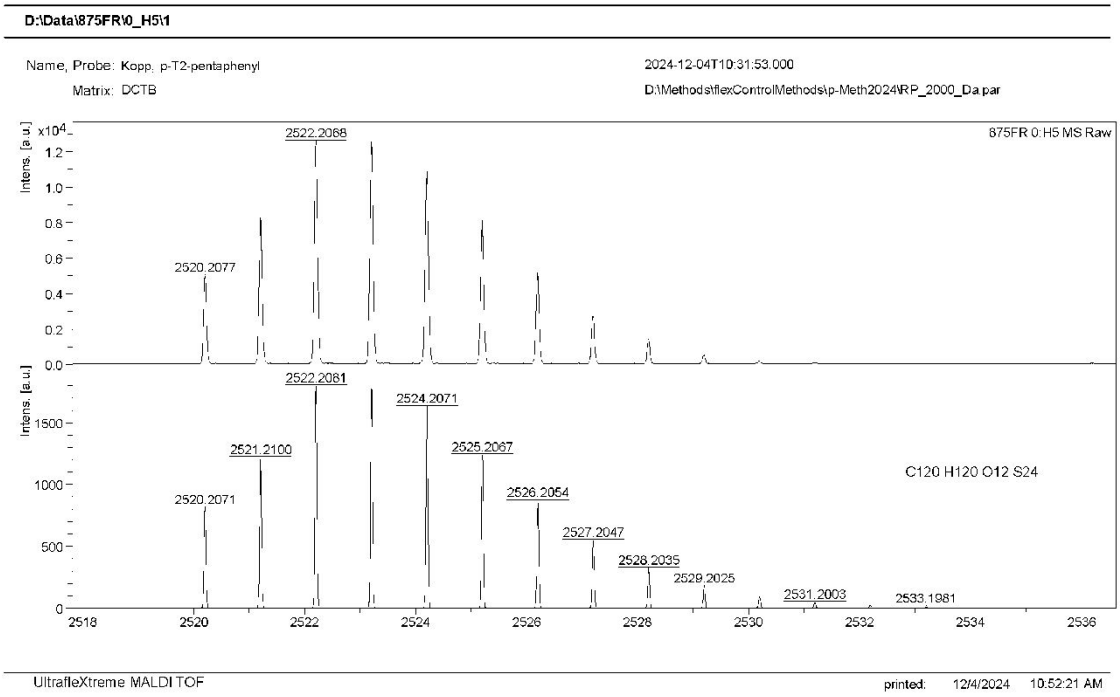

Figure S36: MALDI(+)-HRMS of 4,4’’’’-Bis[{Bis(8-methoxycarbonyl-2,2,6,6-tetramethylbenzo-[1,2-d;4,5-d’]-bis-[1,3]dithiol-4-yl)-(8-yl-2,2,6,6-tetramethylbenzo-[1,2-d;4,5-d’]-bis-[1,3]dithiol-4-yl)}-methanol]-2,2’’’,5,5’’’-tetramethyl-2’’,3’’,5’’,6’’-tetramethoxy-2,2’’’’,5,5’’’’-tetramethyl-p-quinquephenyl **5••**.

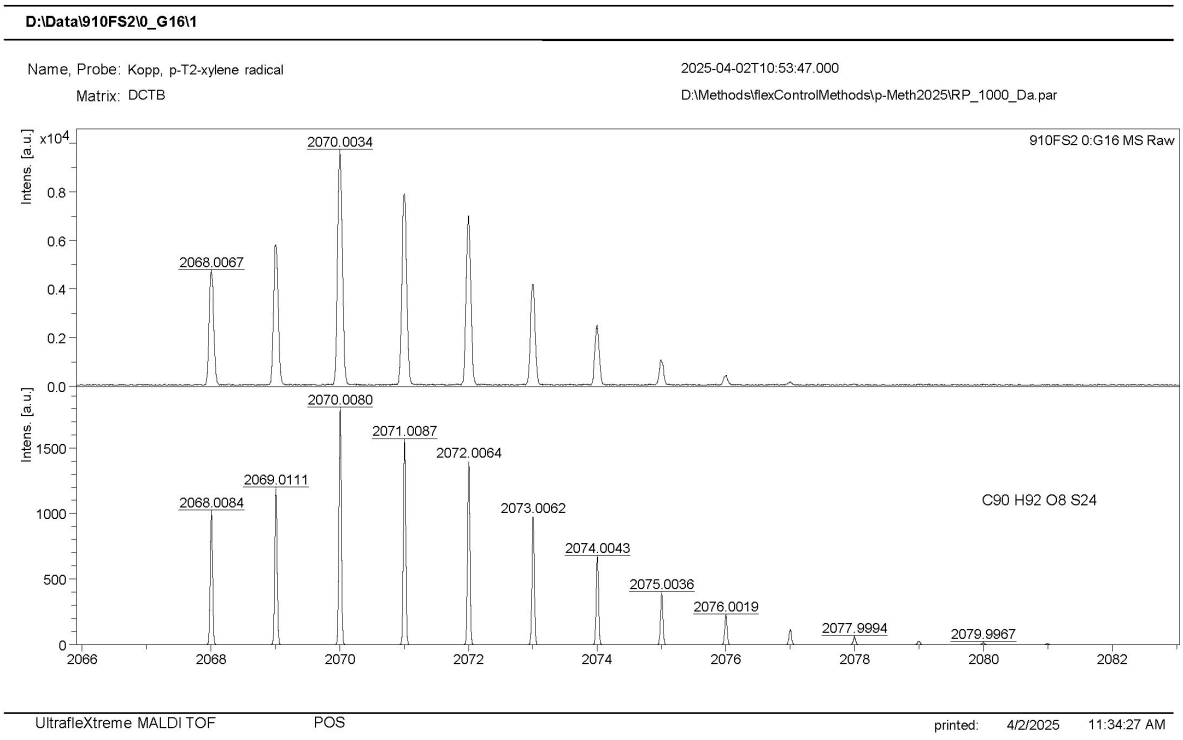

Figure S37: MALDI(+)-HRMs of 1,4-Bis[{Bis(8-methoxycarbonyl-2,2,6,6-tetramethylbenzo-[1,2-d;4,5-d’]-bis-[1,3]dithiol-4-yl)-(8-yl-2,2,6,6-tetramethylbenzo-[1,2-d;4,5-d’]-bis-[1,3]dithiol-4-yl)}-methyl radical]-*p-xylene* ***6••***.

3.3. MALDI(+) mass spectra of trityl biradicals

The additional signal which is +46 m/z of the expected mass arises from a coupling product of impurity **A**, while the smaller signal at +16 m/z can be explained by partial oxidation. This, however, happens during the mass spectrometry.

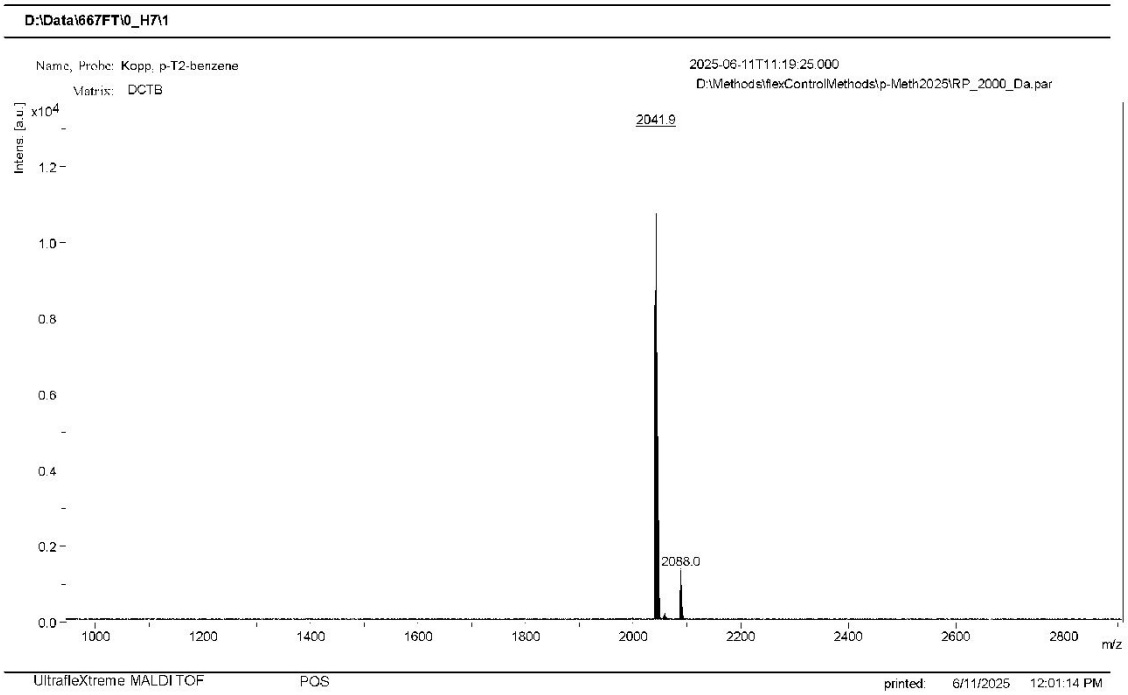

Figure S38: MALDI(+) mass spectrum of 1,4-Bis[{Bis(8-methoxycarbonyl-2,2,6,6-tetramethylbenzo-[1,2-d;4,5-d']-bis-[1,3]dithiol-4-yl)-(8-yl-2,2,6,6-tetramethylbenzo-[1,2-d;4,5-d']-bis-[1,3]dithiol-4-yl)}-methyl radical]-benzene **1••**.

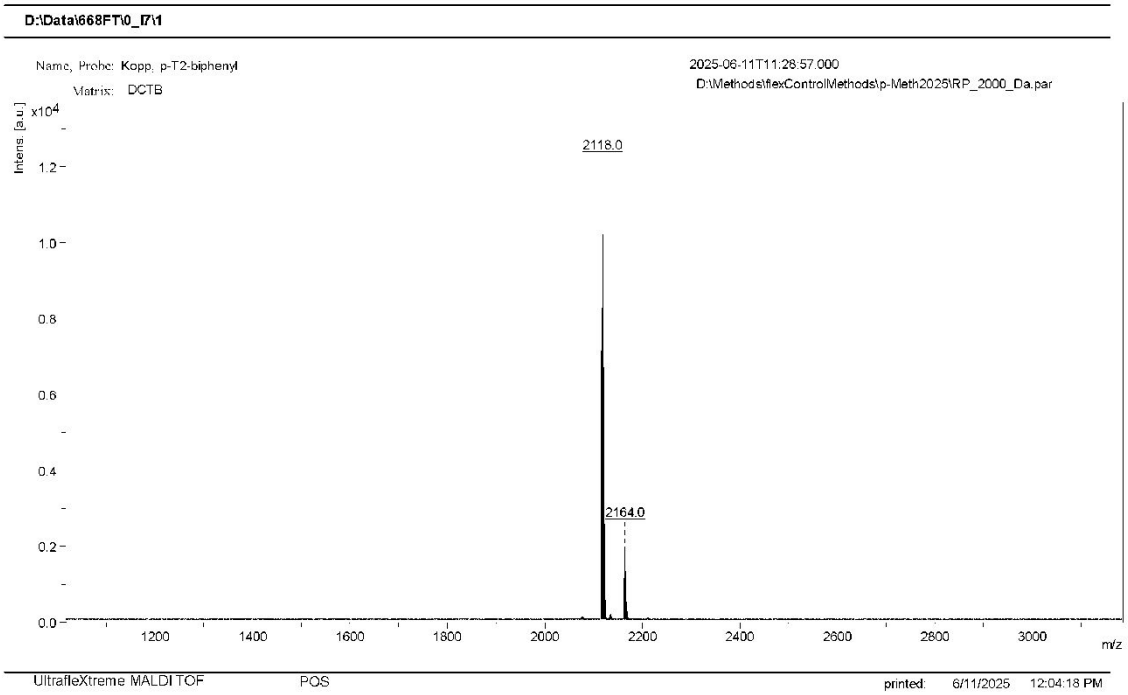

Figure S39: MALDI(+) mass spectrum of 4,4'-Bis[{Bis(8-methoxycarbonyl-2,2,6,6-tetramethylbenzo-[1,2-d;4,5-d']-bis-[1,3]dithiol-4-yl)-(8-yl-2,2,6,6-tetramethylbenzo-[1,2-d;4,5-d']-bis-[1,3]dithiol-4-yl)}-methyl radical]-biphenyl **2••**.

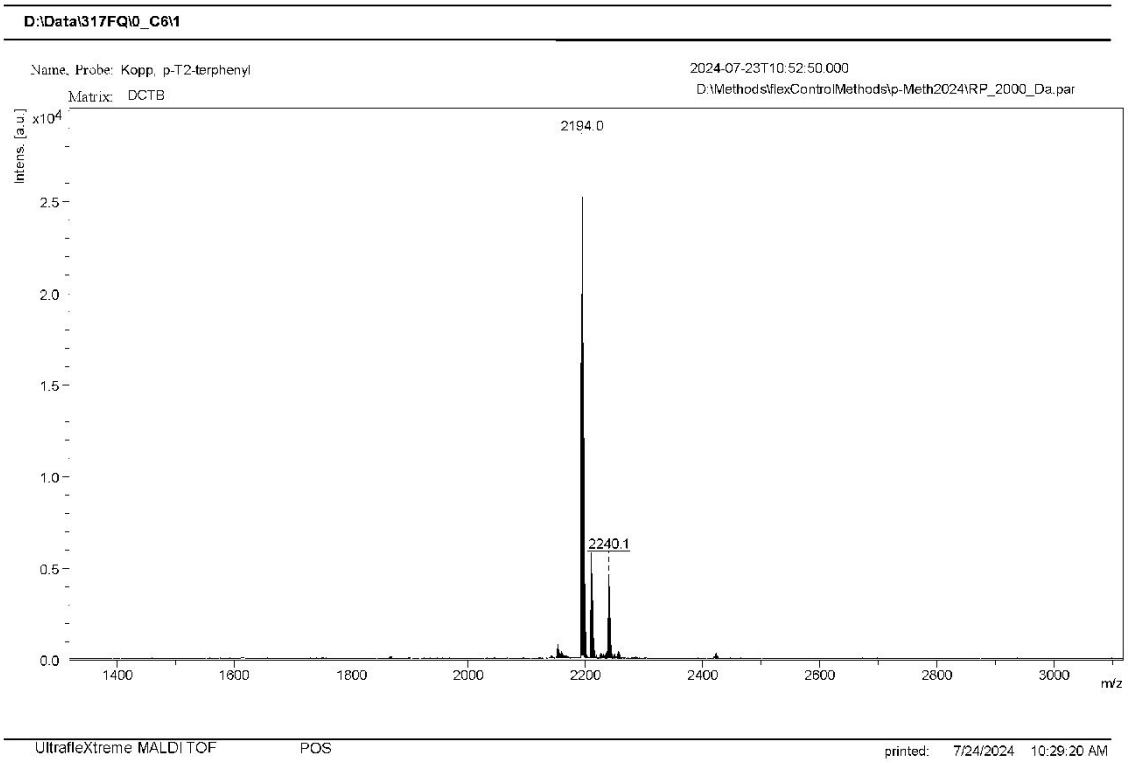

Figure S40: MALDI(+) mass spectrum of 4,4''-Bis[{Bis(8-methoxycarbonyl-2,2,6,6-tetramethylbenzo-[1,2-d;4,5-d']-bis-[1,3]dithiol-4-yl)-(8-yl-2,2,6,6-tetramethylbenzo-[1,2-d;4,5-d']-bis-[1,3]dithiol-4-yl)}-methyl radical]-p-terphenyl **3••**.

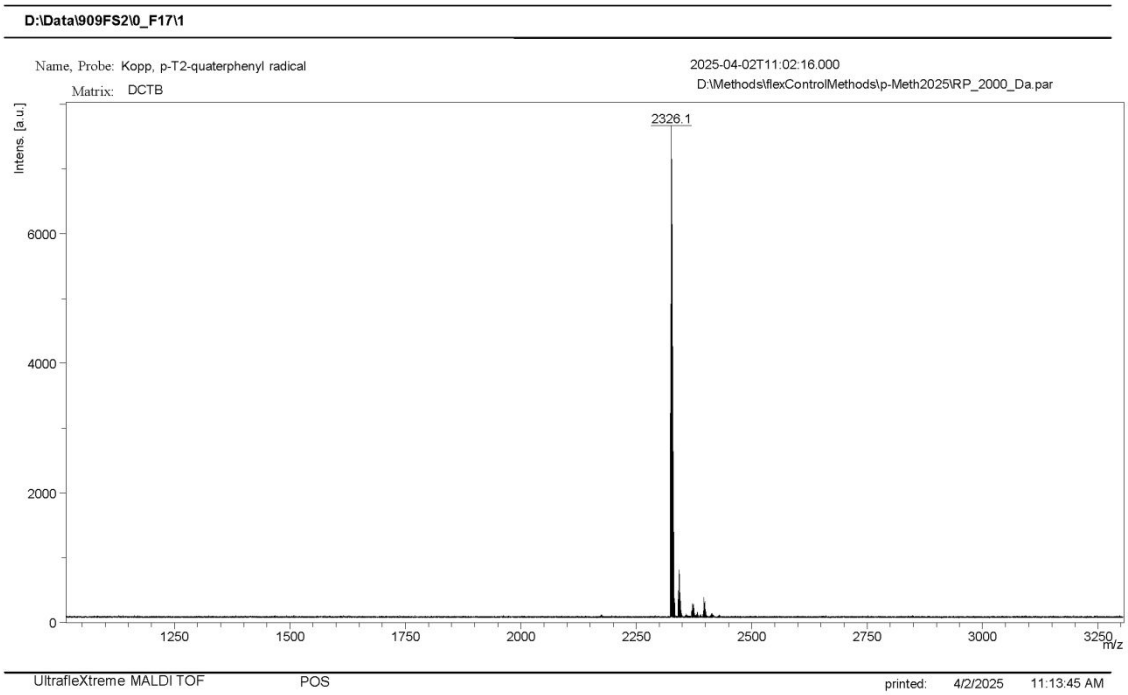

Figure S41: MALDI(+) mass spectrum of 4,4'''-Bis[{Bis(8-methoxycarbonyl-2,2,6,6-tetramethylbenzo-[1,2-d;4,5-d']-bis-[1,3]dithiol-4-yl)-(8-yl-2,2,6,6-tetramethylbenzo-[1,2-d;4,5-d']-bis-[1,3]dithiol-4-yl)}-methyl radical]-2,2''',5,5'''-tetramethyl- p-quaterphenyl **4••**.

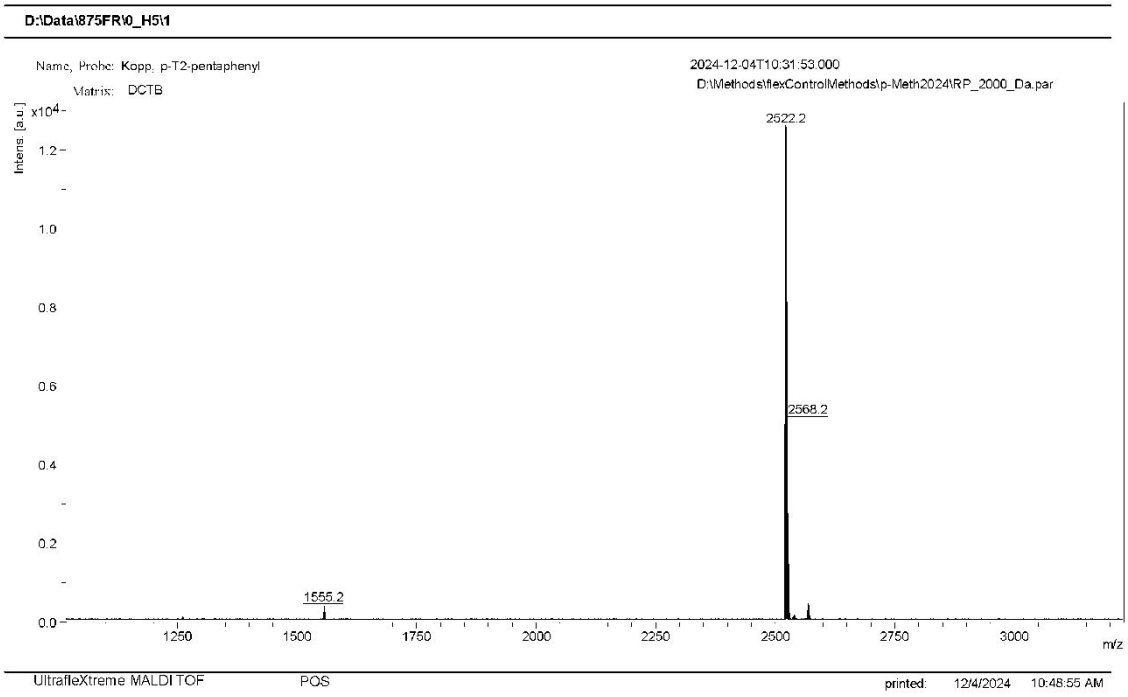

Figure S42: MALDI(+) mass spectrum of 4,4’’’’-Bis[{Bis(8-methoxycarbonyl-2,2,6,6-tetramethylbenzo-[1,2-d;4,5-d’]-bis-[1,3]dithiol-4-yl)-(8-yl-2,2,6,6-tetramethylbenzo-[1,2-d;4,5-d’]-bis-[1,3]dithiol-4-yl)}-methanol]-2,2’’’,5,5’’’-tetramethyl-2’’,3’’,5’’,6’’-tetramethoxy-2,2’’’’,5,5’’’’-tetramethyl-p-quinquephenyl **5••**.

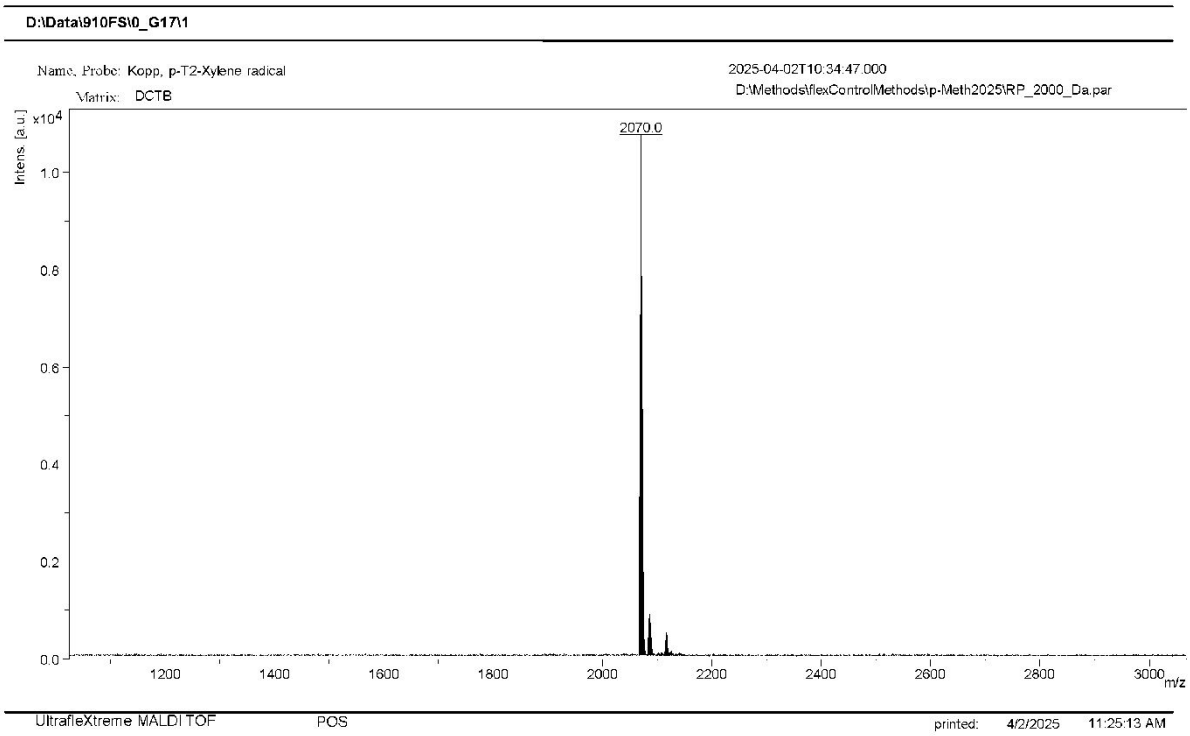

Figure S43: MALDI(+) mass spectrum of 1,4-Bis[{Bis(8-methoxycarbonyl-2,2,6,6-tetramethylbenzo-[1,2-d;4,5-d’]-bis-[1,3]dithiol-4-yl)-(8-yl-2,2,6,6-tetramethylbenzo-[1,2-d;4,5-d’]-bis-[1,3]dithiol-4-yl)}-methyl radical]-*p-xylene* ***6••***.

3.4. Medium Pressure Liquid Chromatography

The purity of Biradicals **1••** **5••** was assessed by analytical medium pressure liquid chromatography. The green line in the chromatogram shows the gradient percentage of tetrahydrofuran to n-hexane. The chromatogram around zero time was not shown because of the zero-adjustment of the detector. The signals around 8 minutes arise from the solvent system itself and are also visible without injection of sample (Figure S44).

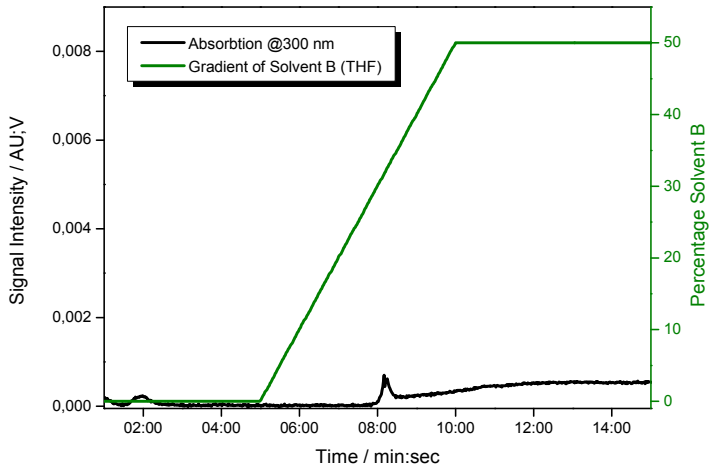

Figure S44: MPLC-chromatogram without injection of sample.

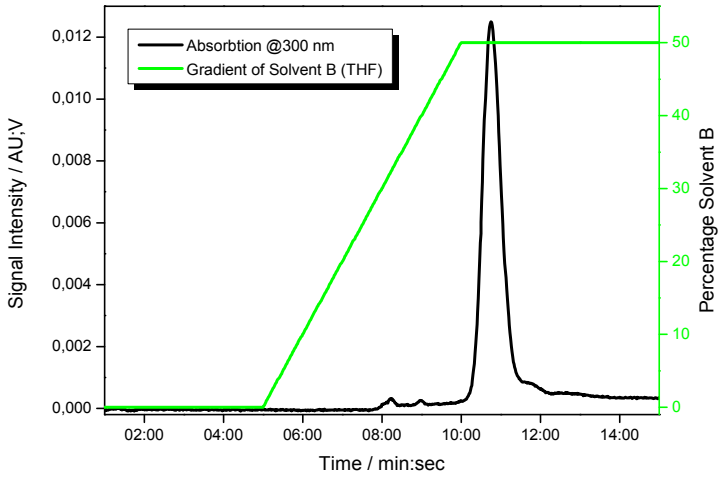

Figure S45: MPLC-chromatogram of **1••** (t = 10 min 45 sec).

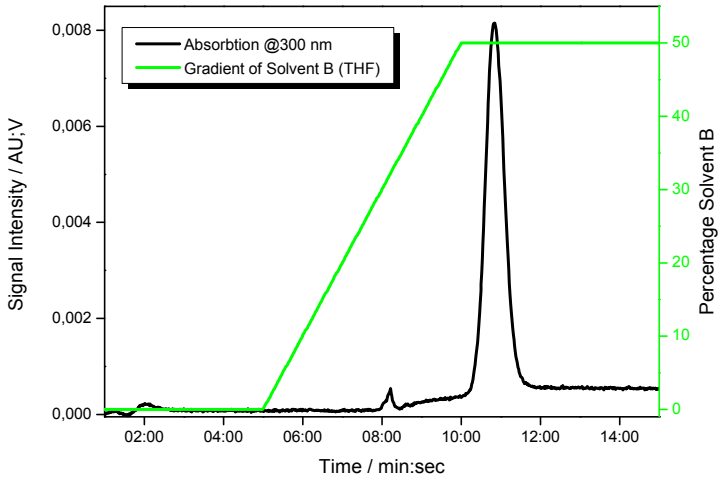

Figure S46: MPLC-chromatogram of **2••** (t = 10 min 50 sec).

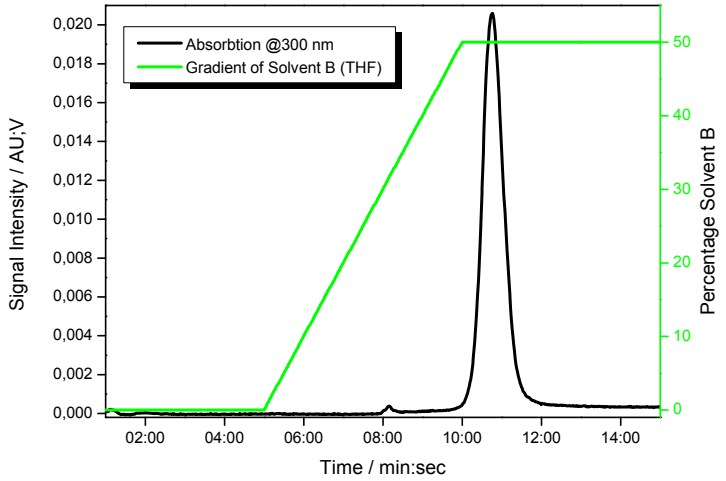

Figure S47: MPLC-chromatogram of **3••** (t = 10 min 46 sec).

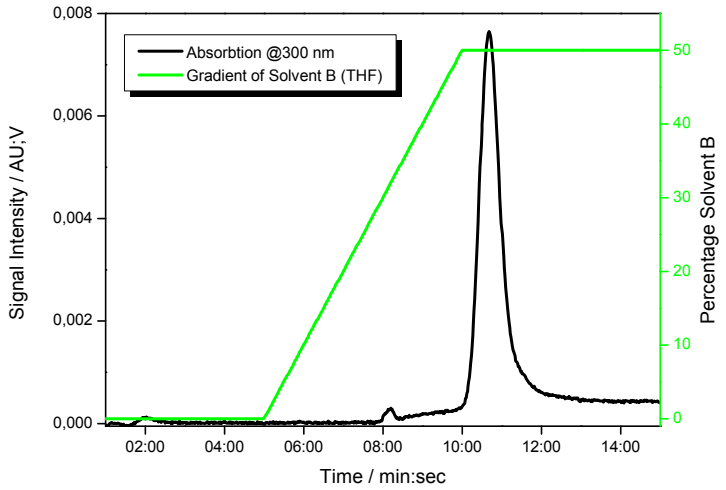

Figure S48: MPLC-chromatogram of **4••** (t = 10 min 41 sec).

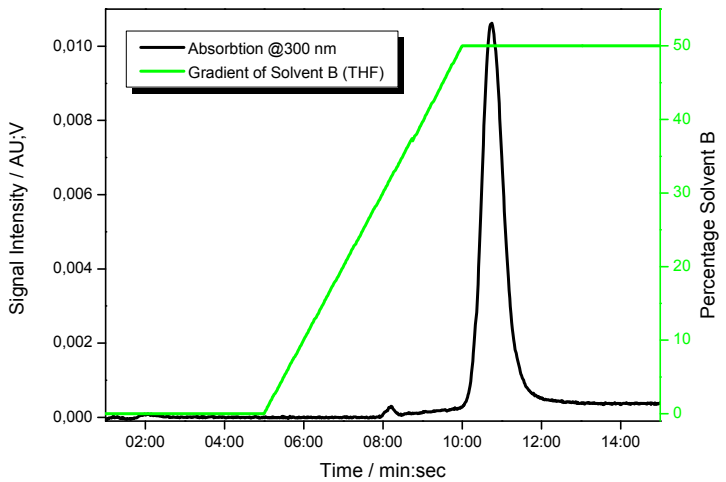

Figure S49: MPLC-chromatogram of **5••** (t = 10 min 45 sec).

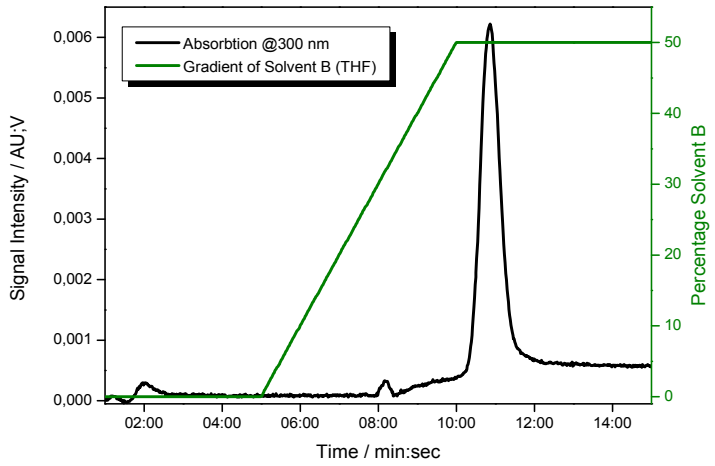

Figure S50: MPLC-chromatogram of **6••** (t = 10 min 52 sec).

4. cw EPR data

4.1. cw EPR, X-band, room temperature

In order to determine the isotropic properties of the biradicals, all samples were measured in degassed deuterated toluene at room temperature. The spectra were recorded at X-band (9.86 GHz) at a modulation amplitude of 0.2 G, 10 kHz modulation frequency, and 0.1805 mW microwave power. The conversion time was set to 20.81 ms with a time constant of 10.24 ms. All spectra were field-corrected using Mn^{2+}-doped MgO.[3] For the sake of plotting all spectra on the same magnetic field axis, the frequency was recalculated to 9.86000 GHz. Room-temperature spectra were fitted using the *pepper* routine in *Easyspin,*[4] assuming two S=1/2 systems, each with their own set of hyperfine interactions, that are assumed to be equal. Hyperfine interaction is only non-zero for nuclei in the same trityl. Furthermore, exchange coupling is introduced. Since, in the case of biradical **4••** the exchange coupling is obtained from the cw-EPR simulation, the sign is unknown. In the cases of biradicals **1••**-**3••**, and **6••** the singlet-triplet splitting obtained from the temperature-dependent half-field measurement is used in the simulation. Best-fit parameters are shown in Table S1.

The ^{13}C-hyperfine splitting in the spectra of **1•• – 6••** in the liquid solution cw EPR spectra are given by the ^{13}C-hyperfine coupling constant of the respective C-atom and the magnitude of *J*. If *J* is 0, the observed ^{13}C splitting is only given by the ^{13}C-hyperfine coupling constant. If *J* is much larger than the ^{13}C-hyperfine coupling constant, then the apparent splitting is half the ^{13}C hyperfine coupling constant. If *J* is on the order of the ^{13}C-hyperfine coupling, the apparent splitting heavily depends on the ratio of *J* and the ^{13}C-hyperfine coupling constant.

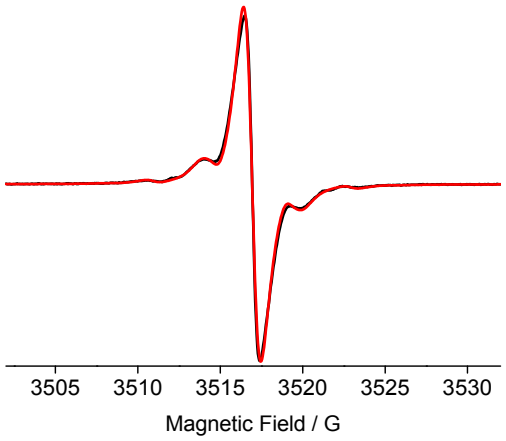

Figure S51: cw X-Band (9.86 GHz) EPR spectrum at room temperature of 1,4-Bis[{Bis(8-methoxycarbonyl-2,2,6,6-tetramethylbenzo-[1,2-d;4,5-d']-bis-[1,3]dithiol-4-yl)-(8-yl-2,2,6,6-tetramethylbenzo-[1,2-d;4,5-d']-bis-[1,3]dithiol-4-yl)}-methyl radical]-benzene **1••**.

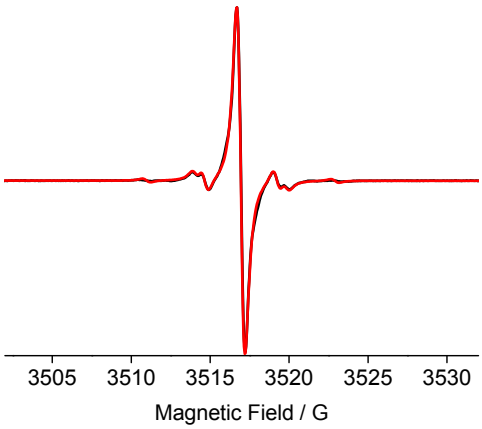

Figure S52: cw X-Band (9.86 GHz) EPR spectrum at room temperature of 4,4'-Bis[{Bis(8-methoxycarbonyl-2,2,6,6-tetramethylbenzo-[1,2-d;4,5-d']-bis-[1,3]dithiol-4-yl)-(8-yl-2,2,6,6-tetramethylbenzo-[1,2-d;4,5-d']-bis-[1,3]dithiol-4-yl)}-methyl radical]-biphenyl **2••**.

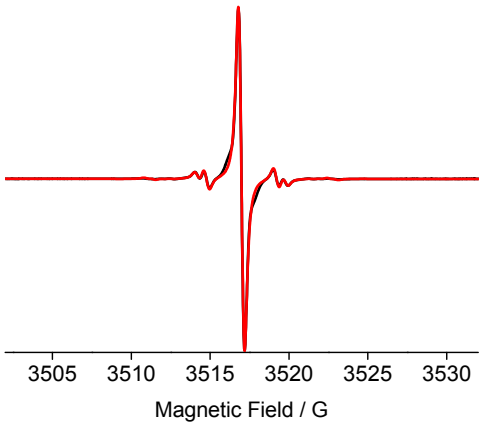

Figure S53: cw X-Band (9.86 GHz) EPR spectrum at room temperature of 4,4''-Bis[{Bis(8-methoxycarbonyl-2,2,6,6-tetramethylbenzo-[1,2-d;4,5-d']-bis-[1,3]dithiol-4-yl)-(8-yl-2,2,6,6-tetramethylbenzo-[1,2-d;4,5-d']-bis-[1,3]dithiol-4-yl)}-methyl radical]-p-terphenyl **3••**.

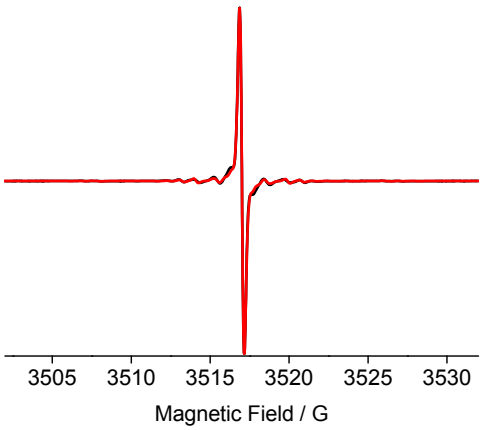

Figure S54: cw X-Band (9.86 GHz) EPR spectrum at room temperature of 4,4'''-Bis[{Bis(8-methoxycarbonyl-2,2,6,6-tetramethylbenzo-[1,2-d;4,5-d']-bis-[1,3]dithiol-4-yl)-(8-yl-2,2,6,6-tetramethylbenzo-[1,2-d;4,5-d']-bis-[1,3]dithiol-4-yl)}-methyl radical]-2,2''',5,5'''-tetramethyl-p-quaterphenyl **4••**.

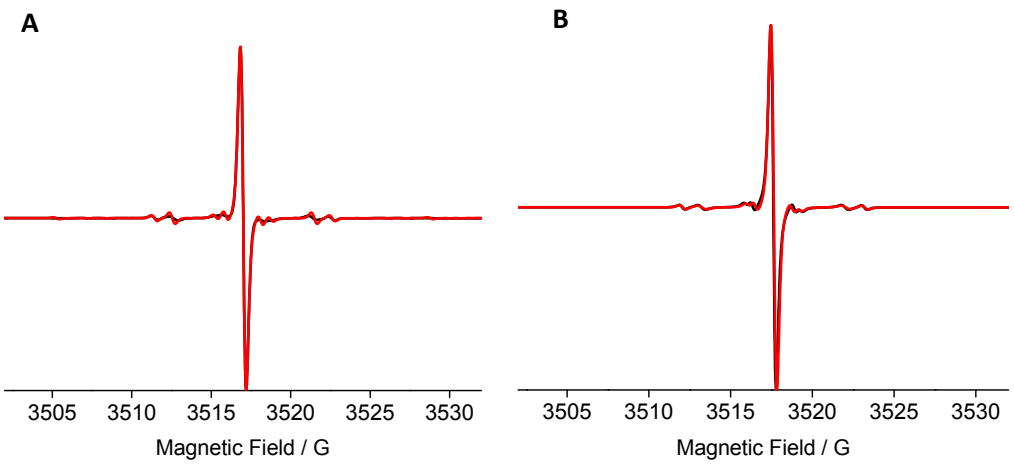

Figure S55: cw X-Band (9.86 GHz) EPR spectrum at room temperature of 4,4’’’’-Bis[{Bis(8-methoxycarbonyl-2,2,6,6-tetramethylbenzo-[1,2-d;4,5-d’]-bis-[1,3]dithiol-4-yl)-(8-yl-2,2,6,6-tetramethylbenzo-[1,2-d;4,5-d’]-bis-[1,3]dithiol-4-yl)}-methanol]-2,2'''',5,5''''-tetramethyl-2’’,3’’,5’’,6’’-tetramethoxy-2,2’’’’,5,5’’’’-tetramethyl-p-quinquephenyl **5••**. (A) Simulation assuming isotropic hyperfine coupling constants. (B) Simulation including hyperfine anisotropy from Bowman et al. and a rotational correlation time τ_{corr} of 6 ns.

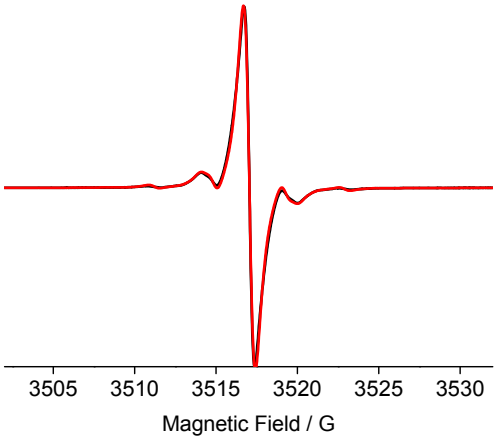

Figure S56: cw X-Band (9.86 GHz) EPR spectrum at room temperature of 1,4-Bis[{Bis(8-methoxycarbonyl-2,2,6,6-tetramethylbenzo-[1,2-d;4,5-d’]-bis-[1,3]dithiol-4-yl)-(8-yl-2,2,6,6-tetramethylbenzo-[1,2-d;4,5-d’]-bis-[1,3]dithiol-4-yl)}-methyl radical]-*p*-xylene **6••**.

Table S1: EPR parameters for the simulation* of the room temperature cw-EPR spectra at X-Band.

Compound	*g*-value	$A_{C,\ ipso}$ / MHz	$A_{C,\ ortho}$ / MHz	$A_{C,central}$ / MHz	*J* / GHz
1••	2.0031	31.2	24.9	65.1	-235
2••	2.0031	31.2	24.9	65.1	-131
3••	2.0031	31.2	24.9	65.1	-94
4••	2.0031	31.2	24.9	65.1	0.0170(1)
5••	2.0031	31.2	24.9	65.1	-
6••	2.0031	31.2	24.9	65.1	-82

*Only J of **4••** and **5••** were fitted.

4.2. cw EPR, X-band, 100K

All cw X-Band EPR spectra obtained at 100 K were measured at a frequency of 9.46 GHz with a modulation amplitude of 0.4 G, 100 kHz modulation frequency, and a microwave power of 0.004674 mW. The conversion time was set to 30.10 ms with a time constant of 20.48 ms. Before each measurement, there was a waiting time of at least 30 min to ensure proper adjustment of the temperature. The spectra were field-corrected using Mn^{2+}-doped MgO[3] as an internal standard. The spectra were fitted, using the *pepper* routine in *EasySpin*[4] assuming triplet radicals (S = 1) with a zero-field splitting parameter *D*, and an isotropic *g*-value. Best fit parameters are given in table S2.

The zero-field splitting parameter *D* depends on the distance *r* between the two spins and the orientation of distance vector *r* with respect to the external magnetic field B_0 expressed by the angle θ:

$$D = \frac{3}{4}\frac{\mu_0}{4\pi}(g_e\beta_e)^2\left\langle\frac{1-3\cos^2\theta}{r^3}\right\rangle$$

This gives rise to a distinct splitting, the so called Pake pattern. If *r* is parallel to B_0 (θ = 0°), *D* is twice as large as if r is perpendicular to B_0 (θ = 90°). The Pake pattern is only resolved in cases where *D* is larger than the linewidth, which is the case for **1$^{\bullet\bullet}$ – 3$^{\bullet\bullet}$** and **6$^{\bullet\bullet}$** but not for **4$^{\bullet\bullet}$** and **5$^{\bullet\bullet}$**.

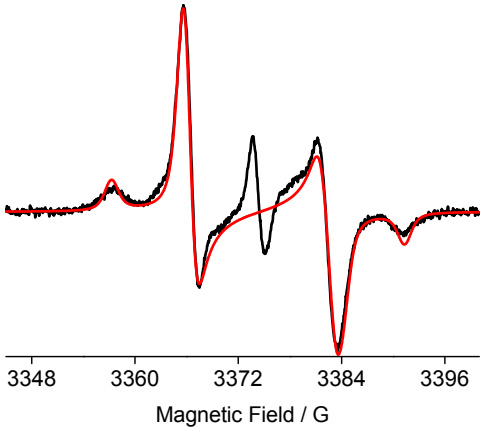

Figure S57: cw X-Band (9.46 GHz) EPR spectrum at 100 K of 1,4-Bis[{Bis(8-methoxycarbonyl-2,2,6,6-tetramethylbenzo-[1,2-d;4,5-d']-bis-[1,3]dithiol-4-yl)-(8-yl-2,2,6,6-tetramethylbenzo-[1,2-d;4,5-d']-bis-[1,3]dithiol-4-yl)}-methyl radical]-benzene **1$^{\bullet\bullet}$**. The central line was excluded from the simulation and arises from double quantum transition & residual monoradical impurities.

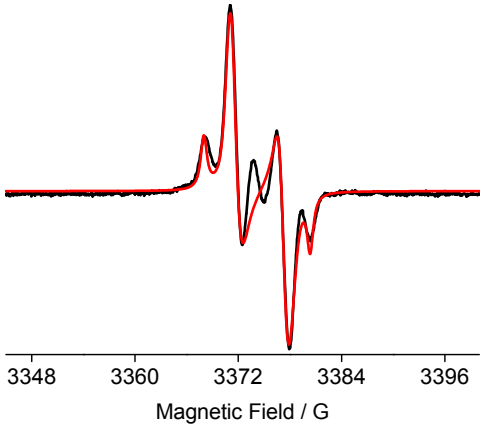

Figure S58: cw X-Band (9.46 GHz) EPR spectrum at 100 K of 4,4'-Bis[{Bis(8-methoxycarbonyl-2,2,6,6-tetramethylbenzo-[1,2-d;4,5-d']-bis-[1,3]dithiol-4-yl)-(8-yl-2,2,6,6-tetramethylbenzo-[1,2-d;4,5-d']-

bis-[1,3]dithiol-4-yl)}-methyl radical]-biphenyl **2••**. The central line was excluded from the simulation and arises from double quantum transition & residual monoradical impurities.

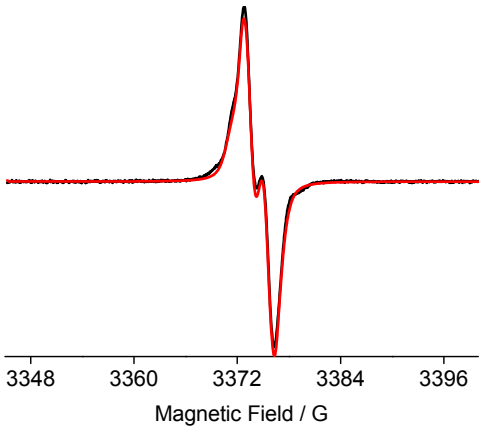

Figure S59: cw X-Band (9.46 GHz) EPR spectrum at 100 K of 4,4''-Bis[{Bis(8-methoxycarbonyl-2,2,6,6-tetramethylbenzo-[1,2-d;4,5-d']-bis-[1,3]dithiol-4-yl)-(8-yl-2,2,6,6-tetramethylbenzo-[1,2-d;4,5-d']-bis-[1,3]dithiol-4-yl)}-methyl radical]-p-terphenyl **3••**.

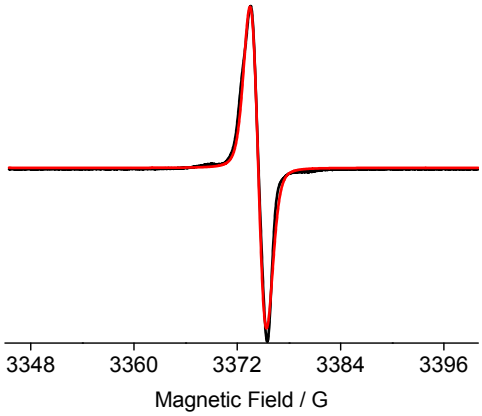

Figure S60: cw X-Band (9.46 GHz) EPR spectrum at 100 K of 4,4'''-Bis[{Bis(8-methoxycarbonyl-2,2,6,6-tetramethylbenzo-[1,2-d;4,5-d']-bis-[1,3]dithiol-4-yl)-(8-yl-2,2,6,6-tetramethylbenzo-[1,2-d;4,5-d']-bis-[1,3]dithiol-4-yl)}-methyl radical]-2,2''',5,5'''-tetramethyl- p-quaterphenyl **4••**.

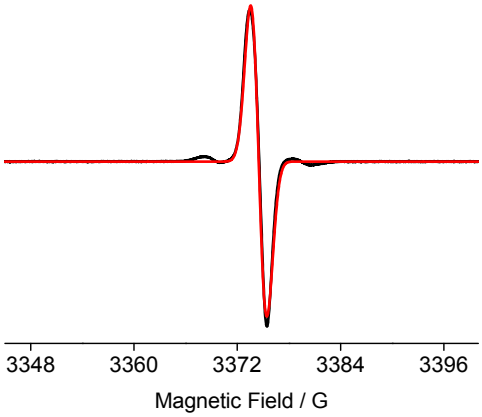

Figure S61: cw X-Band (9.46 GHz) EPR spectrum at 100 K of 4,4''''-Bis[{Bis(8-methoxycarbonyl-2,2,6,6-tetramethylbenzo-[1,2-d;4,5-d']-bis-[1,3]dithiol-4-yl)-(8-yl-2,2,6,6-tetramethylbenzo-[1,2-d;4,5-d']-bis-[1,3]dithiol-4-yl)}-methanol]-2,2''',5,5'''-tetramethyl-2'',3'',5'',6''-tetramethoxy-2,2'''',5,5''''-tetramethyl-p-quinquephenyl **5••**.

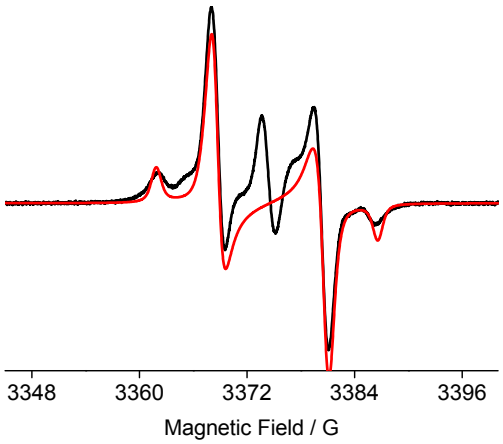

Figure S62: cw X-Band (9.46 GHz) EPR spectrum at 100 K of 1,4-Bis[{Bis(8-methoxycarbonyl-2,2,6,6-tetramethylbenzo-[1,2-d;4,5-d']-bis-[1,3]dithiol-4-yl)-(8-yl-2,2,6,6-tetramethylbenzo-[1,2-d;4,5-d']-bis-[1,3]dithiol-4-yl)}-methyl radical]-p-*xylene* **6••**.

Table S2: EPR parameters for the simulation of the cw X-Band EPR spectra at 100 K.

Comp.	*g*	*D* / MHz	*r* / Å
1••	2.0031	47.8	
2••	2.0031	17.3	
3••	2.0031	7.6	
4••	2.0031	0	-
5••	2.0031	0	-
6••	2.0031	34.7	
Mono•	2.0032	-	-

4.3. Temperature-dependent cw-EPR measurement in fluid solution, X-Band

All cw X-Band EPR spectra obtained in solution were measured at a frequency of 9.46 GHz with a modulation amplitude of 0.4 G, 100 kHz modulation frequency, and a microwave power of 0.005823 mW. The conversion time was set to 20.48 ms with a time constant of 10.24 ms. Before each measurement, there was a waiting time of at least 15 min to ensure proper adjustment of the temperature. The temperature-dependent spectra for each biradical were fitted globally using the *chili* routine in *EasySpin*[4] assuming triplet radicals (S = 1) with a zero-field splitting parameter *D* from the previous fitting of the cw spectra at 100 K, an isotropic -value, and a rotational correlation time τ_{rot}.

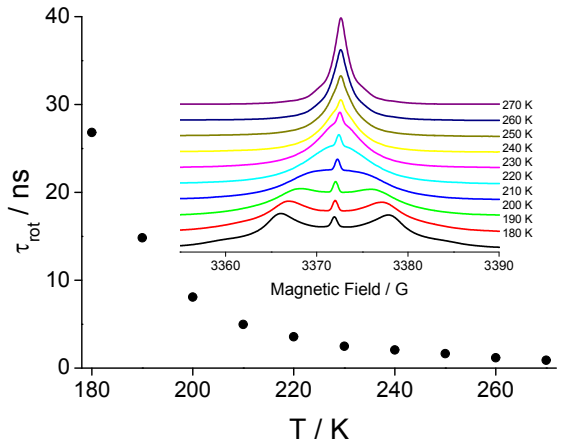

Figure S63: Temperature-dependent cw X-Band spectra of biradical **1••** and fitted rotational correlation times τ_{rot} plotted against the measurement temperature.

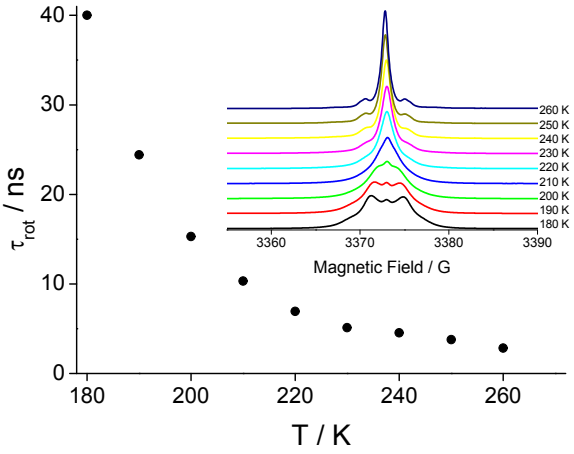

Figure S64: Temperature-dependent cw X-Band spectra of biradical **2••** and fitted rotational correlation times τ_{rot} plotted against the measurement temperature.

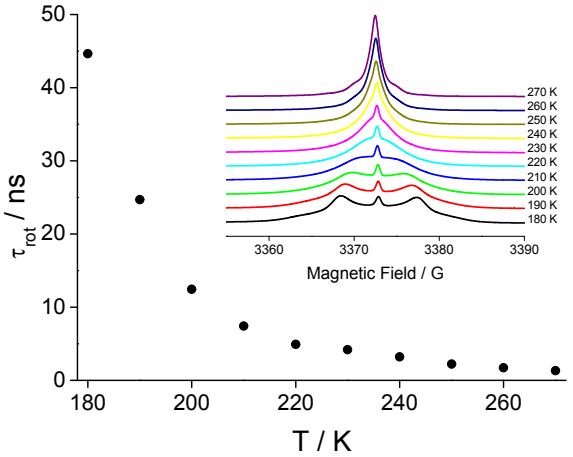

Figure S65: Temperature-dependent cw X-Band spectra of biradical **6••** and fitted rotational correlation times τ_{rot} plotted against the measurement temperature.

4.4. Temperature-dependent half-field cw-EPR measurement, X-Band

To assess the exchange coupling constant for the biradicals that are in the strong coupling limit, the half-field cw-EPR spectrum intensity was measured in dependence of the temperature.

For the analysis, the cw spectrum was first integrated. The integrated spectrum is background-corrected by a polynomial of 3rd order and then integrated again to obtain the total signal intensity. Each measurement was performed in duplicates and the exchange coupling constants obtained from the fit[5] as well as their standard deviation are shown in table S3.

Table S3: Experimental *J* values obtained from the Bleaney-Bowers fit[5] of the half-field measurements.

Compound	*J* / cm^{-1}	*J* / GHz
1••	-7.83±0.55	-235±17
2••	-4.38±1.25	-131±37
3••	-3.14±0.40	-94±12
6••	-2.72±0.30	-82±9

4.4.1. Biradical 1••

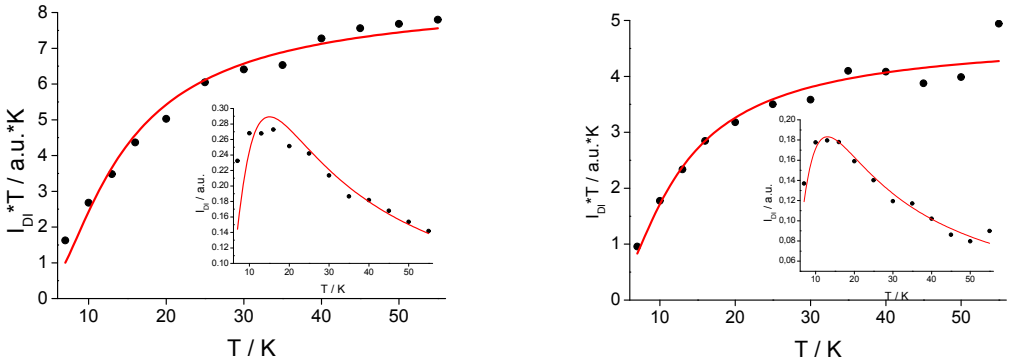

Figure S66: Bleaney-Bowers fit of the temperature-dependent half-field signal of biradical **1••** (50 µm, 11.14 mW, 1 G mod. amp.). Left: *J* = -8.38±0.39 cm^{-1}. Right: *J* = -7.28±0.50 cm^{-1}.

4.4.2. Biradical 2••

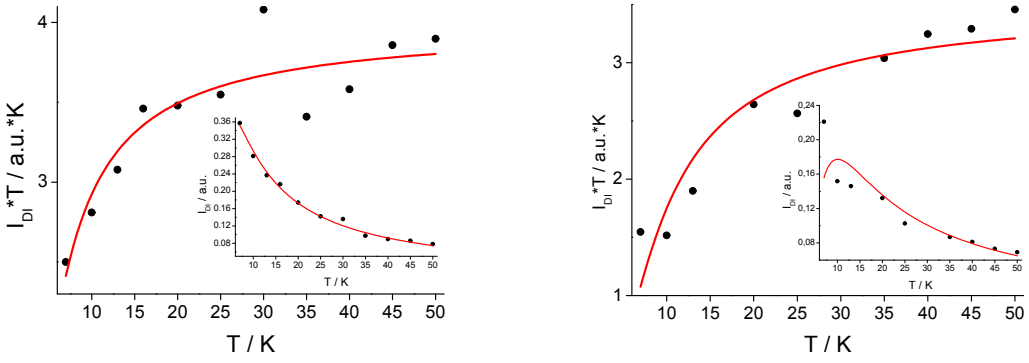

Figure S67: Bleaney-Bowers fit of the temperature-dependent half-field signal of biradical **2••** (500 µm, 11.14 mW, 1 G mod. amp.). Left: *J* = -3.13±0.36 cm^{-1}. Right: *J* = -5.62±0.30 cm^{-1}.

4.4.3. Biradical 3••

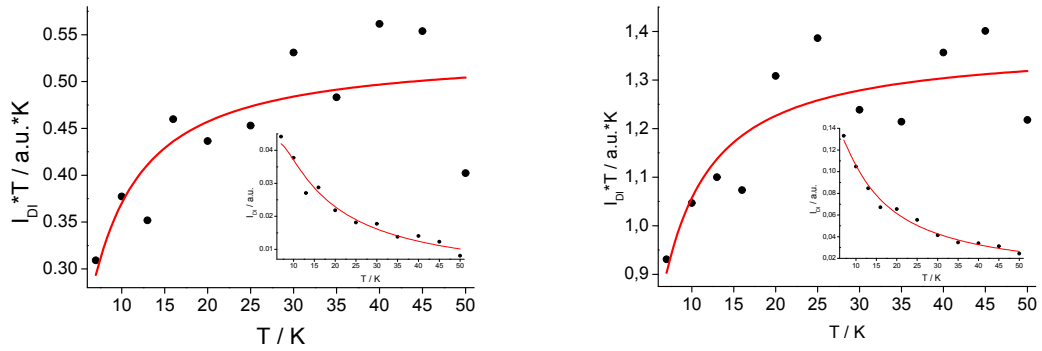

Figure S68: Bleaney-Bowers fit of the temperature-dependent half-field signal of biradical **3••** (500 µm, 86.41 mW, 1 G mod. amp.). Left: J = -3.53±0.70 cm^{-1}. Right: J = -2.74±0.46 cm^{-1}.

4..4. Biradical 6••

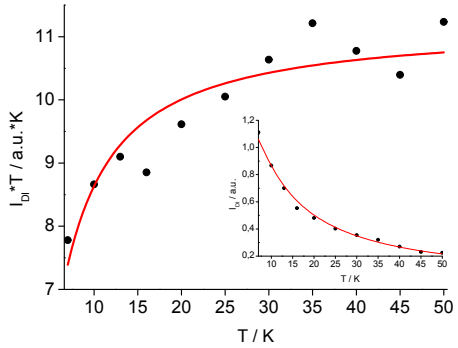

Figure S69: Bleaney-Bowers fit of the temperature-dependent half-field signal of biradical **6••** (500 µm, 86.41 mW, 1 G mod. amp.). J = -2.73±0.30 cm^{-1}.

5. Pulsed EPR data

5.1. Echo-detected field-swept EPR spectra, Q-Band

Echo-detected field-swept spectra of the frozen solutions were detected at 80 K and Q-band frequency (33.7 GHz) with a power attenuation of 2 dB. The PulseSpel parameters used for the detection are shown in table S3.

Table S4: PulseSpel parameters for the echo-detected field-swept EPR spectra at 80 K.

Parameter	Value
π/2	12 ns
π	24 ns
τ_1	250 ns
Shots per point	10
Shot Repetition Time	10000 µs
Scans	1
Number of points	1024
Center field	33.7 GHz
Sweep width	100 G

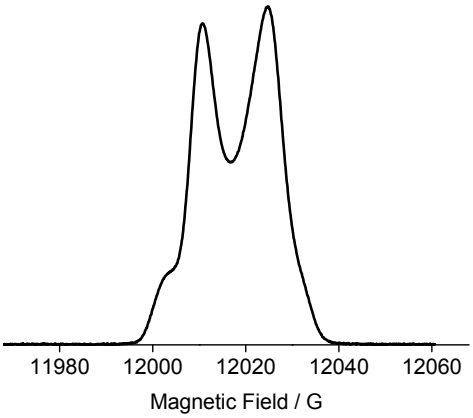

Figure S70: Echo-detected field-swept EPR spectrum at 80 K of 1,4-Bis[{Bis(8-methoxycarbonyl-2,2,6,6-tetramethylbenzo-[1,2-d;4,5-d']-bis-[1,3]dithiol-4-yl)-(8-yl-2,2,6,6-tetramethylbenzo-[1,2-d;4,5-d']-bis-[1,3]dithiol-4-yl)}-methyl radical]-benzene **1$^{\bullet\bullet}$**.

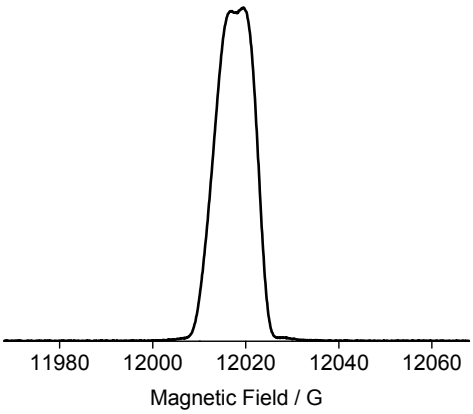

Figure S71: Echo-detected field-swept EPR spectrum at 80 K of 4,4'-Bis[{Bis(8-methoxycarbonyl-2,2,6,6-tetramethylbenzo-[1,2-d;4,5-d']-bis-[1,3]dithiol-4-yl)-(8-yl-2,2,6,6-tetramethylbenzo-[1,2-d;4,5-d']-bis-[1,3]dithiol-4-yl)}-methyl radical]-biphenyl **2$^{\bullet\bullet}$**.

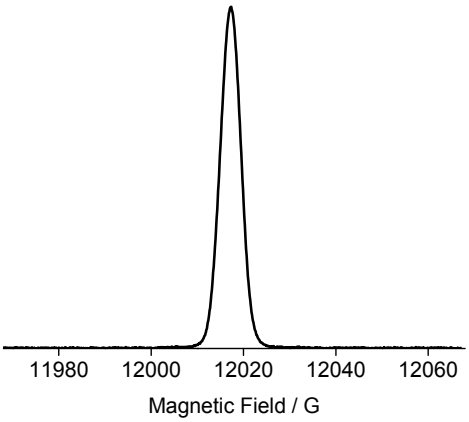

Figure S72: Echo-detected field-swept EPR spectrum at 80 K of 4,4''-Bis[{Bis(8-methoxycarbonyl-2,2,6,6-tetramethylbenzo-[1,2-d;4,5-d']-bis-[1,3]dithiol-4-yl)-(8-yl-2,2,6,6-tetramethylbenzo-[1,2-d;4,5-d']-bis-[1,3]dithiol-4-yl)}-methyl radical]-*p*-terphenyl **3$^{\bullet\bullet}$**.

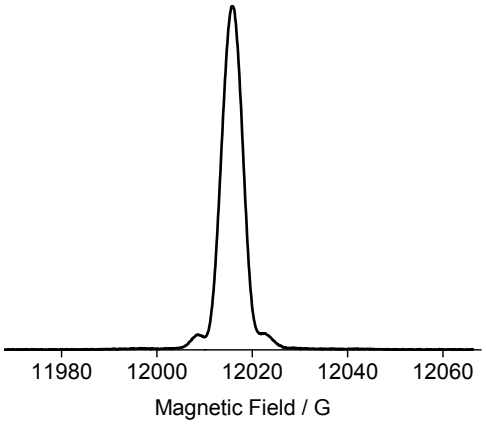

Figure S73: Echo-detected field-swept EPR spectrum at 80 K of 4,4’’’-Bis[{Bis(8-methoxycarbonyl-2,2,6,6-tetramethylbenzo-[1,2-d;4,5-d’]-bis-[1,3]dithiol-4-yl)-(8-yl-2,2,6,6-tetramethylbenzo-[1,2-d;4,5-d’]-bis-[1,3]dithiol-4-yl)}-methyl radical]-2,2''',5,5'''-tetramethyl-*p*-quaterphenyl **4••**.

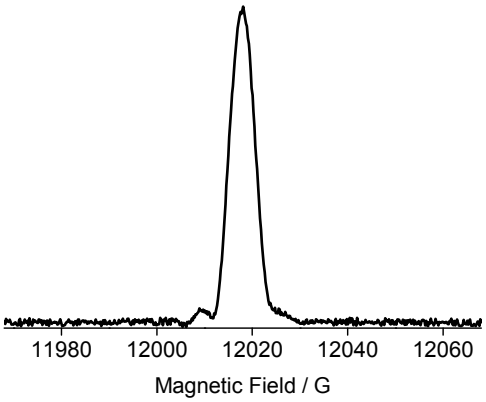

Figure S74: Echo-detected field-swept EPR spectrum at 80 K of 4,4’’’’-Bis[{Bis(8-methoxycarbonyl-2,2,6,6-tetramethylbenzo-[1,2-d;4,5-d’]-bis-[1,3]dithiol-4-yl)-(8-yl-2,2,6,6-tetramethylbenzo-[1,2-d;4,5-d’]-bis-[1,3]dithiol-4-yl)}-methanol]-2,2''',5,5'''-tetramethyl-2’’,3’’,5’’,6’’-tetramethoxy-2,2’’’’,5,5’’’’-tetramethyl-*p*-quinquephenyl **5••**.

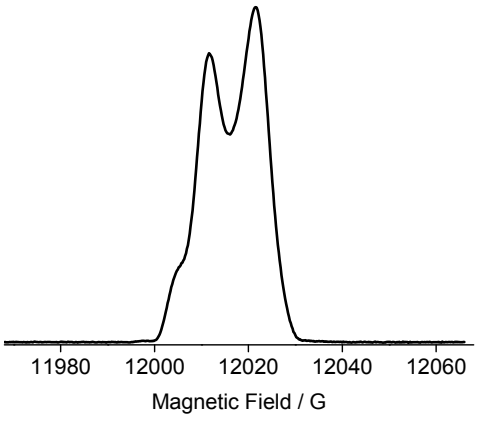

Figure S75: Echo-detected field-swept EPR spectrum at 80 K of 1,4-Bis[{Bis(8-methoxycarbonyl-2,2,6,6-tetramethylbenzo-[1,2-d;4,5-d’]-bis-[1,3]dithiol-4-yl)-(8-yl-2,2,6,6-tetramethylbenzo-[1,2-d;4,5-d’]-bis-[1,3]dithiol-4-yl)}-methyl radical]-*p*-xylene **6••**.

Echo-detected field-swept spectra of the liquid solutions were detected at room temperature and Q-band frequency (33.7 GHz) with a power attenuation of 3 dB. Echoes were only observed for biradicals 3-5. The PulseSpel parameters used for the detection are shown in table S4.

Table S5: PulseSpel parameters for the echo-detected field-swept EPR spectra at room temperature.

Parameter	Value
π/2	16 ns
π	32 ns
τ_1	1800 ns
Shots per point	50
Shot Repetition Time	2000 µs

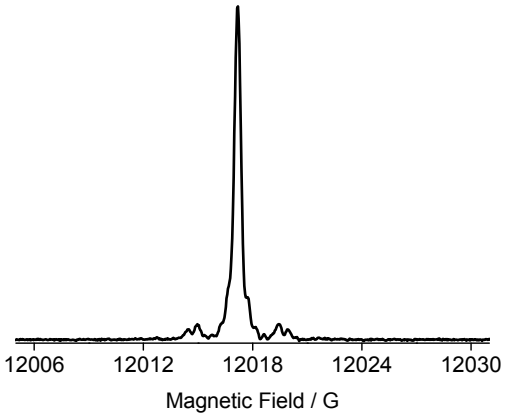

Figure S76: Echo-detected field-swept EPR spectrum at room temperature of 4,4''-Bis[{Bis(8-methoxycarbonyl-2,2,6,6-tetramethylbenzo-[1,2-d;4,5-d']-bis-[1,3]dithiol-4-yl)-(8-yl-2,2,6,6-tetramethylbenzo-[1,2-d;4,5-d']-bis-[1,3]dithiol-4-yl)}-methyl radical]-p-terphenyl ***3***$^{\bullet\bullet}$.

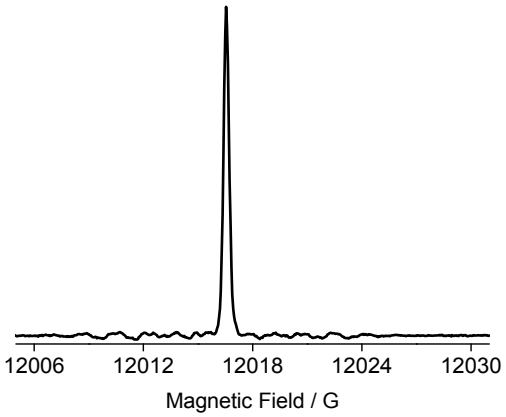

Figure S77: Echo-detected field-swept EPR spectrum at room temperature of 4,4'''-Bis[{Bis(8-methoxycarbonyl-2,2,6,6-tetramethylbenzo-[1,2-d;4,5-d']-bis-[1,3]dithiol-4-yl)-(8-yl-2,2,6,6-tetramethylbenzo-[1,2-d;4,5-d']-bis-[1,3]dithiol-4-yl)}-methyl radical]-2,2''',5,5'''-tetramethyl-p-quaterphenyl ***4***$^{\bullet\bullet}$.

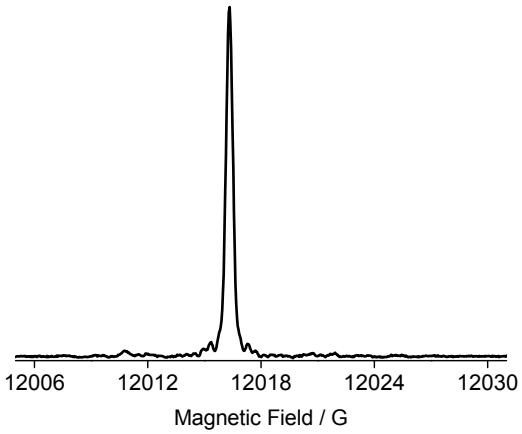

Figure S78: Echo-detected field-swept EPR spectrum at room temperature of 4,4’’’’-Bis[{Bis(8-methoxycarbonyl-2,2,6,6-tetramethylbenzo-[1,2-d;4,5-d’]-bis-[1,3]dithiol-4-yl)-(8-yl-2,2,6,6-tetramethylbenzo-[1,2-d;4,5-d’]-bis-[1,3]dithiol-4-yl)}-methanol]-2,2''',5,5'''-tetramethyl-2’’,3’’,5’’,6’’-tetramethoxy-2,2’’’’,5,5’’’’-tetramethyl-p-quinquephenyl ***5*••**.

5.2. T_m and T_1 at room temperature and 80 K, Q-Band

Two-pulse ESEEM and Inversion recovery experiments were performed using the same parameters as for the measurement of the field sweeps. The delay after the inversion pulse for the inversion recovery experiment was set to 400 ns. In the case of biradical **5••**, the power attenuation was set to 8 dB and 12 dB for the measurement at 80 K and at room temperature, respectively. The inversion recovery curves were fitted with a mono-exponential decay:

$$\mathrm{I(T)} = \mathrm{A}\left(1 - \mathrm{e}^{-\frac{\mathrm{T}}{\mathrm{T_1}}}\right)$$

The two-pulse ESEEM experiments were simulated using the following stretched exponential decay:

$$\mathrm{I}(2\tau) = \mathrm{A}\mathrm{e}^{\left(-\frac{2\tau}{\mathrm{T_m}}\right)^{\mathrm{b}}}$$

Best-fit parameters are summarized in tables S5 and S6 for the low temperature and room temperature experiments, respectively.

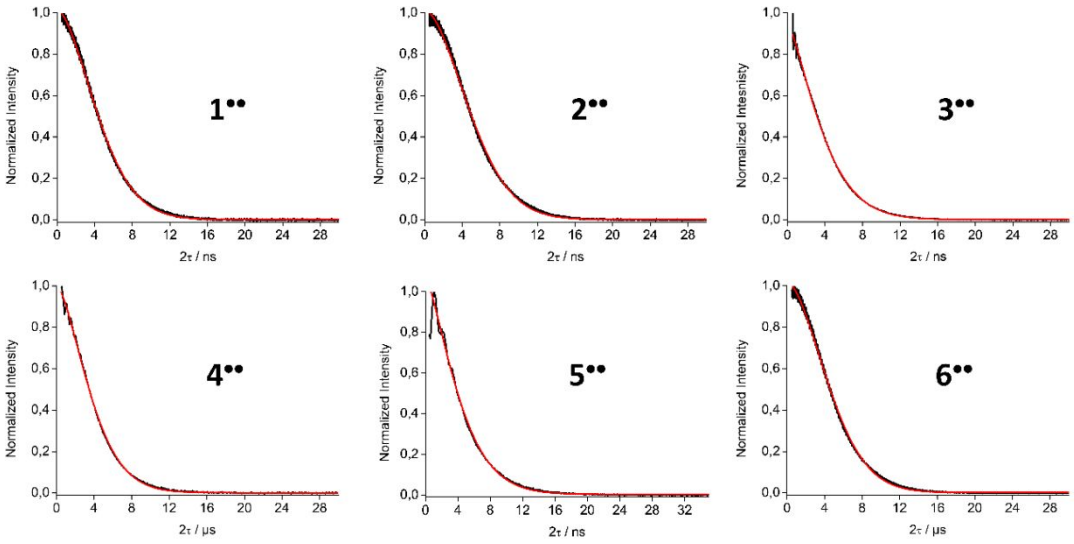

Figure S79: Two-pulse ESEEM data at 80 K for biradicals **1•• – 6••**. **Black:** experimental data, **Red:** stretched exponential fit.

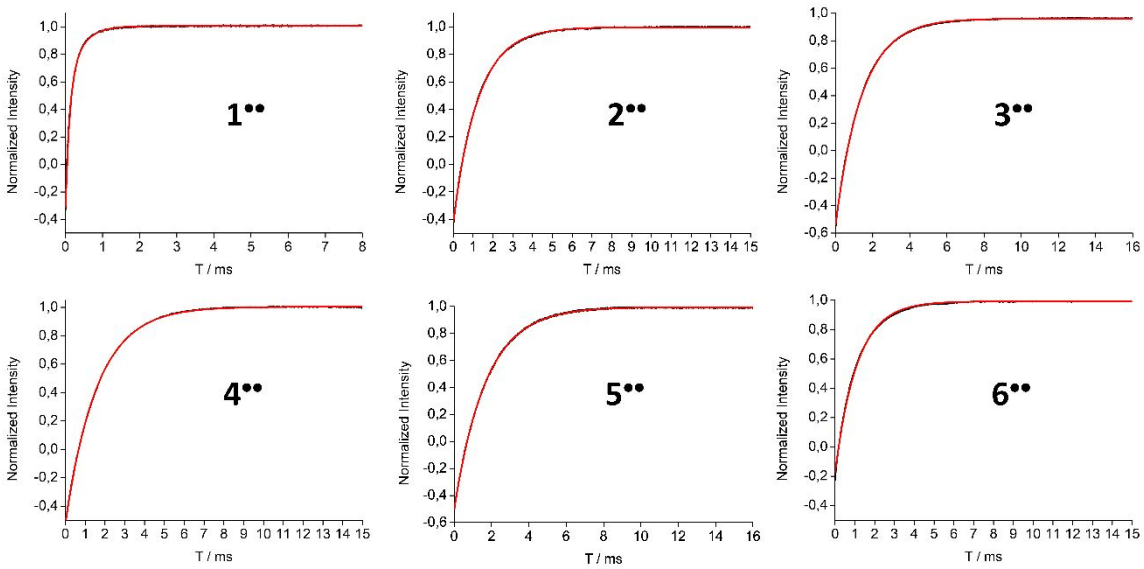

Figure S80: Inversion recovery data at 80 K for biradicals **1•• – 6••**. **Black:** experimental data, **Red:** mono-exponential fit.

Table S6: Fitting parameters for the echo-decays of the two-pulse ESEEM and inversion recovery experiments at 80 K for biradicals **1•• – 6••**.

Compound	T_m / µs	b	T_1 / ms
1••	5.40±0.01	1.68±0.01	0.38±0.01 (36%); 0.11±0.01 (64%)
2••	6.10±0.01	1.76±0.01	1.26±0.00
3••	4.35±0.02	1.37±0.01	1.43±0.00
4••	4.38±0.01	1.52±0.01	1.61±0.00
5••	4.84±0.03	1.36±0.02	1.70±0.00
6••	5.60±0.01	1.71±0.01	1.11±0.00

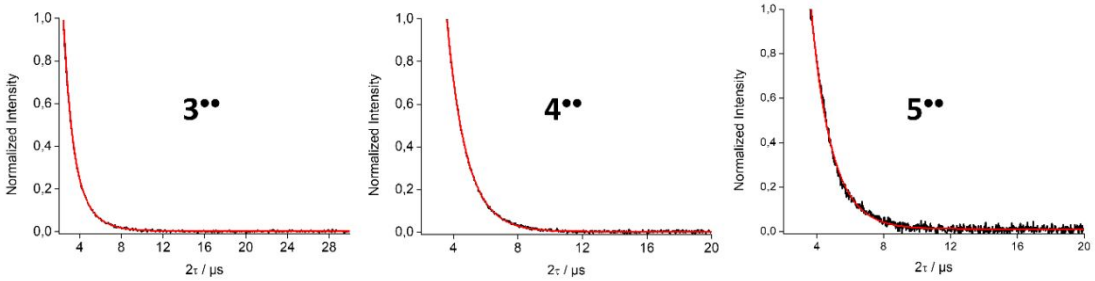

Figure S81: Two-pulse ESEEM data at room temperature for biradicals **3•• – 5••**. **Black:** experimental data, **Red:** mono-exponential fit.

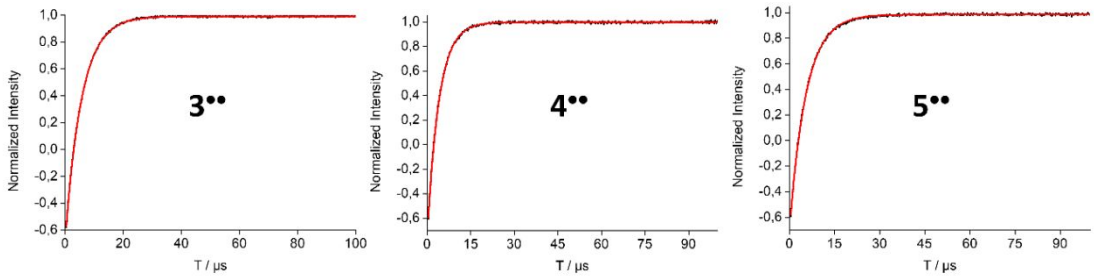

Figure S82: Inversion recovery data at 80 K for biradicals **3•• – 5••**. **Black:** experimental data, **Red:** mono-exponential fit.

Table S7: Fitting parameters for the echo-decays of the two-pulse ESEEM and inversion recovery experiments at room temperature for biradicals **3•• – 5••**.

Compound	T_m / µs	T_1 / µs
3••	1.16±0.01	5.64±0.01
4••	1.21±0.00	4.02±0.01
5••	1.25±0.01	5.51±0.01

5.3. Double Quantum Coherence Experiments (DQC)

The double quantum coherence experiments were performed at the maximum of the echo-detected field-swept EPR spectra of samples **2•• – 5••**. The DQC experiment consists of a six-pulse sequence of the following form: $\pi/2–\tau_1–\pi–\tau_1–\pi/2–T–\pi–T–\pi/2–\tau_2–\pi–\tau_2–$echo.[6,7] The inter-pulse delays τ_1 and τ_2 are incremented and decremented, respectively. In the experiment the echo intensity is shown a function of τ_1- τ_2. A standard 64-step phase-cycle was used to avoid unwanted echoes. The microwave phase was adjusted using the Hahn echo sequence. Here, the echo in the real channel was maximized.

Each measurement was performed at 80 K with the PulseSpel parameters given in the following table S8.

All datasets were mirrored around zero and then analyzed using the DEERAnalysis toolbox[8] in Matlab. The automated comparative DEER analyzer was used for the data assessment. Here, the consensus between the automated Tikhonov regularization and the DEERNet distribution is calculated. The consensus fit, background, and distribution are shown in the following figures. The distributions in the main article are the ones from the automated Tikhonov regularization. Biradical **6••** could only be analyzed by a conventional Tikhonov regularization.

Table S8: PulseSpel parameters used for the detection of the DQC time traces of compounds **2•• – 6••**.

Compound	$\pi/2$	π	τ_1	τ_1 increment τ_2 decrement	τ_2	T	Shots per point	Shot repetition time
2••	12 ns	24 ns	240 ns	2 ns	240 ns	50 ns	3	2000 µs
3••	12 ns	24 ns	250 ns	2 ns	250 ns	50 ns	10	3500 µs
4••	10 ns	20 ns	250 ns	4 ns	250 ns	50 ns	3	7000 µs
5••	12 ns	24 ns	250 ns	4 ns	250 ns	50 ns	3	8000 µs
6••	12 ns	24 ns	250 ns	2 ns	250 ns	50 ns	3	4000 µs

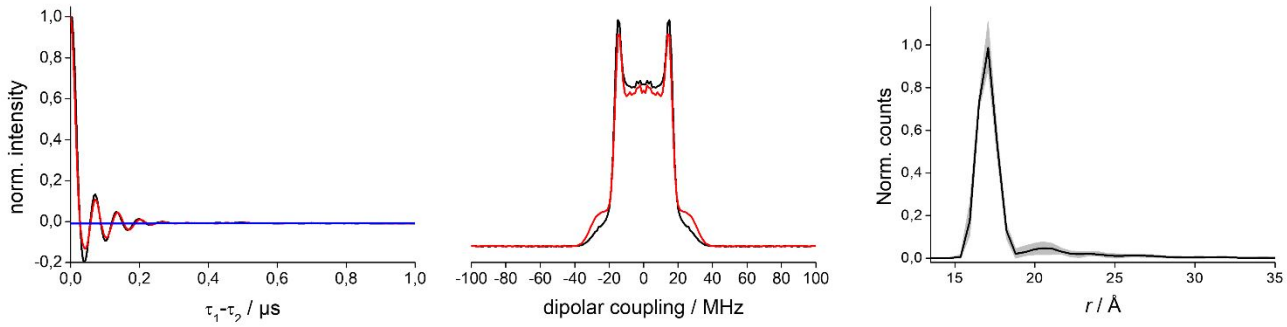

Figure S83: DQC data obtained for biradical **2••**. The experimental data are shown in black, the fits after the consensus analysis are shown in red, and the background in blue. **Left:** Experimental time trace and consensus fit. **Middle:** Experimental Pake pattern and fit. **Right:** Consensus distance distribution and its validation shown as the grey area.

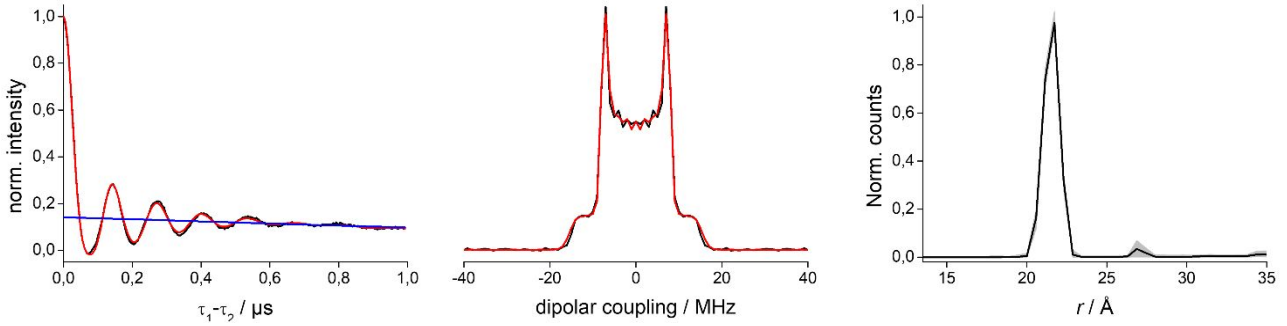

Figure S84: DQC data obtained for biradical **3••**. The experimental data are shown in black, the fits after the consensus analysis are shown in red, and the background in blue. **Left:** Experimental time trace and consensus fit. **Middle:** Experimental Pake pattern and fit. **Right:** Consensus distance distribution and its validation shown as the grey area.

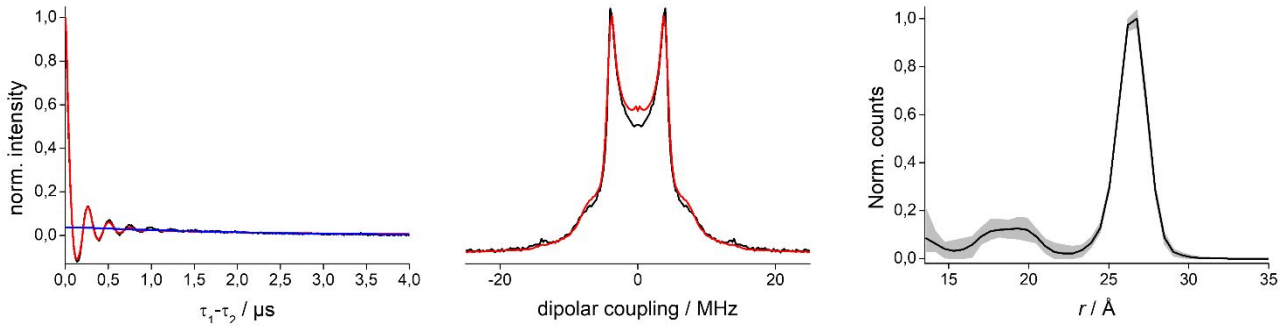

Figure S85: DQC data obtained for biradical **4••**. The experimental data are shown in black, the fits after the consensus analysis are shown in red, and the background in blue. **Left:** Experimental time trace and consensus fit. **Middle:** Experimental Pake pattern and fit. **Right:** Consensus distance distribution and its validation shown as the grey area.

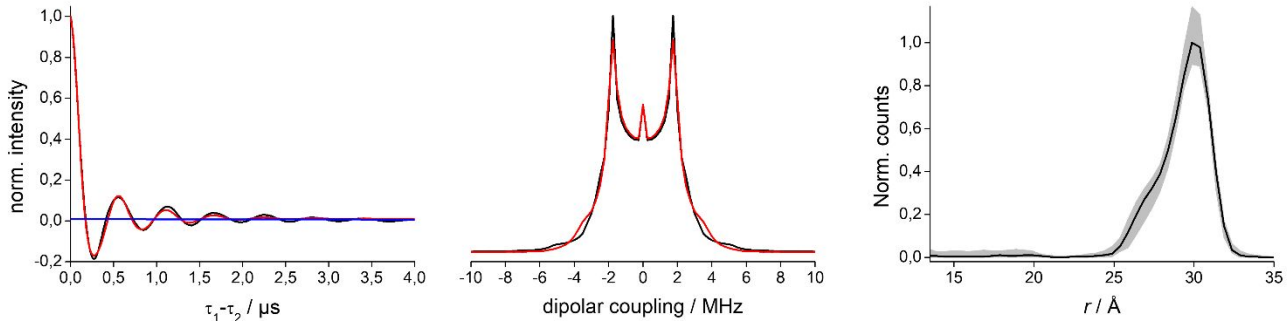

Figure S86: DQC data obtained for biradical **5••**. The experimental data are shown in black, the fits after the consensus analysis are shown in red, and the background in blue. **Left:** Experimental time trace and consensus fit. **Middle:** Experimental Pake pattern and fit. **Right:** Consensus distance distribution and its validation shown as the grey area.

For biradical **5••**, a shoulder appears in the distance distribution at shorter distances, which has been observed for a trityl biradical of similar length before.[9] The observation was explained by the occurrence of dipolar coupling in both the weak and the strong coupling limit. Based on the differences in the **g**-tensor components, the difference in Larmor frequency between the tritys Δω can be as large as 16 MHz at Q-band. In turn, and again depending on the trityl orientation, Δω can become smaller than ω_D, causing the dipolar coupling to be in the strong coupling limit. In that case, the distances appear to be times shorter. This effect is not important for the other biradicals, because their large J-values diminish the differences in the g-values, causing the large dipolar coupling to be always in the strong coupling limit.

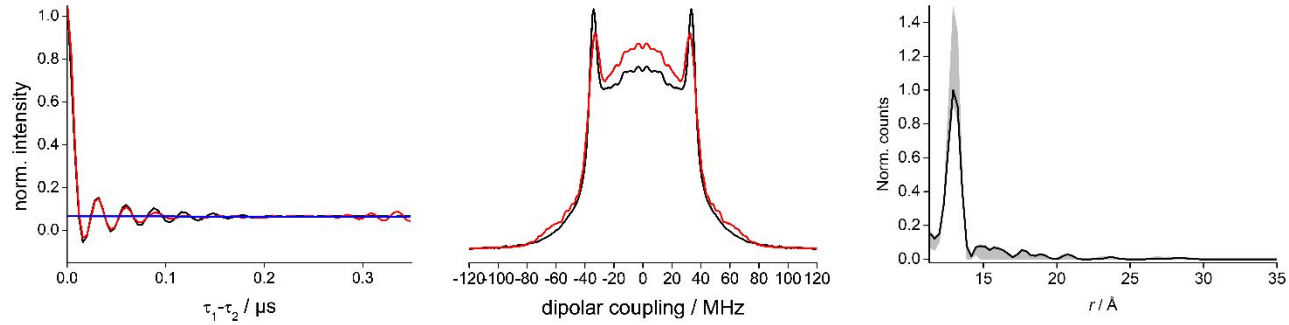

Figure S87: DQC data obtained for biradical **6••**. The experimental data are shown in black, the fits after the *Tikhonov regularization* are shown in red, and the background in blue. **Left:** Experimental time trace and *fit*. **Middle:** Experimental Pake pattern and fit. **Right:** *D*istance distribution and its validation shown as the grey area.

6. Distance dependence of exchange coupling

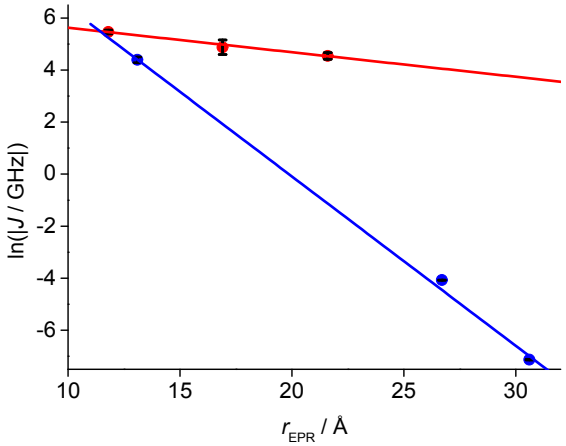

Figure S88: Distance dependence of *J*. Plot of the experimentally determined *J*s for **1•• – 6••** against r_{EPR}. The standard deviations are given as black bars. The exponential fits are shown as dashed lines. Blue: β = 0.65(2) Å^{-1}. Red: β = 0.09(1) Å^{-1}.

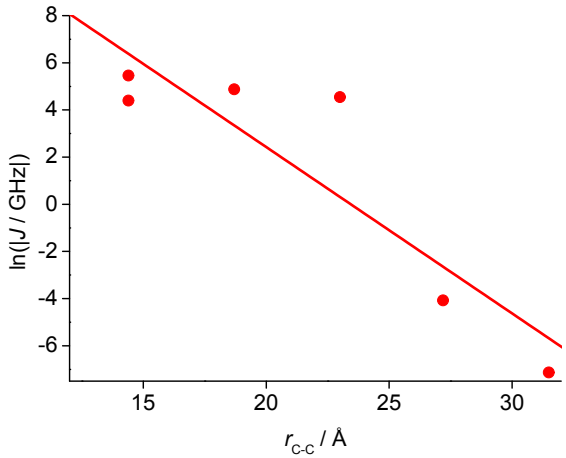

Figure S89: Distance dependence of *J*. Plot of the experimentally determined *J*s for **1•• – 6••** against r_{C-C}. The standard deviations are given as black bars. The exponential fit using all biradicals is shown as a red curve. β = 0.71(17) Å^{-1}.

7. Computational Data

7.1. General procedures and results

All quantum chemical calculations were performed using the ORCA software package (version 6.0.1).[10,11] Each molecule was considered to be a neutral open shell triplet species.

For the geometry optimization every structure was preoptimized using semi-empirical tight binding model GFN2-xTB (version 6.6.1).[12] After preoptimization each structure was further optimized using unrestricted Kohn-Sham (UKS) DFT without constraining any part of the molecule. The optimization was done using r^{2}SCAN-3c/def2-mTZVPP level of theory[13] and with a D4 London dispersion correction.[14] The structures were visualized using the Avogadro software (version 1.2.0).[15] Using the optimized structures, the exchange coupling constant *J* was determined by performing a broken symmetry calculation (keyword "BrokenSym 1,1" in the scf block) with the following convention:

$$J = -\frac{E_{HS} - E_{BS}}{\langle S^2 \rangle_{HS} - \langle S^2 \rangle_{BS}}$$

where E_{HS} is the energy of the high-spin state and E_{BS} is the energy of the broken symmetry state. The exchange coupling constant was determined using eight different functionals, i.e., M06L,[16] TPSS,[17] r²SCAN-3c, TPSSh-D4,[17,18] B3LYP-D4,[19] PBE0-D4,[20–22] ωB97X-D4rev,[23–25] and ωB97X-V.[23,26] In each case a def2-TZVP[27] basis set was employed.

For the determination of the inter-spin distances $r_{spin\text{-}spin}$, the Mulliken spin density population in each structure was taken into account. The distances were weighted using the following formulas:

$$\omega_D = \frac{\mu_0 g^2 \beta_e{}^2}{4\pi h} \sum_{a=1}^{i} \sum_{b=i+1}^{N} \frac{1}{r_{ab}{}^3} \rho_a \rho_b$$

$$r_{spin-spin} = \sqrt[3]{\frac{\mu_0 g^2 \beta_e{}^2}{4\pi h} \cdot \frac{1}{\omega_D}}$$

The summary of the data is shown in table S10.

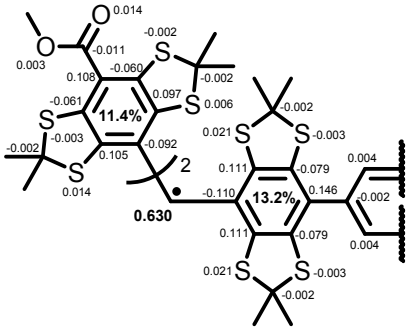

Figure S90: Spin density populations of **1••** obtained from the r²SCAN-3c/def2-mTZVPP level of theory.

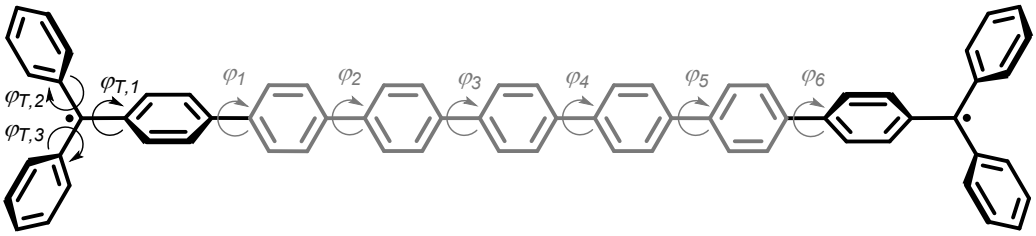

Figure S91. Simplified structure of oligo(p-phenylene)-bridged trityl biradical and assignment of dihedral angles φ_i and $\varphi_{T,i}$.

Table S9. Dihedral angles $\varphi_{T,i}$ of the trityl phenyl units relative to the trityl plane (see Figure S91) calculated for biradicals **1•• – 6••**.

Comp.	$\varphi_{T,1}$ / °	$\varphi_{T,2}$ / °	$\varphi_{T,3}$ / °
1••	45.2	46.0	43.5
2••	45.2	45.9	43.2
3••	44.6	46.1	42.4
4••	44.5	47.0	43.7
5••	44.5	46.9	43.7
6••	45.0	46.9	42.9

Table S10: Geometrical C-C distances of the central carbons of each trityl, Inter-spin distances, and dihedral angles between the phenyl units φ_i (see Figure S91) calculated for biradicals **1•• – 6••**.

Comp.	$r_{C\text{-}C}$ / Å	$r_{spin\text{-}spin}$ / Å	φ_1 / °	φ_2 / °	φ_3 / °	φ_4 / °	φ_5 / °	φ_6 / °
1••	14.4	13.2	63.1	63.1	-	-	-	-
2••	18.7	18.3	64.1	37.3	64.5	-	-	-
3••	23.0	22.9	65.2	39.0	39.1	64.4	-	-
4••	27.2	26.9	81.6	50.7	38.7	53.1	83.3	-
5••	31.5	31.4	79.5	51.7	50.1	61.3	55.9	81.1
6••	14.4	13.4	79.9	80.5	-	-	-	-

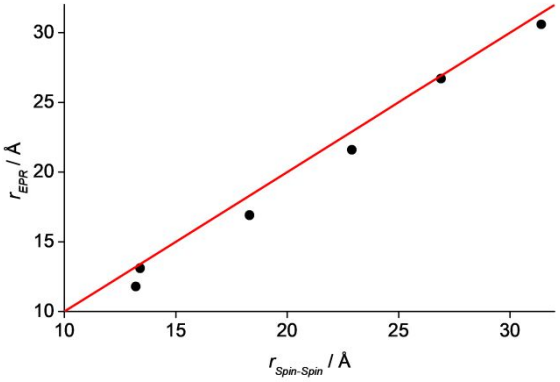

Figure S92. Plot of the experimental inter-spin distances r_{EPR} (average of r_{DQC} and r_{cw} in Table 1) against the geometric distances $r_{C\text{-}C}$. The red line indicates the 1:1 correlation.

Table S11: Square cosine of φ_i (see Figure S91) calculated for biradicals **1•• – 6••**.

Comp.	$cos^2\varphi_1$	$cos^2\varphi_2$	$cos^2\varphi_3$	$cos^2\varphi_4$	$cos^2\varphi_5$	$cos^2\varphi_6$	$\prod_i^n \cos^2\varphi_i$	J_{exp} / GHz
1••	0.205	0.205	-	-	-	-	0.0419	-235(17)
2••	0.191	0.633	0.185	-	-	-	0.0224	-131(37)
3••	0.176	0.604	0.602	0.187	-	-	0.0119	-94(12)
4••	0.021	0.401	0.609	0.361	0.014	-	0.0000	|0.0170(1)|
5••	0.033	0.384	0.411	0.231	0.314	0.024	0.0004	<|0.0008|
6••	0.031	0.027	-	-	-	-	0.0008	-82(9)

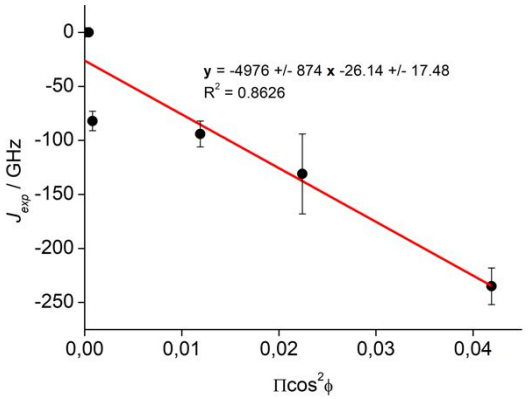

Figure S93: Plot of J versus $\prod_i^n cos^2\varphi_i$.

Table S12: Average condensed spin density on diradical carbons of **1•• – 6••** at triplet state.

Comp.	M06L	TPSS	r²SCAN-3c	TPSSh-D4	B3LYP-D4	PBE0-D4	ωB97X-D4rev	ωB97X-V
1••	1.117	0.643	0.657	0.689	0.643	0.720	0.637	0.637
2••	1.109	0.642	0.656	0.689	0.642	0.719	0.636	0.636
3••	1.130	0.654	0.666	0.699	0.651	0.728	0.644	0.644
4••	1.101	0.651	0.662	0.695	0.647	0.724	0.639	0.639
5••	1.101	0.649	0.661	0.694	0.646	0.723	0.638	0.638
6••	1.097	0.648	0.661	0.693	0.645	0.722	0.638	0.638

7.2. DFT-optimized structures, spin density plots, frontiers orbitals and coordinates

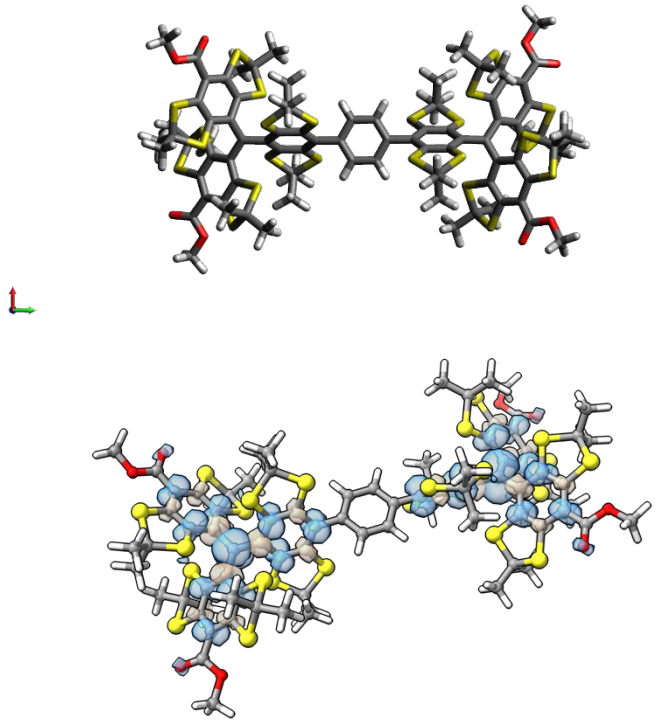

Figure S94: DFT-optimized structure and spin density surface (isovalue ±0.002) of biradical **1**$^{\bullet\bullet}$.

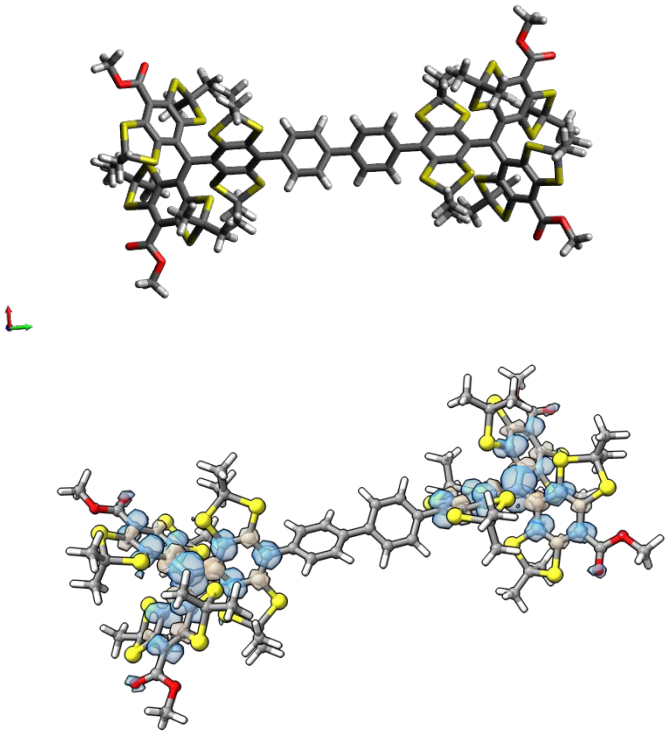

Figure S93: DFT-optimized structure and spin density surface (isovalue ±0.002) of biradical **2**$^{\bullet\bullet}$.

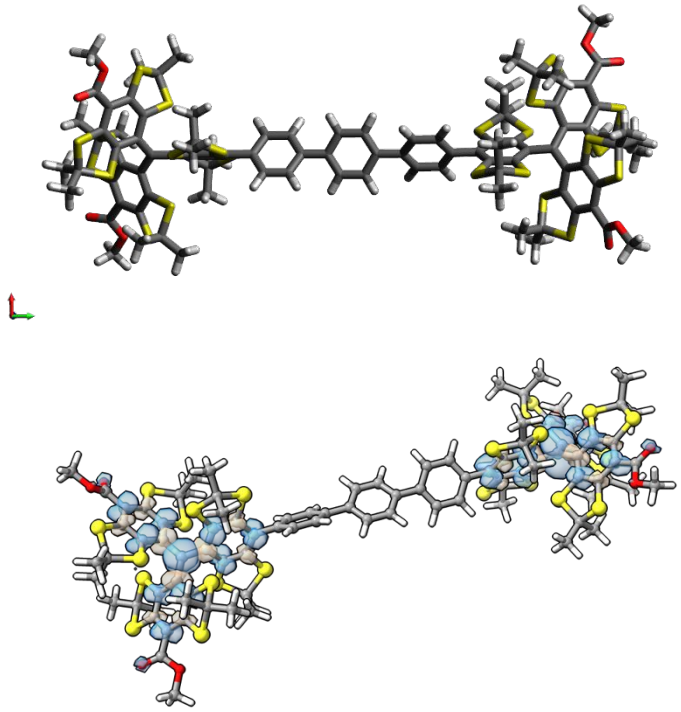

Figure S94: DFT-optimized structure and spin density surface (isovalue ±0.002) of biradical **3••**.

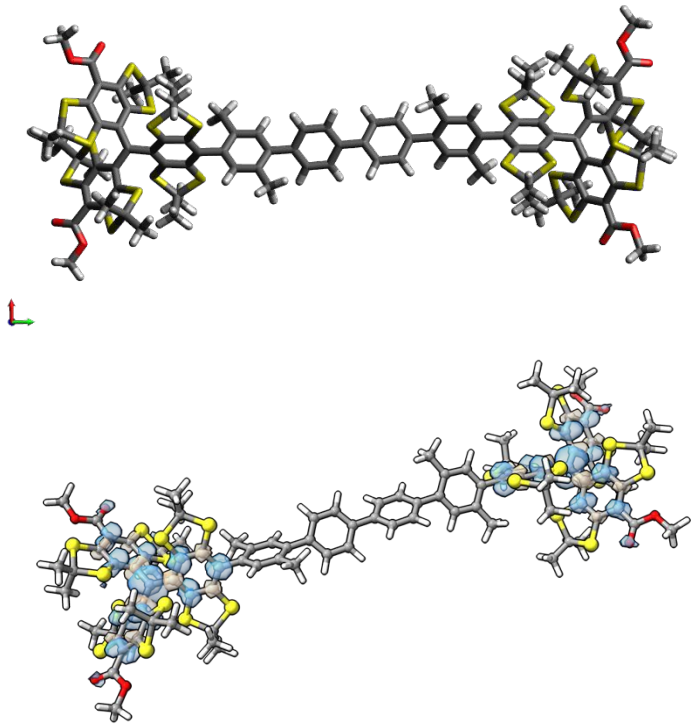

Figure S95: DFT-optimized structure and spin density surface (isovalue ±0.002) of biradical **4••**.

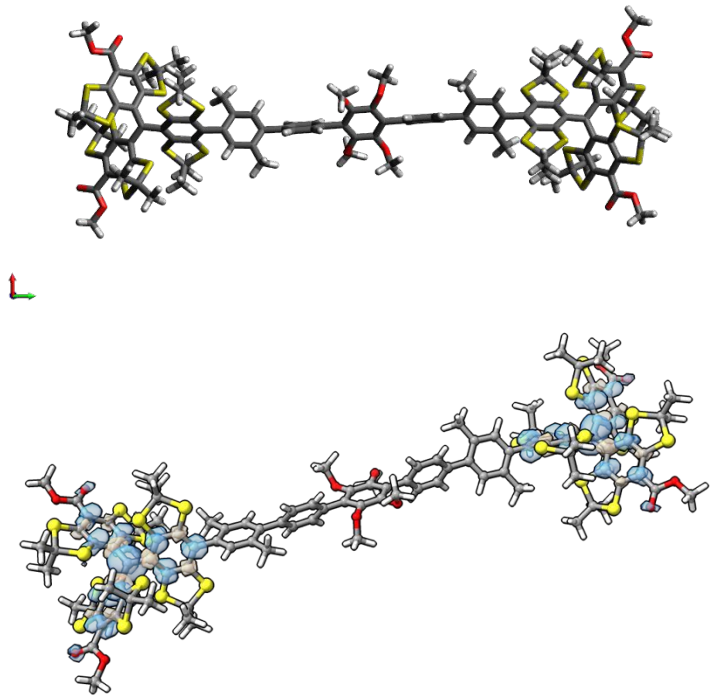

Figure S96: DFT-optimized structure and spin density surface (isovalue ±0.002) of biradical **5**••.

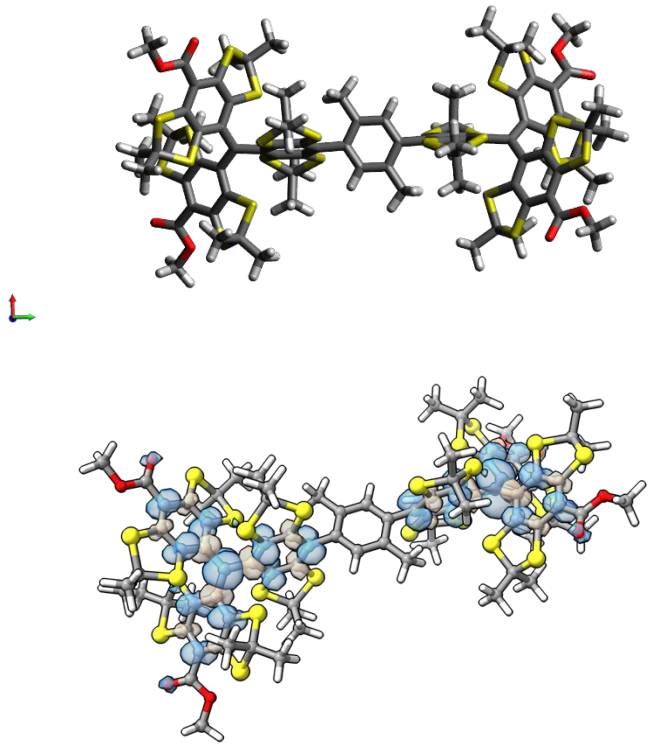

Figure S97: DFT-optimized structure and spin density surface (isovalue ±0.002) of biradical ***6***••.

Coordinates of the structures shown above, calculated with r^{2}SCAN-3c/def2-mTZVPP:

Biradical **1**••

C	2.16172	9.72621	1.67391	C	1.04651	9.01791	1.21315

C	1.18991	7.93046	0.32826	C	-2.17133	-9.72004	1.67004
C	2.49327	7.57569	-0.07712	C	-1.05287	-9.01383	1.21401
C	3.61416	8.28062	0.37426	C	-1.19046	-7.92664	0.32787
C	3.45836	9.36305	1.26327	C	-2.49138	-7.56972	-0.08335
S	2.80319	6.25361	-1.21439	C	-3.61550	-8.27250	0.36338
C	4.41594	6.95493	-1.78455	C	-3.46552	-9.35486	1.25346
S	5.16908	7.73312	-0.28261	S	-2.79395	-6.24733	-1.22227
S	1.82867	11.05861	2.79084	C	-4.40560	-6.94559	-1.79915
C	0.20106	10.35745	3.33453	S	-5.16654	-7.72244	-0.30046
S	-0.52224	9.55874	1.83160	S	-1.84559	-11.05253	2.78907
C	0.41276	9.31832	4.43065	C	-0.21912	-10.35417	3.33960
C	-0.71000	11.48951	3.79200	S	0.51218	-9.55703	1.83971
C	5.31480	5.82625	-2.27323	C	-0.43364	-9.31447	4.43464
C	4.18251	8.00712	-2.86332	C	0.68797	-11.48779	3.80113
C	0.03247	7.19260	-0.15714	C	-5.30033	-5.81515	-2.29136
C	0.59997	3.57206	0.79114	C	-4.16975	-7.99812	-2.87706
C	0.58706	4.96959	0.85302	C	-0.02955	-7.19096	-0.15265
C	0.06406	5.74100	-0.21221	C	-0.59682	-3.56942	0.79178
C	-0.45017	5.03928	-1.32777	C	-0.58514	-4.96691	0.85454
C	-0.47316	3.64101	-1.35594	C	-0.05854	-5.73933	-0.20815
C	0.05740	2.88434	-0.30333	C	0.46136	-5.03870	-1.32174
S	-0.90713	5.84295	-2.82985	C	0.48508	-3.64046	-1.35083
C	-1.93994	4.42643	-3.42780	C	-0.04960	-2.88276	-0.30104
S	-1.05484	2.89889	-2.85396	S	0.92490	-5.84383	-2.82099
S	1.16324	2.72734	2.24228	C	1.96031	-4.42788	-3.41597
C	2.05366	4.20583	2.92127	S	1.07319	-2.89971	-2.84705
S	1.03653	5.66604	2.41208	S	-1.16531	-2.72347	2.24016
C	2.09511	4.12394	4.44172	C	-2.05925	-4.20098	2.91666
C	3.44913	4.30760	2.31428	S	-1.04119	-5.66219	2.41218
C	-1.99209	4.44393	-4.94985	C	-2.10631	-4.11814	4.43690
C	-3.33019	4.49813	-2.80530	C	-3.45254	-4.30217	2.30456
C	-3.60791	8.16730	-0.46122	C	2.01844	-4.44673	-4.93779
C	-2.44914	7.46551	-0.11582	C	3.34810	-4.49911	-2.78797
C	-1.17769	7.90876	-0.53934	C	3.61014	-8.17408	-0.43675
C	-1.11699	9.06214	-1.34766	C	2.45129	-7.46865	-0.09914
C	-2.26746	9.79175	-1.68184	C	1.18105	-7.90951	-0.52880
C	-3.53552	9.32840	-1.26598	C	1.12201	-9.06363	-1.33622
S	0.37472	9.53300	-2.16887	C	2.27245	-9.79667	-1.66288
C	-0.15579	11.27767	-2.41787	C	3.53931	-9.33624	-1.24015
S	-1.98667	11.20480	-2.71280	S	-0.36624	-9.53159	-2.16525
S	-5.12389	7.51185	0.17653	C	0.16101	-11.27800	-2.40909
C	-4.30076	6.57159	1.54847	S	1.99377	-11.21037	-2.69354
S	-2.66697	6.02619	0.88614	S	5.12415	-7.52184	0.20891
C	-4.09929	7.47928	2.75860	C	4.29555	-6.57694	1.57439
C	-5.14233	5.34836	1.89269	S	2.66722	-6.02812	0.90145
C	0.52798	11.84985	-3.65435	C	4.08428	-7.48207	2.78477
C	0.14057	12.10185	-1.16865	C	5.13849	-5.35553	1.92163

C	-0.51709	-11.84984	-3.64883	H	-3.83009	5.42266	-3.11663
C	-0.14472	-12.09984	-1.16062	H	-5.06935	7.83652	3.12330
C	0.03204	1.40289	-0.33192	H	-3.48233	8.34382	2.49729
C	-1.18676	0.71830	-0.34310	H	-3.59644	6.92613	3.56043
C	-1.21439	-0.66855	-0.33481	H	-5.27966	4.70178	1.02225
C	-0.02396	-1.40134	-0.33078	H	-6.12604	5.66383	2.25765
C	1.19487	-0.71677	-0.33776	H	-4.65912	4.77381	2.69055
C	1.22247	0.67010	-0.33058	H	1.61143	11.88436	-3.49547
C	4.59189	10.16423	1.76100	H	0.18654	12.87632	-3.82667
O	4.50675	11.32225	2.12008	H	0.31605	11.25106	-4.54349
O	5.74461	9.46325	1.79678	H	-0.35123	11.67432	-0.29034
C	6.90940	10.21617	2.18988	H	-0.21351	13.13003	-1.30697
C	-4.80988	9.92821	-1.70007	H	1.22003	12.11749	-0.97805
O	-5.89875	9.40926	-1.53423	H	-0.89452	-9.78443	5.31105
O	-4.65972	11.10830	-2.33429	H	-1.08741	-8.51118	4.08318
C	-5.87467	11.70001	-2.83353	H	0.52719	-8.87491	4.72697
C	-4.60257	-10.15406	1.74632	H	0.84194	-12.22501	3.00892
O	-4.52084	-11.31202	2.10639	H	0.24602	-11.98785	4.66991
O	-5.75436	-9.45130	1.77650	H	1.66061	-11.08689	4.10733
C	-6.92208	-10.20223	2.16465	H	-5.46267	-5.06586	-1.51225
C	4.81456	-9.94030	-1.66568	H	-6.26979	-6.21654	-2.60633
O	5.90392	-9.42437	-1.49376	H	-4.84275	-5.33011	-3.16044
O	4.66487	-11.12069	-2.29947	H	-5.12650	-8.42765	-3.19582
C	5.88118	-11.71646	-2.79053	H	-3.53225	-8.80263	-2.49939
H	0.86884	9.78938	5.30899	H	-3.67441	-7.54257	-3.74199
H	1.06967	8.51626	4.08224	H	-2.68081	-3.23747	4.74382
H	-0.54849	8.87698	4.71885	H	-1.10337	-4.05447	4.86597
H	-0.86188	12.22639	2.99907	H	-2.61275	-5.00199	4.83989
H	-0.27260	11.99039	4.66261	H	-3.39777	-4.37404	1.21448
H	-1.68322	11.08690	4.09410	H	-4.04298	-3.41875	2.57394
H	5.47546	5.07718	-1.49357	H	-3.95818	-5.20042	2.67758
H	6.28474	6.22955	-2.58428	H	2.51818	-5.36053	-5.27684
H	4.86159	5.34050	-3.14419	H	2.60459	-3.59406	-5.29724
H	5.13972	8.43862	-3.17800	H	1.01945	-4.40191	-5.37824
H	3.54177	8.81027	-2.48823	H	3.28646	-4.49705	-1.69589
H	3.69175	7.55063	-3.73036	H	3.94779	-3.64078	-3.11236
H	2.66919	3.24391	4.75126	H	3.84920	-5.42392	-3.09651
H	1.09064	4.05968	4.86709	H	5.05115	-7.84139	3.15587
H	2.59932	5.00843	4.84608	H	3.46651	-8.34531	2.52110
H	3.39831	4.37874	1.22397	H	3.57815	-6.92621	3.58264
H	4.03919	3.42477	2.58640	H	5.28318	-4.71092	1.05093
H	3.95277	5.20645	2.68856	H	6.11898	-5.67323	2.29330
H	-2.49070	5.35733	-5.29163	H	4.65201	-4.77813	2.71544
H	-2.57672	3.59084	-5.31079	H	-1.60152	-11.88146	-3.49614
H	-0.99139	4.39886	-5.38639	H	-0.17725	-12.87736	-3.81806
H	-3.27276	4.49714	-1.71299	H	-0.29857	-11.25259	-4.53741
H	-3.92859	3.63949	-3.13121	H	0.34315	-11.67247	-0.28004

H	0.20743	-13.12911	-1.29558	H	-6.36738	11.02234	-3.53619
H	-1.22530	-12.11240	-0.97620	H	-7.75299	-9.49966	2.09712
H	-2.11441	1.28296	-0.35005	H	-6.80953	-10.57501	3.18639
H	-2.16418	-1.19501	-0.32799	H	-7.07210	-11.04816	1.48815
H	2.12254	-1.28143	-0.34056	H	5.56964	-12.63418	-3.29012
H	2.17223	1.19656	-0.32043	H	6.55828	-11.93669	-1.96068
H	7.74163	9.51476	2.12683	H	6.37997	-11.04112	-3.49114
H	6.79145	10.58959	3.21078	C	2.16172	9.72621	1.67391
H	7.06138	11.06180	1.51342				
H	-5.56264	12.61789	-3.33253				
H	-6.55739	11.91956	-2.00811				

Biradical **2••**

C	2.52048	11.89986	0.85120	C	-2.44791	9.69793	0.62638
C	1.30345	11.21387	0.76883	C	-1.35363	10.07189	-0.18280
C	1.16484	10.07509	-0.04913	C	-1.51851	11.17331	-1.04725
C	2.28708	9.65430	-0.79241	C	-2.70218	11.92545	-1.06809
C	3.50638	10.33566	-0.72007	C	-3.79342	11.53559	-0.26030
C	3.63758	11.46403	0.11418	S	-0.33656	11.53603	-2.30890
S	2.22597	8.27113	-1.89806	C	-0.88566	13.28116	-2.50966
C	3.62225	8.88461	-2.94319	S	-2.72015	13.26376	-2.22858
S	4.79337	9.70047	-1.76390	S	-4.90862	9.85986	1.70263
S	2.55187	13.30122	1.93166	C	-3.72738	8.96590	2.82114
C	1.12299	12.70627	2.95162	S	-2.38253	8.32218	1.73343
S	-0.01165	11.84839	1.77046	C	-3.14894	9.93156	3.85128
C	1.60419	11.73063	4.02052	C	-4.45001	7.79813	3.48192
C	0.40381	13.90483	3.55864	C	-0.60239	13.74662	-3.93349
C	4.31648	7.70142	-3.60596	C	-0.20602	14.17058	-1.47286
C	3.11178	9.89306	-3.96682	C	-2.51485	-11.89965	0.92825
C	-0.09319	9.34456	-0.12408	C	-1.29756	-11.21678	0.82570
C	0.76270	5.77438	0.79947	C	-1.16921	-10.07950	0.00398
C	0.73524	7.17277	0.80819	C	-2.30157	-9.65822	-0.72367
C	-0.08713	7.89220	-0.09192	C	-3.52126	-10.33623	-0.63086
C	-0.90720	7.13703	-0.96334	C	-3.64240	-11.46214	0.20828
C	-0.91079	5.73889	-0.92128	S	-2.25383	-8.27812	-1.83375
C	-0.06574	5.03430	-0.05435	C	-3.66812	-8.88992	-2.85531
S	-1.80471	7.86425	-2.29637	S	-4.82269	-9.70013	-1.65607
C	-2.94280	6.41603	-2.49450	S	-2.53263	-13.29948	2.01085
S	-1.90049	4.92111	-2.13918	C	-1.08533	-12.70815	3.00662
S	1.76202	4.99979	2.03837	S	0.03191	-11.85316	1.80687
C	2.77168	6.52188	2.37133	C	-1.54606	-11.73136	4.08353
S	1.60583	7.94076	2.13847	C	-0.35916	-13.90864	3.60154
C	3.26401	6.50256	3.81257	C	-4.36971	-7.70597	-3.50915
C	3.91989	6.62493	1.37329	C	-3.17700	-9.90155	-3.88524
C	-3.44444	6.35804	-3.93137	C	0.08821	-9.35039	-0.08985
C	-4.08574	6.51479	-1.49017	C	-0.75528	-5.77717	0.83387
C	-3.64312	10.42274	0.60002	C	-0.72709	-7.17549	0.84722

C	0.08360	-7.89788	-0.06122	O	-6.12523	11.69148	0.18745
C	0.89315	-7.14534	-0.94482	O	-5.14854	13.30594	-1.03794
C	0.89782	-5.74707	-0.90656	C	-6.44434	13.91965	-1.17876
C	0.06271	-5.03973	-0.03221	C	-4.89294	-12.23164	0.34315
S	1.77407	-7.87599	-2.28718	O	-4.94603	-13.40666	0.64906
C	2.91120	-6.42949	-2.50111	O	-5.98926	-11.47958	0.10971
S	1.87407	-4.93296	-2.13780	C	-7.24136	-12.19346	0.13818
S	-1.74015	-4.99844	2.08173	C	5.12575	-12.15138	-0.37488
C	-2.74445	-6.51989	2.43322	O	6.13088	-11.67813	0.12310
S	-1.58052	-7.93869	2.19148	O	5.14193	-13.29274	-1.09222
C	-3.21851	-6.49515	3.88050	C	6.43818	-13.89956	-1.25665
C	-3.90501	-6.62780	1.45018	H	2.30033	12.23542	4.70028
C	3.39698	-6.37524	-3.94355	H	2.11493	10.87644	3.56676
C	4.06496	-6.52719	-1.50917	H	0.74995	11.35543	4.59627
C	3.65081	-10.42131	0.57947	H	0.05697	14.59512	2.78546
C	2.45350	-9.70114	0.62625	H	1.07868	14.44009	4.23553
C	1.34766	-10.07783	-0.16565	H	-0.45704	13.56659	4.14601
C	1.50109	-11.17947	-1.03187	H	4.67855	6.98461	-2.86453
C	2.68763	-11.92629	-1.07395	H	5.16389	8.05315	-4.20459
C	3.79123	-11.53212	-0.28517	H	3.62008	7.19289	-4.28144
S	0.29771	-11.54843	-2.27127	H	3.94755	10.27740	-4.56282
C	0.85219	-13.29072	-2.48212	H	2.61799	10.73372	-3.47098
S	2.69144	-13.26350	-2.23592	H	2.38709	9.41167	-4.63325
S	4.93202	-9.85470	1.66183	H	3.92951	5.64632	3.96663
C	3.76569	-8.96658	2.80044	H	2.43299	6.43754	4.51906
S	2.40103	-8.32657	1.73544	H	3.83946	7.41155	4.01892
C	3.20763	-9.93550	3.83878	H	3.54596	6.64984	0.34563
C	4.49496	-7.79707	3.45088	H	4.59192	5.76640	1.48730
C	0.54406	-13.75810	-3.90014	H	4.48392	7.54837	1.54928
C	0.19731	-14.18355	-1.43238	H	-4.03832	7.25155	-4.15183
C	-0.04717	3.55279	-0.04213	H	-4.09414	5.48602	-4.06277
C	-1.17678	2.82866	0.34956	H	-2.61719	6.29499	-4.64239
C	-1.15615	1.44217	0.36191	H	-3.70495	6.57245	-0.46635
C	-0.01102	0.73499	-0.02663	H	-4.73753	5.63797	-1.57936
C	1.11618	1.46692	-0.42166	H	-4.67355	7.41949	-1.68375
C	1.10111	2.85343	-0.42461	H	-3.95422	10.34441	4.46991
C	0.00708	-0.74033	-0.02294	H	-2.62582	10.75614	3.35856
C	-1.12504	-1.47434	-0.39968	H	-2.43455	9.40613	4.49579
C	-1.10968	-2.86085	-0.39624	H	-4.85974	7.11030	2.73784
C	0.04367	-3.55822	-0.02544	H	-5.26899	8.17275	4.10587
C	1.17798	-2.83202	0.34837	H	-3.75984	7.24956	4.13223
C	1.15722	-1.44548	0.35431	H	0.47827	13.75028	-4.11348
C	4.88746	12.23826	0.22630	H	-0.96297	14.77219	-4.06855
O	4.94124	13.41443	0.52762	H	-1.08565	13.10062	-4.67050
O	5.98251	11.48944	-0.02290	H	-0.41169	13.81869	-0.45796
C	7.23223	12.20800	-0.01787	H	-0.56824	15.20063	-1.57006
C	-5.12622	12.16163	-0.32550	H	0.87984	14.15763	-1.62318

H	-2.23339	-12.23388	4.77383	H	-0.53988	-13.76817	-4.05891
H	-2.06050	-10.87488	3.63834	H	0.90800	-14.78154	-4.04209
H	-0.68156	-11.35980	4.64618	H	1.00899	-13.10938	-4.64649
H	-0.02814	-14.60028	2.82266	H	0.42215	-13.83148	-0.42163
H	-1.02355	-14.44159	4.29051	H	0.56173	-15.21201	-1.53776
H	0.51301	-13.57275	4.17336	H	-0.89143	-14.17494	-1.56040
H	-4.71731	-6.98662	-2.76327	H	-2.06991	3.36369	0.65939
H	-5.22798	-8.05642	-4.09287	H	-2.03044	0.89779	0.70732
H	-3.68305	-7.20093	-4.19708	H	2.00400	0.94132	-0.76162
H	-4.02334	-10.28455	-4.46705	H	1.98006	3.40789	-0.74081
H	-2.67757	-10.74290	-3.39627	H	-2.01731	-0.95057	-0.73067
H	-2.46191	-9.42335	-4.56424	H	-1.99248	-3.41693	-0.69857
H	-3.88323	-5.63917	4.03933	H	2.07517	-3.36537	0.64921
H	-2.37865	-6.42589	4.57607	H	2.03579	-0.89937	0.68584
H	-3.78996	-7.40405	4.09807	H	7.99238	11.46715	-0.26673
H	-3.54412	-6.65723	0.41798	H	7.41704	12.63867	0.97002
H	-4.57588	-5.76900	1.56889	H	7.21270	13.00951	-0.76149
H	-4.46654	-7.55064	1.63718	H	-6.27697	14.80597	-1.79132
H	3.98714	-7.27002	-4.16871	H	-6.84269	14.19441	-0.19828
H	4.04639	-5.50440	-4.08396	H	-7.13980	13.23273	-1.66896
H	2.56198	-6.31246	-4.64549	H	-8.00279	-11.45078	-0.10115
H	3.69542	-6.58217	-0.48107	H	-7.41145	-12.61944	1.13074
H	4.71662	-5.65127	-1.60757	H	-7.23700	-12.99804	-0.60234
H	4.64969	-7.43299	-1.70697	H	6.26507	-14.78438	-1.86979
H	4.02441	-10.34636	4.44348	H	6.85396	-14.17605	-0.28393
H	2.67906	-10.76127	3.35391	H	7.12214	-13.20739	-1.75558
H	2.50233	-9.41320	4.49572				
H	4.88930	-7.10646	2.70110				
H	5.32589	-8.16969	4.06004				
H	3.81392	-7.25228	4.11384				

Biradical **3••**

C	2.26921	13.89684	1.76362	C	4.18724	11.91450	-2.68077
C	1.09918	13.28484	1.29971	C	-0.06698	11.51757	-0.01752
C	1.15223	12.15925	0.45534	C	0.27830	7.88368	0.98038
C	2.42180	11.67497	0.07686	C	0.30345	9.28183	1.03861
C	3.59679	12.27952	0.53482	C	-0.14769	10.06551	-0.04621
C	3.53075	13.39432	1.39497	C	-0.68464	9.38315	-1.16205
S	2.62905	10.31178	-1.03843	C	-0.69180	7.98568	-1.21165
C	4.30808	10.85568	-1.59009	C	-0.20371	7.21369	-0.14959
S	5.10539	11.57591	-0.08288	S	-1.34742	10.20594	-2.57848
S	2.04422	15.29574	2.82253	C	-1.10214	8.75618	-3.70966
C	0.33726	14.79042	3.34264	S	-1.40374	7.25752	-2.66202
S	-0.42349	13.98807	1.85948	S	0.84228	7.02423	2.42191
C	0.40925	13.79493	4.49579	C	1.76012	8.48726	3.10630
C	-0.46416	16.03278	3.71105	S	0.76876	9.96639	2.59919
C	5.10568	9.64417	-2.05465	C	1.79610	8.40055	4.62641

C	3.15760	8.56520	2.50211	S	-0.24269	-9.98225	2.79771
C	0.32673	8.74706	-4.24222	C	-0.62501	-8.47183	5.07531
C	-2.13086	8.81571	-4.83093	C	-2.56853	-8.63133	3.46600
C	-3.58233	12.82905	-0.51425	C	0.30858	-8.65857	-5.13009
C	-2.50558	12.04858	-0.07441	C	2.22916	-8.74770	-3.48780
C	-1.18397	12.32523	-0.48924	C	3.11116	-12.55034	-1.48287
C	-0.98423	13.41340	-1.36965	C	2.15378	-11.83371	-0.75909
C	-2.05185	14.20963	-1.80407	C	0.79395	-12.21798	-0.75801
C	-3.36723	13.91717	-1.38454	C	0.42275	-13.33337	-1.53246
S	0.57876	13.73070	-2.13018	C	1.37196	-14.06841	-2.25814
C	0.18777	15.49928	-2.47709	C	2.72254	-13.66050	-2.27403
S	-1.61393	15.51805	-2.91628	S	-1.26800	-13.74094	-1.82647
S	-5.16420	12.40837	0.14919	C	-0.90623	-15.47200	-2.34080
C	-4.64754	10.70830	0.68960	S	0.74740	-15.42763	-3.19476
S	-2.87023	10.85164	1.16828	S	4.77727	-11.96127	-1.30571
C	-5.47087	10.30207	1.90617	C	4.46016	-11.08273	0.29232
C	-4.80061	9.71639	-0.45921	S	2.73292	-10.44720	0.17563
C	1.00031	15.97430	-3.67560	C	4.58591	-12.05660	1.46026
C	0.44430	16.35075	-1.23834	C	5.42649	-9.91145	0.42161
C	-1.72040	-13.95356	2.42799	C	-1.96507	-15.94132	-3.33245
C	-0.79127	-13.30104	1.60940	C	-0.83360	-16.37981	-1.11620
C	-1.16352	-12.18425	0.83424	C	-0.23238	5.73229	-0.19076
C	-2.50790	-11.75963	0.88975	C	-1.05848	5.01920	0.68142
C	-3.44445	-12.40896	1.70022	C	-1.06687	3.63132	0.67107
C	-3.05398	-13.50807	2.49121	C	-0.24503	2.91438	-0.20629
S	-3.11677	-10.41344	-0.08782	C	0.57743	3.63621	-1.08188
C	-4.86203	-11.02337	-0.06793	C	0.58063	5.02268	-1.07848
S	-5.09837	-11.77235	1.60848	C	-0.21246	-2.86630	-0.14108
S	-1.10641	-15.32610	3.36129	C	-1.23346	-3.60437	-0.75277
C	0.65171	-14.74142	3.30003	C	-1.22379	-4.99133	-0.72757
S	0.85582	-13.94956	1.64158	C	-0.19462	-5.68310	-0.08389
C	0.90616	-13.71924	4.40297	C	0.82597	-4.95319	0.53047
C	1.58685	-15.93938	3.40497	C	0.81783	-3.56631	0.49928
C	-5.81218	-9.84391	-0.23167	C	-0.22245	-1.39124	-0.16752
C	-5.06494	-12.07611	-1.15225	C	0.96226	-0.66399	-0.33804
C	-0.19397	-11.47556	0.01235	C	0.95349	0.72226	-0.35756
C	-0.30730	-7.86422	1.15164	C	-0.23964	1.43906	-0.20216
C	-0.29606	-9.26309	1.18502	C	-1.42460	0.71180	-0.03352
C	-0.18740	-10.01942	-0.00562	C	-1.41652	-0.67455	-0.01889
C	-0.06771	-9.30499	-1.21993	C	4.72894	14.08849	1.90194
C	-0.05862	-7.90581	-1.23611	O	4.75730	15.25922	2.22640
C	-0.18678	-7.16404	-0.05546	O	5.79960	13.27116	1.99079
S	-0.09867	-10.08596	-2.80270	C	7.02710	13.90925	2.39624
C	0.71706	-8.66359	-3.66307	C	-4.54057	14.71561	-1.78674
S	0.05690	-7.14087	-2.82877	O	-5.59021	14.74652	-1.17381
S	-0.41338	-7.04033	2.71581	O	-4.33790	15.40258	-2.92931
C	-1.05459	-8.53339	3.61532	C	-5.42624	16.25472	-3.33776

C	-3.99019	-14.24400	3.36086	H	1.40180	-16.66180	2.60587
O	-3.85671	-15.40838	3.68196	H	1.44852	-16.43684	4.37125
O	-5.01246	-13.47292	3.78796	H	2.62928	-15.60649	3.34884
C	-6.01066	-14.15629	4.57216	H	-5.65652	-9.09430	0.54855
C	3.63462	-14.37206	-3.18548	H	-6.85023	-10.19158	-0.18883
O	3.31691	-15.33002	-3.86679	H	-5.65878	-9.37535	-1.20990
O	4.86771	-13.82714	-3.23756	H	-6.09225	-12.45662	-1.11698
C	5.79434	-14.47908	-4.12686	H	-4.37537	-12.91362	-1.01318
H	0.88856	14.26282	5.36340	H	-4.87845	-11.63604	-2.13845
H	0.98736	12.91104	4.21076	H	-1.07538	-7.59830	5.55888
H	-0.60011	13.47162	4.77469	H	0.46173	-8.40952	5.17103
H	-0.51128	16.73786	2.87727	H	-0.98063	-9.36340	5.60329
H	-0.00361	16.53081	4.57132	H	-2.85709	-8.67748	2.41215
H	-1.48350	15.75027	3.99562	H	-3.04573	-7.75854	3.92641
H	5.18173	8.88957	-1.26750	H	-2.93269	-9.54176	3.95633
H	6.11448	9.95190	-2.35098	H	0.67251	-9.56914	-5.61817
H	4.62530	9.19561	-2.93139	H	0.76412	-7.80271	-5.63974
H	5.18368	12.25331	-2.98684	H	-0.77680	-8.60304	-5.24315
H	3.61835	12.77584	-2.31960	H	2.50255	-8.75414	-2.42878
H	3.66604	11.49750	-3.55027	H	2.70864	-7.88937	-3.97234
H	2.35403	7.50971	4.93458	H	2.60476	-9.67275	-3.94054
H	0.78980	8.35306	5.04965	H	5.60282	-12.46377	1.50075
H	2.31521	9.27476	5.03433	H	3.87830	-12.88320	1.35144
H	3.11094	8.63439	1.41168	H	4.36822	-11.53833	2.40132
H	3.73228	7.67303	2.77669	H	5.32821	-9.21810	-0.41761
H	3.67572	9.45615	2.87587	H	6.45766	-10.27969	0.45926
H	0.50951	9.65526	-4.82797	H	5.23276	-9.37018	1.35416
H	0.48205	7.86986	-4.88091	H	-2.94611	-15.97189	-2.84541
H	1.04648	8.71847	-3.41905	H	-1.73195	-16.95696	-3.67047
H	-3.15007	8.82202	-4.43669	H	-2.01837	-15.28315	-4.20309
H	-2.01103	7.95226	-5.49433	H	-0.07939	-16.02607	-0.40746
H	-1.97545	9.72038	-5.42855	H	-0.57537	-17.39947	-1.42506
H	-6.53027	10.24305	1.63360	H	-1.80219	-16.39748	-0.60291
H	-5.35543	11.01734	2.72420	H	-1.69476	5.56083	1.37647
H	-5.16111	9.31012	2.25287	H	-1.69659	3.09500	1.37539
H	-4.19126	10.01309	-1.31769	H	1.20391	3.10148	-1.79043
H	-5.85061	9.66782	-0.77039	H	1.21712	5.56842	-1.76908
H	-4.47558	8.71913	-0.14016	H	-2.03047	-3.08375	-1.27624
H	2.06848	15.94095	-3.43460	H	-2.02273	-5.54976	-1.20801
H	0.74652	17.01407	-3.90870	H	1.63215	-5.48125	1.03263
H	0.81327	15.35676	-4.55766	H	1.60788	-3.01456	1.00094
H	-0.14232	15.99257	-0.38771	H	1.90019	-1.19508	-0.47531
H	0.17413	17.39350	-1.44132	H	1.88976	1.26152	-0.47239
H	1.50418	16.30254	-0.96234	H	-2.36717	1.24231	0.07005
H	0.75131	-14.18194	5.38447	H	-2.34791	-1.21326	0.13237
H	0.22652	-12.86799	4.30457	H	7.77998	13.12083	2.38512
H	1.93584	-13.34805	4.33981	H	6.92052	14.33160	3.39911

H	7.28980	14.70727	1.69626	H	-6.44104	-14.98393	4.00165
H	-5.08272	16.74371	-4.24961	H	6.72426	-13.91729	-4.03463
H	-5.64499	16.99148	-2.55989	H	5.42066	-14.44793	-5.15407
H	-6.32199	15.65783	-3.52954	H	5.93869	-15.52129	-3.82932
H	-6.76762	-13.40408	4.79538				
H	-5.56663	-14.54665	5.49196				

Biradical **4**$^{\bullet\bullet}$

C	2.34973	16.30498	1.33332	C	-3.82606	15.35361	-0.17906
C	1.23043	15.49565	1.10900	S	-0.30012	16.01434	-1.99070
C	1.26608	14.45080	0.16293	C	-1.05512	17.69251	-2.02639
C	2.46542	14.24563	-0.55073	S	-2.88459	17.42159	-1.86711
C	3.58667	15.05465	-0.33876	S	-4.81215	13.34073	1.51947
C	3.54137	16.09123	0.61502	C	-3.58241	12.48142	2.61245
S	2.62698	12.98840	-1.78793	S	-2.11258	12.13568	1.55267
C	3.98259	13.86954	-2.68417	C	-3.18954	13.39011	3.77368
S	4.98806	14.69239	-1.36515	C	-4.17563	11.16378	3.09709
S	2.16318	17.56636	2.56158	C	-0.76366	18.35731	-3.36696
C	0.78117	16.68814	3.43000	C	-0.54534	18.52551	-0.85412
S	-0.19429	15.85697	2.09704	C	-2.30983	-16.31384	1.35143
C	1.33845	15.64893	4.39708	C	-1.19852	-15.50106	1.10147
C	-0.10046	17.70994	4.13669	C	-1.26030	-14.45414	0.15923
C	3.39804	14.91225	-3.63093	C	-2.47744	-14.25017	-0.52383
C	4.84805	12.85288	-3.41783	C	-3.59138	-15.06187	-0.28537
C	0.10592	13.60743	-0.07641	C	-3.51968	-16.10082	0.66415
C	1.12828	10.02395	0.58383	S	-2.67236	-12.99119	-1.75450
C	1.07335	11.41995	0.67118	C	-4.04811	-13.87447	-2.61802
C	0.25308	12.16761	-0.20823	S	-5.01920	-14.69994	-1.27482
C	-0.47126	11.44898	-1.18884	S	-2.08936	-17.57806	2.57100
C	-0.43766	10.05264	-1.22928	C	-0.68943	-16.69721	3.40786
C	0.35296	9.31961	-0.34193	S	0.25112	-15.86068	2.05304
S	-1.33150	12.22543	-2.51890	C	-1.22696	-15.66097	4.38919
C	-2.42735	10.76443	-2.83781	C	0.21198	-17.71716	4.09167
S	-1.36253	9.27324	-2.51757	C	-3.48480	-14.91639	-3.57840
S	2.08292	9.18409	1.81233	C	-4.93316	-12.85958	-3.33015
C	3.05176	10.69657	2.28217	C	-0.10762	-13.60862	-0.10787
S	1.88218	12.11902	2.07761	C	-1.11987	-10.02806	0.58393
C	3.47805	10.60021	3.74121	C	-1.05896	-11.42407	0.66826
C	4.24291	10.86796	1.34578	C	-0.25955	-12.16880	-0.23254
C	-2.86949	10.77184	-4.29497	C	0.43839	-11.44710	-1.22999
C	-3.61094	10.78499	-1.87753	C	0.40074	-10.05077	-1.26746
C	-3.57692	14.17602	0.56450	C	-0.36887	-9.32055	-0.35939
C	-2.30139	13.60460	0.58743	S	1.26646	-12.21979	-2.58259
C	-1.22792	14.19490	-0.11348	C	2.34905	-10.75541	-2.92842
C	-1.48763	15.36356	-0.85620	S	1.28886	-9.26784	-2.57955
C	-2.75458	15.96594	-0.86631	S	-2.04784	-9.19281	1.83603

C	-3.00098	-10.70902	2.32525	C	2.42333	5.05846	-1.90287
S	-1.83114	-12.12666	2.09358	C	-2.51277	-5.06304	-1.82651
C	-3.39548	-10.61547	3.79338	C	1.80135	-7.87306	0.94901
C	-4.21173	-10.88420	1.41501	C	4.67793	16.99411	0.87544
C	2.75321	-10.76047	-4.39663	O	4.56913	18.12686	1.30230
C	3.55758	-10.77306	-1.99950	O	5.86820	16.41780	0.60653
C	3.59343	-14.17271	0.42285	C	7.01511	17.27846	0.75541
C	2.31758	-13.60519	0.48738	C	-5.22336	15.81508	-0.26192
C	1.22511	-14.19489	-0.18404	O	-6.17799	15.16983	0.13126
C	1.46491	-15.36023	-0.93845	O	-5.35689	17.02247	-0.84648
C	2.73293	-15.95832	-0.99071	C	-6.71221	17.48564	-1.00307
C	3.82345	-15.34517	-0.33478	C	-4.64750	-17.00672	0.95092
S	0.24477	-16.01093	-2.03783	O	-4.52553	-18.14118	1.36951
C	1.00320	-17.68673	-2.10137	O	-5.84544	-16.43100	0.71688
S	2.83585	-17.41011	-2.00041	C	-6.98670	-17.29387	0.89398
S	4.85467	-13.33881	1.34473	C	5.21926	-15.79988	-0.46537
C	3.65572	-12.48893	2.47844	O	6.18314	-15.15441	-0.09566
S	2.15415	-12.14127	1.46505	O	5.33931	-17.00044	-1.06659
C	3.30049	-13.40507	3.64596	C	6.69071	-17.45615	-1.27116
C	4.25959	-11.17223	2.95256	H	1.94157	16.14109	5.16876
C	0.67067	-18.34953	-3.43338	H	1.96725	14.92620	3.86920
C	0.53371	-18.52348	-0.91509	H	0.51614	15.10509	4.87640
C	0.33543	7.83539	-0.35916	H	-0.50386	18.44330	3.43369
C	-0.68974	7.14060	0.30142	H	0.47941	18.23561	4.90329
C	-0.67105	5.75179	0.24154	H	-0.93244	17.20357	4.63865
C	0.32276	5.03767	-0.43948	H	2.76895	14.42250	-4.38292
C	1.34477	5.74132	-1.10227	H	4.20625	15.45374	-4.13585
C	1.32488	7.13460	-1.04306	H	2.78242	15.63119	-3.08262
C	-0.35454	-5.03806	-0.44916	H	5.26177	12.11124	-2.72966
C	-1.40045	-5.74362	-1.07141	H	5.67196	13.36257	-3.92931
C	-1.37374	-7.13693	-1.01579	H	4.25201	12.33785	-4.17903
C	-0.35517	-7.83628	-0.37434	H	4.15070	9.74633	3.87635
C	0.69337	-7.13942	0.24652	H	2.61631	10.48105	4.40238
C	0.66768	-5.75060	0.19017	H	4.02665	11.50411	4.02777
C	-0.27734	-3.55904	-0.45634	H	3.91403	10.95554	0.30632
C	0.89793	-2.91730	-0.86449	H	4.91474	10.00643	1.43522
C	0.99900	-1.53371	-0.85497	H	4.79239	11.78053	1.60470
C	-0.07151	-0.73578	-0.43302	H	-3.47120	11.66513	-4.49427
C	-1.24443	-1.37844	-0.01661	H	-3.49704	9.89694	-4.49612
C	-1.34491	-2.76189	-0.02850	H	-2.01360	10.75890	-4.97411
C	0.03292	0.73582	-0.43057	H	-3.27350	10.79790	-0.83689
C	1.22135	1.37512	-0.05481	H	-4.23640	9.89932	-2.03885
C	1.32318	2.75842	-0.06375	H	-4.21325	11.68496	-2.04780
C	0.24157	3.55885	-0.44784	H	-4.07241	13.62725	4.37860
C	-0.94942	2.92059	-0.81366	H	-2.75508	14.32335	3.40398
C	-1.05195	1.53701	-0.80707	H	-2.44572	12.88944	4.40442
C	-1.76626	7.87816	1.04760	H	-4.44459	10.51561	2.25880

H	-5.07171	11.35627	3.69741	H	0.77305	-18.03228	0.03229
H	-3.45436	10.63989	3.73413	H	1.01892	-19.50621	-0.93680
H	0.31571	18.50835	-3.47847	H	-0.55310	-18.66005	-0.96059
H	-1.24088	19.34257	-3.40458	H	-1.44504	5.19120	0.76109
H	-1.12820	17.75380	-4.20177	H	2.09733	7.70057	-1.55953
H	-0.75600	18.03328	0.09949	H	-2.16502	-7.70446	-1.50110
H	-1.02772	19.50985	-0.85883	H	1.45967	-5.18845	0.68003
H	0.53992	18.65868	-0.93387	H	1.73081	-3.51680	-1.22272
H	-1.81125	-16.15556	5.17368	H	1.90880	-1.06058	-1.21452
H	-1.86928	-14.93918	3.87654	H	-2.07472	-0.78496	0.35657
H	-0.39531	-15.11570	4.85039	H	-2.25356	-3.23573	0.33128
H	0.60127	-18.44795	3.37813	H	2.06424	0.77882	0.28403
H	-0.34775	-18.24623	4.87082	H	2.24527	3.22945	0.26409
H	1.05378	-17.20869	4.57473	H	-1.79451	3.52282	-1.13700
H	-2.87331	-14.42649	-4.34466	H	-1.97536	1.06676	-1.13424
H	-4.30415	-15.45840	-4.06445	H	-1.33604	8.56042	1.78992
H	-2.85660	-15.63492	-3.04408	H	-2.43372	7.18154	1.56154
H	-5.33279	-12.11958	-2.63196	H	-2.36528	8.49109	0.36300
H	-5.76742	-13.37118	-3.82255	H	2.06310	4.13255	-2.35929
H	-4.35672	-12.34216	-4.10473	H	3.28766	4.79850	-1.28008
H	-4.06897	-9.76482	3.94379	H	2.78298	5.72049	-2.69576
H	-2.52002	-10.49261	4.43560	H	-2.17628	-4.13135	-2.28907
H	-3.93343	-11.52207	4.09141	H	-3.35529	-4.81439	-1.17006
H	-3.90518	-10.97047	0.36866	H	-2.89667	-5.72225	-2.61032
H	-4.88449	-10.02513	1.51963	H	1.40355	-8.57498	1.69092
H	-4.75193	-11.79900	1.68535	H	2.47260	-7.17489	1.45591
H	3.35156	-11.65217	-4.61245	H	2.39056	-8.46420	0.23711
H	3.37337	-9.88398	-4.61317	H	7.87211	16.67068	0.46429
H	1.87994	-10.74887	-5.05332	H	7.10722	17.60938	1.79347
H	3.24788	-10.78674	-0.95026	H	6.92034	18.15344	0.10646
H	4.17627	-9.88578	-2.17727	H	-6.62963	18.45013	-1.50481
H	4.15759	-11.67149	-2.18545	H	-7.19088	17.59548	-0.02619
H	4.20200	-13.64273	4.22247	H	-7.28828	16.77972	-1.60769
H	2.85794	-14.33769	3.28443	H	-7.85256	-16.68482	0.63341
H	2.57470	-12.91016	4.30175	H	-7.04700	-17.63266	1.93181
H	4.50424	-10.51981	2.11012	H	-6.91094	-18.16391	0.23591
H	5.17208	-11.36571	3.52727	H	6.59591	-18.41475	-1.78195
H	3.55500	-10.65269	3.61145	H	7.20030	-17.57610	-0.31125
H	-0.41122	-18.50411	-3.51007	H	7.24495	-16.74061	-1.88484
H	1.14972	-19.33305	-3.48903				
H	1.00578	-17.74275	-4.27811				

Biradical **5**••

C	2.29560	18.45415	1.38311	C	3.56736	17.21025	-0.26742
C	1.18516	17.63778	1.14121	C	3.50010	18.24718	0.68463
C	1.24241	16.59312	0.19615	S	2.64349	15.13853	-1.73205
C	2.45444	16.39471	-0.49760	C	4.00882	16.02773	-2.60569

S	4.98793	16.85536	-1.26974	S	-2.65780	-15.17042	-1.68324
S	2.08128	19.71507	2.60718	C	-4.02838	-16.06032	-2.54800
C	0.69176	18.82772	3.45436	S	-4.99959	-16.88673	-1.20549
S	-0.25740	17.99013	2.10625	S	-2.06923	-19.74427	2.65524
C	1.24120	17.79187	4.42949	C	-0.67464	-18.85611	3.49328
C	-0.20739	19.84340	4.14750	S	0.26646	-18.01988	2.13868
C	3.43400	17.06830	-3.56071	C	-1.21831	-17.81913	4.47045
C	4.89170	15.01659	-3.32589	C	0.22865	-19.87099	4.18217
C	0.09046	15.74398	-0.06274	C	-3.45927	-17.10199	-3.50523
C	1.12698	12.16633	0.60847	C	-4.91544	-15.04987	-3.26398
C	1.05798	13.56150	0.69909	C	-0.09448	-15.77541	-0.02980
C	0.24744	14.30519	-0.19255	C	-1.12690	-12.19720	0.64449
C	-0.45398	13.58325	-1.18723	C	-1.05677	-13.59221	0.73640
C	-0.40670	12.18738	-1.23220	C	-0.25174	-14.33674	-0.15959
C	0.37397	11.45762	-0.33291	C	0.44373	-13.61555	-1.15906
S	-1.29664	14.35769	-2.52969	C	0.39555	-12.21976	-1.20510
C	-2.36983	12.88676	-2.87731	C	-0.38026	-11.48919	-0.30235
S	-1.29403	11.40664	-2.54638	S	1.27950	-14.39069	-2.50552
S	2.06655	11.33224	1.85299	C	2.34956	-12.91928	-2.86073
C	3.01369	12.85205	2.34224	S	1.27554	-11.43929	-2.52432
S	1.83454	14.26376	2.12203	S	-2.06040	-11.36175	1.89258
C	3.41685	12.75560	3.80786	C	-3.00358	-12.88153	2.38930
C	4.21849	13.03710	1.42607	S	-1.82466	-14.29277	2.16498
C	-2.78511	12.89813	-4.34234	C	-3.39892	-12.78317	3.85693
C	-3.57134	12.88822	-1.93915	C	-4.21323	-13.06902	1.48001
C	-3.60709	16.29442	0.50511	C	2.75586	-12.93166	-4.32830
C	-2.32927	15.72981	0.55400	C	3.55700	-12.91932	-1.93016
C	-1.24495	16.32556	-0.12530	C	3.60693	-16.32697	0.51118
C	-1.49570	17.49312	-0.87292	C	2.32955	-15.76223	0.56968
C	-2.76545	18.08868	-0.90885	C	1.24011	-16.35784	-0.10148
C	-3.84750	17.47035	-0.24387	C	1.48493	-17.52585	-0.85032
S	-0.28926	18.15041	-1.98345	C	2.75437	-18.12128	-0.89620
C	-1.05189	19.82474	-2.03317	C	3.84167	-17.50276	-0.23987
S	-2.88275	19.54409	-1.91161	S	0.26947	-18.18410	-1.95050
S	-4.85709	15.45256	1.43494	C	1.03180	-19.85840	-2.00467
C	-3.64513	14.59999	2.55264	S	2.86352	-19.57736	-1.89913
S	-2.15243	14.26183	1.52297	S	4.86398	-15.48505	1.43141
C	-3.28091	15.51087	3.72150	C	3.66064	-14.63131	2.55751
C	-4.24110	13.27929	3.02552	S	2.15995	-14.29392	1.53938
C	-0.73647	20.49220	-3.36701	C	3.30567	-15.54112	3.73009
C	-0.57034	20.65911	-0.85004	C	4.26027	-13.31013	3.02452
C	-2.29099	-18.48424	1.43155	C	0.70503	-20.52756	-3.33494
C	-1.18203	-17.66816	1.18229	C	0.56040	-20.69134	-0.81645
C	-1.24505	-16.62397	0.23709	C	0.37263	9.97334	-0.35319
C	-2.46131	-16.42596	-0.44933	C	-0.67849	9.26315	0.24812
C	-3.57297	-17.24100	-0.21152	C	-0.63066	7.87423	0.19836
C	-3.49990	-18.27742	0.74067	C	0.40719	7.17544	-0.42924

C	1.46618	7.89333	-1.01384	O	-4.50004	-20.31989	1.44824
C	1.42330	9.28582	-0.95568	O	-5.82455	-18.61624	0.78800
C	-0.41397	-7.20781	-0.40739	C	-6.96288	-19.48320	0.96348
C	-1.47063	-7.92672	-0.99442	C	5.23866	-17.95555	-0.36352
C	-1.42833	-9.31910	-0.93336	O	6.20026	-17.30665	0.00617
C	-0.37977	-10.00491	-0.32515	O	5.36297	-19.15912	-0.95807
C	0.66944	-9.29353	0.27790	C	6.71590	-19.61329	-1.15536
C	0.62191	-7.90451	0.22519	H	1.83020	18.28740	5.20987
C	-0.36139	-5.72695	-0.41714	H	1.88184	17.07315	3.91046
C	-0.42343	-5.00209	-1.61154	H	0.41534	17.24297	4.89676
C	-0.33343	-3.61744	-1.60964	H	-0.60515	20.57406	3.43850
C	-0.18858	-2.90975	-0.41413	H	0.35708	20.37307	4.92282
C	-0.12778	-3.63104	0.77961	H	-1.04338	19.33127	4.63676
C	-0.20672	-5.01702	0.77810	H	2.81844	16.57652	-4.32251
C	-0.09617	-1.43151	-0.41460	H	4.24739	17.61381	-4.05282
C	0.94950	-0.78011	-1.08573	H	2.80713	17.78403	-3.02107
C	1.04376	0.61551	-1.07291	H	5.29921	14.27723	-2.63157
C	0.08189	1.40000	-0.41981	H	5.72037	15.53147	-3.82429
C	-0.97013	0.74461	0.23620	H	4.31088	14.49803	-4.09643
C	-1.05131	-0.65195	0.25397	H	4.09530	11.90776	3.95176
C	0.17378	2.87623	-0.42408	H	2.54552	12.62644	4.45444
C	0.07338	3.60506	0.76622	H	3.95199	13.66385	4.10590
C	0.16095	4.99009	0.75879	H	3.90583	13.12490	0.38163
C	0.35224	5.69519	-0.43506	H	4.89673	12.18158	1.52432
C	0.44797	4.96373	-1.62403	H	4.75499	13.95407	1.69641
C	0.36118	3.57910	-1.62014	H	-3.39282	13.78599	-4.54755
C	-1.81684	9.97917	0.91926	H	-3.39925	12.01772	-4.56014
C	2.65331	7.22167	-1.65424	H	-1.91675	12.89874	-5.00562
C	-2.65275	-7.25350	-1.64203	H	-3.25380	12.89681	-0.89220
C	1.80644	-10.00879	0.95240	H	-4.18444	11.99741	-2.11879
O	2.11805	1.21307	-1.69684	H	-4.17961	13.78324	-2.11422
O	1.93511	-1.55120	-1.64517	H	-4.17732	15.74302	4.30814
O	-1.96089	1.47392	0.85790	H	-2.84436	16.44660	3.36069
O	-2.12831	-1.28919	0.81453	H	-2.54737	15.01442	4.36743
C	3.19662	1.49816	-0.79300	H	-4.49071	12.63008	2.18203
C	2.11998	-1.41225	-3.06215	H	-5.14941	13.46740	3.60855
C	-2.28432	-1.13456	2.23330	H	-3.52964	12.75886	3.67628
C	-3.00477	1.87400	-0.04336	H	0.34413	20.64907	-3.45617
C	4.62674	19.15724	0.96266	H	-1.21803	21.47495	-3.41379
O	4.50398	20.29027	1.38488	H	-1.08056	19.88742	-4.20955
O	5.82481	18.58727	0.71566	H	-0.79766	20.16475	0.09863
C	6.96395	19.45496	0.88260	H	-1.05772	21.64090	-0.86343
C	-5.24542	17.92364	-0.35595	H	0.51559	20.79802	-0.90772
O	-6.20410	17.27358	0.01916	H	-1.80301	-18.31363	5.25471
O	-5.37407	19.12875	-0.94618	H	-1.86165	-17.10083	3.95419
C	-6.72852	19.58364	-1.13174	H	-0.38968	-17.26987	4.93237
C	-4.62500	-19.18685	1.02664	H	0.62229	-20.60235	3.47159

H	-0.33114	-20.39990	4.96140	H	0.09996	5.53968	1.69458
H	1.06747	-19.35821	4.66586	H	0.56384	5.49015	-2.56702
H	-2.84777	-16.61127	-4.27097	H	0.42677	3.03032	-2.55397
H	-4.27558	-17.64778	-3.99217	H	-1.45060	10.73841	1.61934
H	-2.82968	-17.81731	-2.96823	H	-2.45118	9.27670	1.46629
H	-5.31915	-14.30998	-2.56802	H	-2.43880	10.50081	0.18105
H	-5.74683	-15.56527	-3.75729	H	2.47861	7.01577	-2.71700
H	-4.33908	-14.53176	-4.03816	H	2.88376	6.26656	-1.17441
H	-4.07717	-11.93555	4.00312	H	3.53386	7.86721	-1.58867
H	-2.52420	-12.65234	4.49859	H	-2.46913	-7.04453	-2.70273
H	-3.93181	-13.69134	4.15930	H	-2.88621	-6.29957	-1.16141
H	-3.90609	-13.15804	0.43406	H	-3.53408	-7.89885	-1.58558
H	-4.89159	-12.21387	1.58060	H	1.43900	-10.76187	1.65860
H	-4.74739	-13.98610	1.75459	H	2.44402	-9.30460	1.49340
H	3.36305	-13.81919	-4.53655	H	2.42561	-10.53771	0.21698
H	3.36786	-12.05088	-4.55057	H	3.99204	1.94714	-1.39239
H	1.88340	-12.93351	-4.98618	H	3.55972	0.57481	-0.32380
H	3.24602	-12.92639	-0.88125	H	2.87532	2.20850	-0.01963
H	4.16863	-12.02852	-2.11471	H	2.76501	-2.24193	-3.36048
H	4.16442	-13.81444	-2.10777	H	2.59012	-0.45698	-3.31388
H	4.20671	-15.77260	4.30987	H	1.15840	-1.49333	-3.58559
H	2.86643	-16.47727	3.37365	H	-3.05828	-1.84750	2.52657
H	2.57721	-15.04411	4.38130	H	-2.58832	-0.11666	2.49504
H	4.50389	-12.66197	2.17850	H	-1.34905	-1.38130	2.75256
H	5.17266	-13.49773	3.60131	H	-3.73233	2.42930	0.55301
H	3.55352	-12.78875	3.67962	H	-3.48404	0.99441	-0.49184
H	-0.37626	-20.68486	-3.41447	H	-2.60545	2.52440	-0.83289
H	1.18647	-21.51022	-3.38479	H	7.82961	18.85098	0.60983
H	1.04156	-19.92362	-4.18113	H	7.03474	19.79032	1.92089
H	0.79565	-20.19572	0.12964	H	6.87639	20.32694	0.22861
H	1.04781	-21.67310	-0.83267	H	-6.64120	20.54687	-1.63509
H	-0.52597	-20.83044	-0.86477	H	-7.22752	19.69412	-0.16516
H	-1.44086	7.30260	0.64580	H	-7.28825	18.87242	-1.74543
H	2.24097	9.86223	-1.38345	H	-7.83025	-18.87849	0.69785
H	-2.24422	-9.89647	-1.36331	H	-7.02571	-19.81909	2.00210
H	1.43032	-7.33119	0.67378	H	-6.88113	-20.35493	0.30837
H	-0.52056	-5.53329	-2.55412	H	6.62478	-20.57491	-1.66114
H	-0.38463	-3.07264	-2.54794	H	7.22236	-19.72692	-0.19302
H	-0.00353	-3.09904	1.71832	H	7.27097	-18.90010	-1.77102
H	-0.16139	-5.56333	1.71678				
H	-0.06581	3.07624	1.70345				

Biradical **6**••

C	1.65998	9.75022	2.19264	C	3.44341	8.30689	1.40130
C	0.73763	9.03070	1.42485	C	3.02166	9.39301	2.19450
C	1.14527	7.93382	0.63774	S	3.15685	6.25702	-0.33209
C	2.51351	7.58864	0.64272	C	4.86437	6.96233	-0.39877

S	5.12678	7.76791	1.24731	S	-5.12556	-7.76417	1.24653
S	1.00315	11.09045	3.14406	S	-1.00186	-11.08693	3.14278
C	-0.71536	10.39593	3.16978	C	0.71664	-10.39236	3.16828
S	-0.94533	9.57154	1.53096	S	0.94645	-9.56828	1.52928
C	-0.85885	9.37620	4.29485	C	0.86011	-9.37236	4.29312
C	-1.71722	11.53594	3.30434	C	1.71856	-11.53229	3.30302
C	4.96673	7.99407	-1.51708	C	-4.96577	-7.99028	-1.51786
C	5.87163	5.83248	-0.57228	C	-5.87052	-5.82866	-0.57294
C	0.19103	7.17424	-0.15354	C	-0.18996	-7.17066	-0.15485
C	0.42074	3.56185	0.95281	C	-0.41971	-3.55849	0.95222
C	0.43704	4.96064	0.99496	C	-0.43582	-4.95729	0.99411
C	0.25193	5.72207	-0.18412	C	-0.25076	-5.71848	-0.18512
C	0.07526	5.01204	-1.39497	C	-0.07427	-5.00822	-1.39587
C	0.01951	3.61558	-1.40949	C	-0.01873	-3.61174	-1.41014
C	0.18422	2.87081	-0.23955	C	-0.18350	-2.86721	-0.24007
S	0.07461	5.78815	-2.97911	S	-0.07390	-5.78402	-2.98016
C	-0.80484	4.38430	-3.81156	C	0.80521	-4.37991	-3.81252
S	-0.16025	2.84605	-2.99034	S	0.16059	-2.84190	-2.99088
S	0.53778	2.71573	2.50127	S	-0.53691	-2.71267	2.50082
C	1.24081	4.18112	3.39826	C	-1.23974	-4.17834	3.39753
S	0.45980	5.66676	2.61404	S	-0.45846	-5.66371	2.61306
C	0.84572	4.12017	4.86799	C	-0.84471	-4.11760	4.86729
C	2.75349	4.23448	3.21262	C	-2.75240	-4.23191	3.21182
C	-0.43990	4.36441	-5.28983	C	0.43995	-4.35978	-5.29072
C	-2.30802	4.51155	-3.59206	C	2.30845	-4.50702	-3.59337
C	-3.23205	8.05049	-1.49677	C	3.23292	-8.04685	-1.49857
C	-2.20585	7.38755	-0.81801	C	2.20683	-7.38402	-0.81954
C	-0.87660	7.85954	-0.87085	C	0.87755	-7.85591	-0.87236
C	-0.61266	9.00331	-1.65029	C	0.61346	-8.99945	-1.65207
C	-1.63549	9.69686	-2.31386	C	1.63618	-9.69296	-2.31584
C	-2.95843	9.20364	-2.26930	C	2.95914	-9.19983	-2.27130
S	1.04168	9.49965	-2.02041	S	-1.04097	-9.49548	-2.02226
C	0.57141	11.22332	-2.46378	C	-0.57093	-11.21907	-2.46621
S	-1.10278	11.09973	-3.25506	S	1.10324	-11.09541	-3.25752
S	-4.85143	7.35922	-1.30892	S	4.85234	-7.35563	-1.31088
C	-4.43706	6.47089	0.26749	C	4.43821	-6.46730	0.26560
S	-2.67103	5.95946	0.11459	S	2.67211	-5.95599	0.11309
C	-4.60904	7.41106	1.45719	C	4.61051	-7.40743	1.45528
C	-5.31400	5.23053	0.39028	C	5.31509	-5.22689	0.38819
C	1.56358	11.77905	-3.47921	C	-1.56321	-11.77436	-3.48177
C	0.49513	12.08896	-1.20972	C	-0.49469	-12.08512	-1.21243
C	-1.65877	-9.74676	2.19132	C	0.07651	1.39022	-0.25246
C	-0.73648	-9.02727	1.42342	C	-1.18776	0.78008	-0.24914
C	-1.14415	-7.93032	0.63642	C	-1.23479	-0.61137	-0.24577
C	-2.51236	-7.58504	0.64163	C	-0.07577	-1.38661	-0.25270
C	-3.44220	-8.30323	1.40034	C	1.18850	-0.77648	-0.24962
C	-3.02041	-9.38941	2.19344	C	1.23554	0.61497	-0.24601
S	-3.15574	-6.25332	-0.33300	C	-2.44676	1.60087	-0.24285
C	-4.86328	-6.95855	-0.39954	C	2.44749	-1.59728	-0.24393

C	3.94831	10.20234	3.00714	H	-0.20971	11.67122	-0.48534
O	3.75268	11.36002	3.32140	H	0.17172	13.10210	-1.47530
O	5.04106	9.50873	3.38992	H	1.48042	12.14201	-0.73201
C	6.02690	10.26793	4.11763	H	0.69248	-9.85772	5.26151
C	-4.06864	9.76328	-3.06091	H	0.13532	-8.56147	4.17710
O	-5.13961	9.20646	-3.21974	H	1.86716	-8.93928	4.27878
O	-3.78013	10.95291	-3.62557	H	1.61450	-12.25393	2.48863
C	-4.81502	11.50607	-4.46160	H	1.56777	-12.05031	4.25656
C	-3.94701	-10.19870	3.00620	H	2.73997	-11.13580	3.29805
O	-3.75147	-11.35645	3.32028	H	-4.76956	-7.51258	-2.48452
O	-5.03952	-9.50495	3.38939	H	-5.97043	-8.42836	-1.53169
C	-6.02529	-10.26408	4.11726	H	-4.23526	-8.79193	-1.37574
C	4.06923	-9.75940	-3.06314	H	-5.78969	-5.09509	0.23334
O	5.14014	-9.20252	-3.22217	H	-6.88832	-6.23379	-0.58447
O	3.78063	-10.94898	-3.62782	H	-5.70257	-5.32369	-1.53046
C	4.81536	-11.50202	-4.46414	H	-1.28175	-3.22766	5.33295
H	-0.69120	9.86179	5.26312	H	0.24072	-4.08464	4.98847
H	-0.13411	8.56525	4.17904	H	-1.23736	-4.99464	5.39329
H	-1.86593	8.94317	4.28063	H	-3.01451	-4.29542	2.15180
H	-1.61318	12.25742	2.48979	H	-3.21265	-3.33342	3.63887
H	-1.56635	12.05415	4.25776	H	-3.15773	-5.11799	3.71407
H	-2.73865	11.13950	3.29950	H	0.79284	-5.27863	-5.77126
H	4.77046	7.51638	-2.48373	H	0.93422	-3.51556	-5.78341
H	5.97138	8.43218	-1.53098	H	-0.63962	-4.27286	-5.43530
H	4.23622	8.79571	-1.37491	H	2.55017	-4.53989	-2.52672
H	5.79090	5.09889	0.23400	H	2.82493	-3.65429	-4.04933
H	6.88941	6.23766	-0.58390	H	2.67526	-5.43385	-4.04978
H	5.70361	5.32752	-1.52979	H	5.65386	-7.73657	1.52401
H	1.28259	3.23007	5.33351	H	3.97091	-8.28784	1.34574
H	-0.23971	4.08737	4.98913	H	4.33354	-6.89283	2.38275
H	1.23851	4.99705	5.39417	H	5.17842	-4.55619	-0.46427
H	3.01565	4.29823	2.15263	H	6.36941	-5.51988	0.44248
H	3.21357	3.33580	3.63946	H	5.07258	-4.68463	1.30895
H	3.15895	5.12036	3.71513	H	-2.55861	-11.83980	-3.02885
H	-0.79277	5.28340	-5.77012	H	-1.26715	-12.78708	-3.77627
H	-0.93437	3.52034	-5.78258	H	-1.61736	-11.14647	-4.37439
H	0.63964	4.27738	-5.43466	H	0.21023	-11.66771	-0.48794
H	-2.54951	4.54423	-2.52536	H	-0.17140	-13.09822	-1.47836
H	-2.82470	3.65897	-4.04807	H	-1.47997	-12.13823	-0.73471
H	-2.67484	5.43851	-4.04820	H	-2.19856	-1.11532	-0.23140
H	-5.65236	7.74024	1.52616	H	2.19931	1.11892	-0.23175
H	-3.96943	8.29143	1.34748	H	-2.42022	2.36021	0.54674
H	-4.33187	6.89646	2.38460	H	-3.32428	0.96753	-0.08952
H	-5.17755	4.55982	-0.46221	H	-2.56739	2.13402	-1.19412
H	-6.36829	5.52359	0.44478	H	2.42123	-2.35673	0.54557
H	-5.07133	4.68825	1.31099	H	3.32507	-0.96397	-0.09082
H	2.55900	11.84441	-3.02633	H	2.56777	-2.13027	-1.19532
H	1.26742	12.79186	-3.77333	H	6.84301	9.57136	4.31094
H	1.61772	11.15148	-4.37206	H	5.60203	10.63941	5.05416

H	6.37249	11.11534	3.51905	H	-6.37120	-11.11134	3.51866
H	-4.40503	12.44070	-4.84528	H	4.40535	-12.43667	-4.84775
H	-5.71900	11.69016	-3.87473	H	5.71950	-11.68603	-3.87752
H	-5.05147	10.81940	-5.27910	H	5.05151	-10.81528	-5.28167
H	-6.84122	-9.56739	4.31090				
H	-5.60023	-10.63576	5.05362				

8. References

[1] L. Chen, L. Wu, X. Tan, A. Rockenbauer, Y. Song, Y. Liu, "Synthesis and Redox Properties of Water-Soluble Asymmetric Trityl Radicals" *J. Org. Chem.* **2021**, *86*, 8351–8364.

[2] Y. Liu, F. A. Villamena, J. Sun, Y. Xu, I. Dhimitruka, J. L. Zweier, "Synthesis and Characterization of Ester-Derivatized Tetrathiatriarylmethyl Radicals as Intracellular Oxygen Probes" *J. Org. Chem.* **2008**, *73*, 1490–1497.

[3] O. Burghaus, M. Rohrer, T. Gotzinger, M. Plato, K. Mobius, "A novel high-field/high-frequency EPR and ENDOR spectrometer operating at 3 mm wavelength" *Meas. Sci. Technol.* **1992**, *3*, 765–774.

[4] S. Stoll, A. Schweiger, "EasySpin, a comprehensive software package for spectral simulation and analysis in EPR" *J. Magn. Reson.* **2006**, *178*, 42–55.

[5] B. Bleaney, K.D. Bowers, "Anomalous paramagnetism of copper acetate" *Proc. R. Soc. Lond. A Math. Phys. Sci.* **1952**, *214*, 451–465.

[6] S. Saxena, J. H. Freed, "Double quantum two-dimensional Fourier transform electron spin resonance: Distance measurements" *Chem. Phys. Lett.* **1996**, *251*, 102–110.

[7] S. Saxena, J. H. Freed, "Theory of double quantum two-dimensional electron spin resonance with application to distance measurements" *J. Chem. Phys.* **1997**, *107*, 1317–1340.

[8] G. Jeschke, V. Chechik, P. Ionita, A. Godt, H. Zimmermann, J. Banham, C. R. Timmel, D. Hilger, H. Jung, "DeerAnalysis2006—a comprehensive software package for analyzing pulsed ELDOR data" *Appl. Magn. Reson.* **2006**, *30*, 473–498.

[9] K. Kopp, L. Westhofen, T.Hett, F. Schwering-Sohnrey, M. Mayländer, S. Richert, O. Schiemann, "Synthesis and dark state EPR properties of PDI-trityl dyads and triads" *Chem. Eur. J.* **2024**, *30 (12)*, e202303635.

[10] F. Neese, F. Wennmohs, U. Becker, C. Riplinger, "The ORCA quantum chemistry program package" *J. Chem. Phy.s* **2020**, *152*, DOI 10.1063/5.0004608.

[11] F. Neese, "Software update: The ORCA program system—Version 5.0" *WIREs Computational Molecular Science* **2022**, *12*, DOI 10.1002/wcms.1606.

[12] C. Bannwarth, S. Ehlert, S. Grimme, "GFN2-xTB—An Accurate and Broadly Parametrized Self-Consistent Tight-Binding Quantum Chemical Method with Multipole Electrostatics and Density-Dependent Dispersion Contributions" *J. Chem. Theory Comput.* **2019**, *15*, 1652–1671.

[13] S. Grimme, A. Hansen, S. Ehlert, J.-M. Mewes, "r2SCAN-3c: A 'Swiss army knife' composite electronic-structure method" *J. Chem. Phys.* **2021**, *154*, DOI 10.1063/5.0040021.

[14] E. Caldeweyher, S. Ehlert, A. Hansen, H. Neugebauer, S. Spicher, C. Bannwarth, S. Grimme, "A generally applicable atomic-charge dependent London dispersion correction" *J. Chem. Phys.* **2019**, *150*, DOI 10.1063/1.5090222.

[15] E. Caldeweyher, J.M. Mewes, S. Ehlert, S. Grimme, "Extension and evaluation of the D4 London-dispersion model for periodic systems" *Phys. Chem. Chem. Phys.* **2020**, *22*, 8499-8512.

[16] M. D. Hanwell, D. E. Curtis, D. C. Lonie, T. Vandermeersch, E. Zurek, G. R. Hutchison, "Avogadro: an advanced semantic chemical editor, visualization, and analysis platform" *J. Cheminform.* **2012**, *4*, 17.

[17] Y. Zhao, D. G. Truhlar, "The M06 suite of density functionals for main group thermochemistry, thermochemical kinetics, noncovalent interactions, excited states, and transition elements: two new functionals and systematic testing of four M06-class functionals and 12 other functionals" *Theor. Chem. Acc.* **2008**, *120*, 215–241.

[18] J. Tao, J. P. Perdew, V. N. Staroverov, G. E. Scuseria, "Climbing the Density Functional Ladder: Nonempirical Meta–Generalized Gradient Approximation Designed for Molecules and Solids" *Phys. Rev. Lett.* **2003**, *91*, 146401.

[19] V. N. Staroverov, G. E. Scuseria, J. Tao, J. P. Perdew, "Erratum: 'Comparative assessment of a new nonempirical density functional: Molecules and hydrogen-bonded complexes' [J. Chem. Phys. 119 , 12129 (2003)]" *J. Chem. Phys.* **2004**, *121*, 11507–11507.

[20] A. D. Becke, “Density-functional thermochemistry. III. The role of exact exchange” *J. Chem. Phys.* **1993**, *98*, 5648–5652.
[21] J. P. Perdew, M. Ernzerhof, K. Burke, “Rationale for mixing exact exchange with density functional approximations” *J. Chem. Phys.* **1996**, *105*, 9982–9985.
[22] C. Adamo, V. Barone, “Toward reliable density functional methods without adjustable parameters: The PBE0 model” *J. Chem. Phys.* **1999**, *110*, 6158–6170.
[23] M. Ernzerhof, G. E. Scuseria, “Assessment of the Perdew–Burke–Ernzerhof exchange-correlation functional” *J. Chem. Phys.* **1999**, *110*, 5029–5036.
[24] J.-D. Chai, M. Head-Gordon, “Systematic optimization of long-range corrected hybrid density functionals” *J. Chem. Phys.* **2008**, *128*, DOI 10.1063/1.2834918.
[25] E. Caldeweyher, C. Bannwarth, S. Grimme, “Extension of the D3 dispersion coefficient model” *J. Chem. Phys.* **2017**, *147*, DOI 10.1063/1.4993215.
[26] N. Mardirossian, M. Head-Gordon, “ωB97X-V: A 10-parameter, range-separated hybrid, generalized gradient approximation density functional with nonlocal correlation, designed by a survival-of-the-fittest strategy” *Phys. Chem. Chem. Phys.* **2014**, *16*, 9904.
[27] Weigend, F.; Ahlrichs, R. “Balanced Basis Sets of Split Valence, Triple Zeta Valence and Quadruple Zeta Valence Quality for H to Rn: Design and Assessment of Accuracy” *Phys. Chem. Chem. Phys.* **2005**, *7*, 3297. DOI 10.1039/b508541a.